3/80

CMCRCZ 9, (3), 157-246 (1980)

ΧΗΜΙΚΑ ΧΡΟΝΙΚΑ

ΝΕΑ ΣΕΙΡΑ

CHIMIKA CHRONIKA

NEW SERIES

AN INTERNATIONAL EDITION OF THE GREEK CHEMISTS ASSOCIATION

CHIMICA CHRONIKA, NEW SERIES Volume 9, No 3, pp. 157-246, September 1980

CHIMIKA CHRONIKA/NEW SERIES

Published by the Greek Chemists' Association
27, Kaningos Street, Athens (147), Greece

Correspondence, submission of papers, subscriptions, renewals and changes of address should be sent to Chimika Chronica, New Series, 27 Kaningos street, Athens 147, Greece. Subscriptions are taken by volume at 500 drachmas for members and 1.000 drachmas for Corporations in Greece and 28U.S. dollars to all other countries except Cyprus, where subscriptions are made on request.
Printed in Greece by EPTALOFOS
Ὑπεύθυνος σύμφωνα μὲ τὸν νόμο: Μ. Καραγιάννης, Παρμενίδου 15, Ἀθήνα.

CONTENTS

Chimica Chronika, New Series, 9, 157-177 (1980)

ΜΙΑ ΣΤΟΧΑΣΤΙΚΗ ΘΕΩΡΙΑ ΓΙΑ ΤΗΝ ΚΙΝΗΤΙΚΗ ΜΗ ΣΤΟΙΧΕΙΩΔΩΝ ΑΝΤΙΔΡΑΣΕΩΝ

ΚΥΡΙΑΚΟΣ ΑΘ. ΜΑΣΑΒΕΤΑΣ
Ἐργαστήριο Φυσικῆς-Χημείας Ε. Μ. Πολυτεχνείου

Περίληψη

Στοχαστικὲς θεωρίες τῆς Χημικῆς Κινητικῆς εἶναι ὅσες ἔχουν σὰν Μαθηματικό τους ὑπόβαθρο τὶς στοχαστικὲς ἀνελίξεις. Συγκρινόμενες πρὸς τὶς λοιπὲς θεωρίες, δηλαδὴ τὶς ντετερμινιστικὲς θεωρίες τῆς Χημικῆς Κινητικῆς, πλεονεκτοῦν κατὰ τὸ ὅτι ἐκφράζουν ἀμεσότερα τὸ στατιστικὸ χαρακτῆρα τῶν χημικῶν ἀντιδράσεων καὶ περιέχουν σὰν μερικές τους περιπτώσεις τὶς ἀντίστοιχες ντετερμινιστικὲς θεωρίες. Μοναδικὸ «μειονέκτημα» τους εἶναι τὸ ὅτι, ἐπειδὴ δὲν ἔχουν ἀκόμη χρησιμοποιηθεῖ συστηματικά, δὲν καλύπτουν στὸ παρὸν στάδιο ἐξελίξεως τους μεγάλο πλῆθος ρεαλιστικῶν χημικῶς ἀντιδρώντων συστημάτων.

Σὰν παραδείγματα, ἐνδεικτικὰ τῆς ἐφαρμογῆς στοχαστικῆς μεθοδολογίας στὴ Χημικὴ Κινητική, ἀναπτύσσονται δύο στοχαστικὲς θεωρίες, μία ἐξ ἀνασκοπίσεως σχετικῶν ἐργασιῶν γιὰ στοιχειώδεις ἀντιδράσεις καὶ μία πρωτότυπη γιὰ μὴ στοιχειώδεις ἀντιδράσεις, γίνεται ἀναφορὰ σὲ μερικὰ ἀπὸ τὰ μοντέλα τους καὶ σύγκριση τῶν συμπερασμάτων τους μὲ ἄλλα ἀντίστοιχα τῆς βιβλιογραφίας.

Εἰσαγωγὴ

Οἱ θεωρίες τῆς Χημικῆς Κινητικῆς ταξινομοῦνται στὴ βιβλιογραφία κατὰ ποικίλους τρόπους, ὅπως π.χ. κατὰ Johnston[1], κατὰ Boudart[2], κατὰ Laidler[3] καὶ κατὰ Bunker[4]. Μία ταξινόμηση ὅμως τῶν στοιχείων ἑνὸς συνόλου $S = \{a, b, c, \ldots\}$ ἀπαιτεῖ ἀπὸ σκοπιᾶς Μαθηματικῆς Λογικῆς τὴν ὕπαρξη μιᾶς σχέσεως ἰσοδυναμίας $R \subseteq S^2$ μεταξὺ τῶν στοιχείων του, δηλαδὴ μιᾶς σχέσεως ποὺ εἶναι:

1) ἀνακλαστική, δηλαδὴ $\Delta_{S^2} \subseteq R$, ὅπου Δ_{S^2} εἶναι τὸ σύνολο τῶν στοιχείων τοῦ S^2 ποὺ εἶναι τῆς μορφῆς (a, a). [τὸ $\Delta_{S^2} \subseteq R$ σημαίνει ὅτι γιὰ κάθε $a \in S$ εἶναι $(a, a) \in R$]

2) συμμετρική, δηλαδή $R^{-1} \subseteq R$, [πού σημαίνει ὅτι ἡ $(a, b) \in R$ συνεπάγεται τὴν $(b, a) \in R$]
καί 3) μεταβατική, δηλαδή $R^{\circ} R \subseteq R$, [πού σημαίνει ὅτι ἐκ τῶν $(a, b) \in R$ καί $(b, c) \in R$ ἕπεται ἡ $(a, c) \in R$],
ὁπότε οἱ συνιστῶσες τῆς ταξινομήσεως εἶναι τὰ στοιχεῖα τοῦ πηλίκου-συνόλου S/R. Μόνον τότε ἔχουμε διαμέριση τοῦ S σὲ κλάσεις, τὶς κλάσεις ἰσοδυναμίας τοῦ S modulo R, δηλαδὴ μιὰ οἰκογένεια $(S_i)_{i \in I}$ ὑποσυνόλων τοῦ S τέτοια ὥστε:

i) $S_i \neq \emptyset$. $\forall i \in I$

ii) $S_i \cap S_j = \emptyset$. $\forall i, j \in I$ & $i \neq j$

iii) $\bigcup_{i \in I} S_i = S$

πού φορμαλιστικὰ ἀπηχεῖ τὸ διαισθητικὸ περιεχόμενο τῆς ἐννοίας ταξινόμηση.

Ἐν ὄψει αὐτῆς τῆς αὐστηρᾶς ἀντιμετωπίσεως τῆς ἐννοίας ταξινόμηση ἡ μόνη ἀπαλλαγμένη ἀμφισημιῶν διάκριση σὲ κατηγορίες τῶν θεωριῶν τῆς Χημικῆς Κινητικῆς εἶναι αὐτή, πού μὲ κριτήριο τὸ χαρακτήρα τοῦ Μαθηματικοῦ τους ὑποβάθρου τὶς διακρίνει σὲ ντετερμινιστικὲς καὶ σὲ στοχαστικές. Ἐδῶ θὰ πρέπει νὰ παρατηρήσουμε πῶς ἀπὸ Μαθηματικῆς ἀπόψεως οἱ ὅροι ντετερμινιστικὴ θεωρία καὶ στοχαστικὴ θεωρία εἶναι ἀντιφατικῶς ἀντίθετοι — παρὰ τὸ ὅτι ἀπὸ Φιλοσοφικῆς ἀπόψεως ἡ ἀκριβὴς μορφὴ τῆς ἀντιθέσεως τους εἶναι ἀσαφὴς[5] — ὁπότε ἀποτελοῦν πράγματι τὶς συνιστῶσες μιᾶς σχέσεως ἰσοδυναμίας γιὰ τὸ σύνολο τῶν θεωριῶν τῆς Χημικῆς Κινητικῆς.

Στοχαστικὲς θεωρίες τῆς Χημικῆς Κινητικῆς εἶναι ὅσες ἔχουν σὰν Μαθηματικό τους ὑπόβαθρο τὶς στοχαστικὲς ἀνελίξεις, δηλαδὴ ὅσες σὲ τελευταία ἀνάλυση βασίζονται στὶς ἀρχὲς τῆς πιθανοθεωρίας. Ἕνας χονδρικός, ἀλλὰ ἀρκετὰ κατατοπιστικὸς σὲ πρώτη προσέγγιση, καθορισμὸς τοῦ ἀντικειμένου σπουδῆς τῶν στοχαστικῶν ἀνελίξεων εἶναι τοῦ Feller[6]: «Οἱ ὅροι στοχαστικὲς ἀνελίξεις καὶ τυχαῖες διεργασίες εἶναι συνώνυμοι καὶ πρακτικὰ καλύπτουν ὅλη τὴ Θεωρία πιθανοτήτων ἀπὸ τὸ παιγνίδι τῆς ρίψεως κέρματος μέχρι τὴν ἁρμονικὴ ἀνάλυση. Στὴν πράξη, ὁ ὅρος "στοχαστικὴ ἀνέλιξη" χρησιμοποιεῖται κυρίως ὅταν εἰσάγεται μία παράμετρος χρόνου... Στὶς στοχαστικὲς ἀνελίξεις τὸ μέλλον ποτὲ δὲν προσδιορίζεται μονοσήμαντα, ἀλλὰ ἔχουμε τοὐλάχιστον σχέσεις πιθανότητος πού μᾶς φέρνουν σὲ θέση νὰ μποροῦμε νὰ κάνουμε προβλέψεις».

Ἡ πρώτη ἐφαρμογὴ στοχαστικῆς μεθοδολογίας στὴ Χημικὴ Κινητικὴ φαίνεται ὅτι ὀφείλεται στὸν Kramers[7] καὶ τὸν Delbrück[8]. Τὸ ἀπό τότε, 1940, μέχρι καὶ τώρα χρονικὸ διάστημα ἐξελίξεως τῶν στοχαστικῶν θεωριῶν τῆς Χημικῆς Κινητικῆς μποροῦμε νὰ τὸ χωρίσουμε σὲ δύο περιόδους:

α) Τὴν ἀρχικὴ περίοδο, ἀπὸ τὸ 1940 μέχρι τὸ 1958, ὅπου οἱ σχετικὲς ἐργασίες εἶναι λίγες καὶ κατὰ κανόνα ἀσυσχέτιστες μεταξύ τους. Μία ἐμπεριστατωμένη βιβλιογραφικὴ ἀνασκόπηση — ποὺ εἶναι καὶ ἡ πρώτη τοῦ εἴδους — τῶν χαρακτηριστικοτέρων ἐργασιῶν αὐτῆς τῆς περιόδου περιέχεται στὸ βιβλίο τοῦ Bharucha-Reid[9].

καὶ β) Τὴ σύγχρονη περίοδο, ποὺ πρέπει νὰ θεωρεῖται σὰν μεταβατικὸ στάδιο ἀπὸ τὴν ἀρχική, μὴ συστηματική, πρὸς μιὰ μελλοντικὴ περίοδο ποὺ θὰ εἶναι ἑνοποιητικὴ τῶν τάσεων ποὺ ἔχουν ἤδη ἐκδηλωθεῖ καὶ ταυτόχρονα κριτικὴ τῆς Μαθηματικῆς θεμελιώσεως τους. Ἡ σύγχρονη περίοδος ἀρχίζει ἀπὸ τὸ 1958, χρονιὰ ὅπου ἐμφανίστηκαν οἱ ἐργασίες - σταθμοὶ γιὰ τὴ στοχαστικὴ Χημικὴ Κινητικὴ τοῦ Bartholomay[10] καὶ τῶν Montroll-Shuler[11], καὶ χαρακτηρίζεται καὶ ἀπὸ τὴν προσφορὰ τῶν Jachimowski, Mc Quarrie, Ishida κ.ἄ., ποὺ ἔπαιξαν καθοριστικὸ ρόλο στὴ διαμόρφωση τῶν τωρινῶν κατευθύνσεων ἐρεύνης τῆς στοχαστικῆς Χημικῆς Κινητικῆς. Ἡ πιὸ πρόσφατη βιβλιογραφικὴ ἀνασκόπιση μέρους (μέχρι καὶ τὸ 1973) τῶν ἐργασιῶν αὐτῆς τῆς περιόδου εἶναι τοῦ Ishida[12].

Στοχαστικὲς ἀνελίξεις καὶ Χημικὴ Κινητικὴ

Ὁ ὅρος "στοχαστικὴ ἀνέλιξη" (stochastic process) συντίθεται ἀπὸ τὸν ἐπιθετικὸ προσδιορισμό "στοχαστική", ποὺ προέρχεται ἀπὸ τὸ ρῆμα στοχαζομαι = σκοπεύω, σημαδεύω κατὰ στόχου, εἰκάζω, καὶ ἀπὸ τὸ ὑποκείμενο "ἀνέλιξη", ποὺ εἶναι λέξη προτιμότερη τῆς ἐναλλακτικῆς μεταφράσεως τοῦ process ὡς "διεργασία", γιατὶ ἀποδίδει καλύτερα ἀπὸ Μαθηματικῆς σκοπιᾶς τὴ σχετικὴ ἔννοια.

Μεταφορικά, θὰ λέγαμε ὅτι οἱ στοχαστικὲς ἀνελίξεις ἀποτελοῦν τὴ δυναμικὴ τῆς Θεωρίας πιθανοτήτων στὴν ἔννοια ὅτι περιγράφουν τὴν ἐξέλιξη, συναρτήσει τοῦ χρόνου, ἑνὸς συστήματος ποὺ ὑπόκειται σὲ τυχαῖες διακυμάνσεις. Σὲ ἁδρὲς γραμμές: ἀντικείμενο τῆς Θεωρίας πιθανοτήτων εἶναι οἱ τυχαῖες μεταβλητές, δηλαδὴ μεγέθη ἀγνώστου ἐκ τῶν προτέρων — ἀλλὰ ὁπωσδήποτε κάποιας συγκεκριμμένης — τιμῆς, ἐνῶ ἀντικείμενο τῶν στοχαστικῶν ἀνελίξεων εἶναι οἱ στοχαστικὲς συναρτήσεις, δηλαδὴ συναρτήσεις ἀγνώστου ἐκ τῶν προτέρων μορφῆς. Δοθέντος ὅτι οἱ τυχαῖες μεταβλητὲς στὴν πραγματικότητα εἶναι συναρτήσεις $x \mid \Omega \rightarrow W$ μὲ πεδίο ὁρισμοῦ κάποιο δειγματικὸ χῶρο Ω καὶ πεδίο τιμῶν κάποιο χῶρο καταστάσεων W, θὰ λέγαμε τελικὰ ὅτι, ἀπὸ μὴ Μαθηματικῆς σκοπιᾶς, ἡ στοχαστικὴ ἀνέλιξη εἶναι μιὰ οἰκογένεια τυχαίων μεταβλητῶν[13] $\{x_t, t \in T\}$, ὅπου x_t εἶναι στὴν πράξη συνήθως ἡ παρατήρηση τὴ χρονικὴ στιγμὴ t καὶ T εἶναι τὸ θεωρούμενο πεδίο μεταβολῆς τοῦ χρόνου. Ἔτσι, μιὰ στοχαστικὴ ἀνέλιξη μπορεῖ κατὰ περίπτωση νὰ ἔχει μιὰ ἀπὸ τὶς ἑξῆς τέσσερις διαφορετικὲς φυσικὲς σημασίες[14]:

1. Γιὰ $t \in T$ καὶ $\omega \in \Omega$ μεταβλητές, παριστᾶ μιὰ οἰκογένεια συναρτήσεων τοῦ χρόνου.

2. Γιὰ t μεταβλητὴ καὶ ω σταθερά, παριστᾶ μιά, μόνη, συνάρτηση τοῦ χρόνου.

3. Γιὰ t σταθερὰ καὶ ω μεταβλητή, παριστᾶ μιὰ τυχαία μεταβλητή.

καὶ 4. Γιὰ t σταθερὰ καὶ ω σταθερά, παριστᾶ ἕναν, μόνον, ἀριθμό.

Οἱ στοχαστικὲς ἀνελίξεις ποὺ ἔχουν χρησιμοποιηθεῖ μέχρι σήμερα στὶς θεωρίες τῆς Χημικῆς Κινητικῆς εἶναι ἢ ἀνάγονται σὲ εἰδικὲς περιπτώσεις τῶν ἀνελίξεων Markov· αὐτὲς τὶς ἀνελίξεις τὶς ἐμπνεύσθηκε[15] ὁ Ρῶσσος Μαθηματικὸς A.A. Markov (1856-1922) παρατηρώντας τὶς ἐναλλαγὲς φωνηέντων καὶ συμφώνων στὴν ποιητικὴ νουβέλα τοῦ Pushkin «Εὐγένιος Ὀνιέγκιν» καὶ στὸ διήγημα τοῦ Aksakov «Τὰ παιδικὰ χρόνια τοῦ ἐγγονοῦ τοῦ Μπαγκρώφ»[16]. Ἡ αὐστηρὰ θεμελίωση τῆς γενικῆς θεωρίας τῶν ἀνελίξεων Markov ἔγινε ἀπὸ τὸν Kolmogorov[17].

Διαισθητικὰ μποροῦμε νὰ προσεγγίσουμε τὴν ἔννοια τῶν ἀνελίξεων Markov ὡς ἑξῆς:

Κατὰ τὸ χρονικὸ διάστημα $[o, \zeta)$ ἕνα σωματίδιο μετακινεῖται κατὰ τρόπο τυχαῖο μέσα σὲ ἕνα χῶρο E. Ἔστω ὅτι, ἂν ἡ κατάσταση τοῦ σωματιδίου εἶναι γνωστὴ τὴ χρονικὴ στιγμὴ t, τότε οἱ συμπληρωματικὲς πληροφορίες ἐπὶ τῶν φαινομένων ποὺ παρατηρήθηκαν πρὶν τὴν t (καὶ μάλιστα, εἰδικότερα οἱ πληροφορίες οἱ σχετικὲς μὲ τὸ χαρακτήρα τῆς κινήσεως πρὶν τὴν t) δὲν ἀσκοῦν ἐπίδραση ἐπὶ τῶν προβλέψεων τῶν σχετικῶν μὲ τὴν κίνηση μετὰ τὴν t, δηλαδὴ γιὰ δεδομένο «παρόν», τό «μέλλον» καὶ τό «παρελθόν» εἶναι ἀνεξάρτητα μεταξύ τους. Ὁ χρόνος ζ, ποὺ θὰ σταματήσει ἡ κίνηση, μπορεῖ καὶ αὐτὸς ἀκόμη νὰ εἶναι τυχαῖος.

Γιὰ νὰ ὁρίσουμε αὐστηρὰ τὴν ἔννοια τῶν ἀνελίξεων Markov, ἄς ὑποθέσουμε ὅτι ἔχουμε:

i) μιὰ συνάρτηση $\zeta(\omega)$ ὁρισμένη σὲ ἕναν ὁποιοδήποτε χῶρο Ω, ἡ ὁποία παίρνει τιμὲς μὴ ἀρνητικές· ἡ $\zeta(\omega)$ μπορεῖ νὰ πάρει καὶ τὴν τιμὴ $+\infty$

ii) μιὰ συνάρτηση $x(t, \omega) := x_t(\omega)$ ὁρισμένη γιὰ $\omega \in \Omega$ καὶ $t \in [0, \zeta(\omega))$, ἡ ὁποία παίρνει τὶς τιμές της μέσα σὲ ἕνα μετρήσιμο χῶρο (E, F). Θεωροῦμε ὅτι ἡ σ-ἄλγεβρα F περιλαμβάνει ὅλα τὰ ὑποσύνολα τοῦ E ποὺ ἀποτελοῦνται ἀπὸ ἕνα μόνο σημεῖο.

iii) γιὰ κάθε s $(0 \leqslant s \leqslant t)$, μιὰ σ-ἄλγεβρα M_t^s ἐπὶ τοῦ χώρου

$$\Omega_t = \{\omega : \zeta(\omega) > t\}$$

iv) γιὰ κάθε $s \geqslant 0$ καὶ κάθε $x \in E$, μιὰ συνάρτηση $P_{s,x}(\Sigma)$ ὁρισμένη σὲ μιὰ σ-ἄλγεβρα M^s ἐπὶ τοῦ χώρου Ω, ποὺ περιέχει τὴν M_t^s γιὰ κάθε $t \geqslant s$.

Θὰ λέμε ὅτι αὐτὰ τὰ στοιχεῖα ὁρίζουν τὴν ἀνέλιξη Markov

$$X = (x_t, \zeta, M_t^s, P_{s,x})$$

ἂν πληροῦνται οἱ ἑξῆς συνθῆκες:

α) Ἂν $s \leqslant t \leqslant u$ καὶ $\Sigma \in M_t^s$ τότε $\{\Sigma, \zeta > u\} \in M_u^s$

β) $\{x_t \in \Gamma\} \in M_t^s$ γιὰ κάθε $0 \leqslant s \leqslant t$ καὶ κάθε $\Gamma \in F$.

Γιὰ $\Gamma = E$ ἔχουμε, εἰδικά, $\{\zeta > t\} \in M_t$ γιὰ κάθε s $(0 \leqslant s \leqslant t)$

γ) $P_{s,x}$ εἶναι μιὰ πιθανότητα ἐπὶ τῆς σ-ἄλγεβρας M^s

δ) Γιὰ κάθε $0 \leqslant s \leqslant t$ καὶ κάθε $\Gamma \in F$ ἡ $P'(s, x \cdot t, \Gamma) = P_{s,x}\{x_t \in \Gamma\}$ εἶναι μιὰ F-μετρήσιμη συνάρτηση τῆς x

ε) $P'(s, x \cdot s, E - x) = 0$

καὶ

στ) Ἂν $0 \leqslant s \leqslant t \leqslant u$, $x \in E$ καὶ $\Gamma \in F$, τότε

$$P_{s,x}\{x_u \in \Gamma \mid M_t^s\} = P'(t, x_t \cdot u, \Gamma)$$

Τὸ σύνολο Ω λέγεται χῶρος ἐνδεχομένων, ὁ μετρήσιμος χῶρος (E, F) λέγεται χῶρος καταστάσεων καὶ ἡ συνάρτηση $P'(s, x \cdot t, \Gamma)$ λέγεται συνάρτηση μεταβάσεως τῆς ἀνελίξεως X. Γιὰ δεδομένο w, ἡ συνάρτηση $x_t(\omega)$ $(t \in [0, \zeta(\omega)])$ ὁρίζει στὸ χῶρο E μιὰ πραγματοποίηση τῆς ἀνελίξεως ἀντιστοιχοῦσα στὸ ἐνδεχόμενο ω. Ἡ σ-ἄλγεβρα M_t^s ἑρμηνεύεται σὰν τὸ σύνολο τῶν συμβάντων ποὺ παρατηροῦνται στὸ χρονικὸ διάστημα $[s, t]$. Ἡ $P_{s,x}(\Sigma)$ $(\Sigma \in M^s)$ ἑρμηνεύεται σὰν πιθανότητα τοῦ συμβάντος Σ ὑπὸ τὴ συνθήκη ὅτι τὴ χρονικὴ στιγμὴ s τὸ σωματίδιο εὑρίσκετο στὴν κατάσταση ποὺ καθορίζεται ἀπὸ τὸ σημεῖο x τοῦ χώρου καταστάσεων.

Ἂν καὶ ὁ παραπάνω αὐστηρὸς ὁρισμὸς τῶν ἀνελίξεων Markov μπορεῖ νὰ γενικευθεῖ ἀκόμη παραπέρα, ἀρκεῖ, ὥστε ἀπὸ Μαθηματικῆς μὲν ἀπόψεως νὰ δείξει ὅτι ἡ ἐξομοίωση μιᾶς ἀνελίξεως Markov πρὸς μιὰ στοχαστικὴ συνάρτηση κάποιας εἰδικῆς μορφῆς εἶναι μιὰ ἀντίληψη ἀνεπαρκὴς γιὰ τὴν ἀνάπτυξη τῆς θεωρίας, ἀπὸ Φυσικοχημικῆς δὲ ἀπόψεως νὰ ὑπερκαλύπτει ὅλες τὶς εἰδικὲς μορφὲς ἀνελίξεων Markov, ποὺ ἔχουν χρησιμοποιηθεῖ στὴ στοχαστικὴ Χημικὴ Κινητική.

Γιὰ τὴ στοχαστικὴ Κινητικὴ ἀρκεῖ ἡ θέση ὅτι ἀνέλιξη Markov λέγεται μιὰ στοχαστικὴ ἀνέλιξη $\{x_t, t \in T\}$, ἄν γιὰ κάθε $v = 1, 2, 3, \ldots$ καὶ ὁποιαδήποτε $t_i \in T$ $(i = 0, 1, \ldots, v)$, μὲ τὸ $t_0 < t_1 < \ldots < t_v$, ἡ δεσμευμένη κατανομὴ τῆς $x(t_v)$ δ θεισῶν τῶν $x(t_o), \ldots, x(t_{v-1})$ εἶναι ἡ αὐτὴ μὲ τὴ δεσμευμένη κατανομὴ τῆς $x(t_v)$ δοθείσης μόνον τῆς $x(t_{v-1})$, δηλαδή, φορμαλιστικά, ἄν γιὰ κάθε $x_o, x_1, \ldots, x_v$ καὶ κάθε $v = 1, 2, \ldots$, ἰσχύει ἡ σχέση $P\left[x(t_v) \leqslant x_v \mid x(t_{v-1}) = x_{v-1}, x(t_{v-2}) = x_{v-2}, \ldots, x(t_o) = x_o\right] = P\left[x(t_v) \leqslant x_v \mid x(t_{v-1}) = x_{v-1}\right]$.

Τὸ ἁπλούστερο παράδειγμα στοχαστικῆς θεωρίας τῆς Χημικῆς Κινητικῆς εἶναι ἡ θεωρία Bartholomay[10] γιὰ τὶς μονόδρομες μονομοριακὲς στοιχειώδεις ἀντιδράσεις τοῦ γενικοῦ τύπου $A \rightarrow B$. Κατὰ τὴ θεωρία Bartholomay, ἡ Κινητικὴ τῶν ἀντιδράσεων αὐτοῦ τοῦ τύπου περιγράφεται ἀπὸ μιὰ γραμμικὴ ἀνέλιξη γεννήσεώς καὶ θανάτου[18] ὡς ἑξῆς:

Ἔστω ὅτι ἡ τυχαία μεταβλητὴ $x(t)$ παριστᾶ τὸν ἀριθμὸ τῶν μορίων τοῦ A στὸ ἀντιδρῶν σύστημα κατὰ τὴ χρονικὴ στιγμὴ t καὶ ὅτι

(1) ἡ πιθανότητα μεταβάσεως $(x) \rightarrow (x-1)$ στὸ χρονικὸ διάστημα $(t, t+\Delta t)$ εἶναι $kx\Delta t + O(\Delta t)$, ὅπου k εἶναι μιὰ σταθερὰ καὶ τὸ $O(\Delta t)$ σημαίνει[19] ὅτι $\dfrac{O(\Delta t)}{\Delta t} \rightarrow 0$ γιὰ $\Delta t \rightarrow 0$. [Δηλαδή: ἡ πιθανότητα τοῦ νὰ μετατραπεῖ ἕνα (ἐκ τῶν x τὸ πλῆθος) μόριο τοῦ A, σὲ μόριο τοῦ B κατὰ τὸ μικρὸ χρονικὸ διάστημα μεταξὺ t καὶ $t + \Delta t$, εἶναι ἀνάλογη αὐτοῦ τοῦ μικροῦ χρονικοῦ διαστήματος]

(2) ἡ πιθανότητα μεταβάσεως $(x) \rightarrow (x-j)$, $j > 1$, στὸ διάστημα $(t, t+\Delta t)$ εἶναι τὸ πολὺ $O(\Delta t)$. [Δηλαδή: τὸ χρονικὸ διάστημα Δt θεωρεῖται ὅτι εἶναι ἀρεκτὰ μικρό, ὥστε μόνον ἕνα μόριο τοῦ A νὰ μετατρέπεται σὲ μόριο τοῦ B μεταξὺ t καὶ $t + \Delta t$ καὶ νὰ μὴν πραγματοποιοῦνται ταυτόχρονες μετατροπὲς περισσοτέρων τοῦ ἑνὸς μορίων τοῦ A πρὸς μόρια τοῦ B].

(3) ἡ πιθανότητα τοῦ νὰ μετατραπεῖ ἕνα μόριο τοῦ B σὲ μόριο τοῦ A εἶναι μηδέν. [Δηλαδή: ἡ ἀντίστροφη ἀντίδραση δὲν πραγματοποιεῖται].

Τότε, ἄν τὴ χρονικὴ στιγμὴ $t = 0$ ὑπῆρχαν μόνον μόρια τοῦ A, ἡ πιθανότητα $P_x(t+\Delta t)$ τοῦ νὰ ὑπάρχουν x τὸν ἀριθμὸ μόρια τοῦ A στὸ ἀντιδρῶν σύστημα τὴ χρονικὴ στιγμὴ $t + \Delta t$ εἶναι:

$$P_x(t+\Delta t) = k\ (x+1)\,\Delta t\ P_{x+1}(t) + (1 - kx\,\Delta t)\ P_x(t) + O(\Delta t)$$

Μεταφέροντας τὸ $P_x(t)$ ἀπὸ τὸ δεύτερο στὸ πρῶτο μέλος αὐτῆς τῆς ἐξισώσεως, διαιρώντας διὰ Δt καὶ παίρνοντας τὸ ὅριο γιὰ $\Delta t \to 0$ (διεργασίες, ποὺ ἡ ἐγκυρότητα τους ἔχει συζητηθεῖ ἀρκετὰ διεξοδικὰ π.χ. ἀπὸ τὸν Van Hove[20]), παίρνουμε τὴ διαφόρο-διαφορικὴ ἐξίσωση

$$\frac{dP_x}{dt} = k\,(x+1)\ P_{x+1}(t) - kxP_x(t)$$

Μέσω τῆς γεννήτριας συναρτήσεως τῆς $P_x(t)$, δηλαδὴ τῆς

$$F(s,\ t) = \sum_{x=0}^{\infty} P_x(t)\,s^x\ ,\ |s| < 1$$

ἡ διαφόρο-διαφορικὴ ἐξίσωση μπορεῖ νὰ μετασχηματισθεῖ στὴ διαφορικὴ ἐξίσωση ὡς πρὸς μερικὲς παραγώγους

$$\frac{\partial F}{\partial t} = k\ (1-s)\frac{\partial F}{\partial s}$$

τῆς ὁποίας ἡ λύση, γιὰ τὴν ὁριακὴ συνθήκη $F(s, 0) = s^{x_0}$ ὅπου x_0 ὁ συνολικὸς ἀριθμὸς μορίων τοῦ συστήματος, εἶναι

$$F(s,\ t) = \left[1 + (s-1)\,e^{-kt}\right]^{x_0}$$

Ἐπειδὴ γιὰ τὴ Μαθηματικὴ ἐλπίδα $E\{X(t)\}$ καὶ τὴ διασπορὰ $D^2\{X(t)\}$ ἰσχύουν προφανῶς οἱ σχέσεις

$$E\ \{X(t)\} = \left(\frac{\partial F}{\partial s}\right)_{s=1}$$

$$\text{καὶ}\ \ D^2\{X(t)\} = \left(\frac{\partial^2 F}{\partial s^2}\right)_{s=1} + \left(\frac{\partial F}{\partial s}\right)_{s=1} - \left(\frac{\partial F}{\partial s}\right)^2_{s=1}$$

προκύπτει ὅτι ἐν προκειμένῳ θὰ ἔχουμε

$$E\ \{X(t)\} = x_0\,e^{-kt}$$

$$\text{καὶ}\ \ D^2\{X(t)\} = x_0\,e^{-kt}(1 - e^{-kt})$$

Παρατηροῦμε ὅτι ἡ μέση τιμὴ τῆς στοχαστικῆς θεωρίας συμπίπτει μὲ τὸ ἀποτέλεσμα τῆς ντετερμινιστικῆς θεωρίας, δηλαδὴ ὅτι οἱ δύο θεωρίες «εἶναι συμβιβαστὲς κατὰ τὸν μέσο»· ὅμως, ἡ στοχαστικὴ θεωρία δίνει καὶ ροπὲς ἀνωτέρας τάξεως, ὁπότε ἔτσι εἰσάγεται στὴ Χημικὴ Κινητικὴ καὶ ἡ διαπραγμάτευση τῶν διαφόρων θεωρητικὰ ἀναμενομένων καὶ πειραματικὰ διαπιστουμένων διακυμάνσεων[9] τῶν ποσοτήτων τῶν ἀντιδρώντων καὶ τῶν προϊόντων, οἱ ὁποῖες πάντως γιὰ τὶς πιὸ πολλὲς ἀντιδράσεις εἶναι πρακτικὰ ἀμελητέες.

Αὐτὴ ἡ στοχαστικὴ θεωρία τοῦ Bartholomay (ποὺ ἕνα ἀπὸ τὰ πρῶτα μοντέλα της ὑπῆρξαν οἱ ἀντιδράσεις ραδιενεργῶν διασπάσεων) γενικεύτηκε παραπέρα ἀπὸ τὸν Ishida[21], τὸν Mc Quarrie[22], κ.ἄ, ὥστε νὰ καλύπτει χαλαρότερους περιορισμούς, ὅπως π.χ. ἀμφίδρομη διεξαγωγὴ τῆς ἀντιδράσεως (δηλαδή: A, B ἀντὶ $A \rightarrow B$), μεταβαλλομένη συναρτήσει τοῦ χρόνου εἰδικὴ ταχύτητα τῆς ἀντιδράσεως (δηλαδή: $k(t)$ ἀντὶ k) κ.τ.λ.

Ἐνῶ, ὅμως, σὲ περιπτώσεις σὰν τὶς παραπάνω εἶναι δυνατὴ ἡ ἀκριβὴς ἐπίλυση τῶν διαφόρο-διαφορικῶν ἐξισώσεων τῶν στοχαστικῶν θεωριῶν, σὲ περιπλοκότερες καταστάσεις, ποὺ ἐμφανίζονται κατὰ τὴ ρεαλιστικότερη θεώρηση καὶ αὐτῶν τῶν μονομοριακῶν στοιχειωδῶν ἀντιδράσεων (π.χ. Kim[23], Osipov καὶ Stupochenko[24], κ.ἄ.), εἶναι δυνατὴ μόνον (ἢ ἐνίοτε δὲν ἔχει ἀκόμη μελετηθεῖ οὔτε κἂν κι αὐτή) ἡ προσεγγιστικὴ ἐπίλυση τῶν προκυπτουσῶν διαφόρο-διαφορικῶν ἐξισώσεων. Πιστεύεται, πάντως, ὅτι μὲ τὴν ἐξάπλωση τῆς στοχαστικῆς μεθοδολογίας τέτοιες δυσκολίες, ποὺ ὀφείλονται καθαρὰ καὶ μόνον στὸ ὅτι δὲν ἔχουν ἀκόμη χρησιμοποιηθεῖ συστηματικὰ καὶ σὲ μεγάλη κλίμακα οἱ στοχαστικὲς ἀνελίξεις στὴ Χημικὴ Κινητική, θὰ ξεπεραστοῦν γρήγορα.

Ἂν τώρα ἀντιπαραβάλλουμε τὶς στοχαστικές (ὅπου ἔχουν ἤδη ἐφαρμοσθεῖ) πρὸς τὶς ἀντίστοιχες ντετερμινιστικὲς θεωρίες τῆς Χημικῆς Κινητικῆς, μποροῦμε νὰ ἐπισημάνουμε ὅτι:

— οἱ συναρτήσεις μεταβάσεως καὶ οἱ ἐπιλύσεις τῶν διαφόρο-διαφορικῶν ἐξισώσεων τῶν στοχαστικῶν θεωριῶν καταστρώνονται ὥστε νὰ πληροῦνται οἱ ἀρχὲς καὶ οἱ κανόνες (δηλαδή: τὰ «ἀξιώματα») τῶν ἀντιστοίχων ντετερμινιστικῶν θεωριῶν. Ἔτσι, π.χ. γιὰ μιὰ ἀντίδραση ποὺ χωρεῖ μέσω συστοιχίας στοιχειωδῶν ἀντιδράσεων, στὴ διαμόρφωση τῆς συναρτήσεως μεταβάσεως καὶ τὴν ἐπίλυση τῶν διαφόρο-διαφορικῶν ἐξισώσεων μιᾶς στοχαστικῆς θεωρίας τῆς κινητικῆς της, θὰ πρέπει νὰ ληφθοῦν ὑπ' ὄψη καὶ νὰ καλυφθοῦν καὶ οἱ περιπτώσεις ἰσχύος τῆς ἀρχῆς τῆς μικροσκοπικῆς ἀντιστρεψιμότητας, τοῦ λεπτομερειακοῦ ἰσοζυγίου, τῆς στασίμου καταστάσεως ὡς πρὸς κατάλληλα ἐνδιάμεσα, τῆς ὑπάρξεως καταλλήλου συναρτήσεως Liapounov[25] καὶ τῶν ἀρχῶν διατηρήσεως. Ἐπὶ πλέον, μιὰ στοχαστικὴ θεωρία τῆς Χημικῆς Κινητικῆς εἶναι στὸ σύνολο της δεσμία τῶν ἰδιοτήτων ποὺ διέπουν καὶ κάθε στοχαστικὴ θεωρία[26].

— οἱ στοχαστικὲς θεωρίες ἀνταποκρίνονται φυσικότερα καὶ ἐκφράζουν ἀμεσότερα τὸν ἔμφυτο στατιστικὸ χαρακτήρα τῶν χημικῶν ἀντιδράσεων παρὰ οἱ ντετερμινιστικὲς θεωρίες.

— ἐνῶ κατὰ τὶς ντετερμινιστικὲς θεωρίες ἡ συγκέντρωση (ἤ: ὁ ἀριθμὸς μορίων) δεδομένου χημικοῦ εἴδους εἶναι συνεχὴς πραγματικὴ συνάρτηση τοῦ χρόνου, χωρὶς προβλεπόμενες ἀποκλίσεις ἀπὸ τὶς προκαθοριζόμενες τιμές της, στὶς στοχαστικὲς θεωρίες εἶναι διακριτὴ ἀκέραιη τυχαία μεταβλητὴ καὶ ἡ κινητικὴ περιγράφεται ἀπὸ τὴν συνάρτηση πυκνότητας πιθανότητας αὐτῆς τῆς τυχαίας μεταβλητῆς. Ἡ Μαθηματικὴ ἐλπίδα τῆς ἀντίστοιχης κατανομῆς θὰ ἐκφράζει τότε τὴν συγκέντρωση καὶ ἡ διασπορὰ θὰ χαρακτηρίζει τὴν σύμφυτη μὲ τὴν ἀντίδραση στατιστικὴ διακύμανση της στὴν γειτονιὰ τῆς Μαθηματικῆς ἐλπίδας.

— οἱ ντετερμινιστικὲς θεωρίες ἀποδίδουν τὰ τυχαῖα σφάλματα ἀποκλειστικὰ καὶ μόνο στὶς ἐν γένει ἀδυναμίες τῆς πειραματικῆς διαδικασίας σπουδῆς τῆς κινητικῆς, ἐνῶ οἱ στοχαστικὲς θεωρίες δέχονται ὅτι λόγω τοῦ στατιστικοῦ χαρακτήρα τῶν χημικῶν ἀντιδράσεων πρέπει νὰ ὑπάρχουν ἀποκλίσεις, τὶς ὁποῖες καὶ προβλέπουν καὶ προσπαθοῦν νὰ τοὺς δώσουν ἑρμηνεία σχετικὴ μὲ αὐτὴν ταύτην τὴν ἀντίδραση καὶ ὄχι μὲ τὸν τρόπο πειραματικῆς διεξαγωγῆς της.

— ὑπάρχουν περιπτώσεις ποὺ οἱ ντετερμινιστικὲς θεωρίες δὲν μποροῦν νὰ ἐφαρμοσθοῦν καὶ ἀντιμετωπίζονται ἀποκλειστικὰ καὶ μόνο μὲ στοχαστικὴ μεθοδολογία[27].

— οἱ στοχαστικὲς καὶ οἱ ντετερμινιστικὲς θεωρίες εἶναι «συμβιβαστὲς κατὰ τὸν μέσο» τόσο περισσότερο ὅσο μικρότερη εἶναι ἡ τάξη τῆς ἀντιδράσεως καὶ ὅσο μεγαλύτερος εἶναι ὁ ἀριθμὸς τῶν μορίων τοῦ ἀντιδρῶντος συστήματος.

— οἱ στοχαστικὲς θεωρίες «περιέχουν», κατὰ κάποιον τρόπο, σὰν εἰδικὲς περιπτώσεις τους τὶς ντετερμινιστικές.

— ἡ στοχαστικὴ μεθοδολογία γιὰ τὴ Χημικὴ Κινητικὴ εἶναι, ὅτι ἡ στατιστικὴ μεθοδολογία γιὰ τὴ Θερμοδυναμική.

Μιὰ στοχαστικὴ θεωρία γιὰ μὴ στοιχειώδεις ἀντιδράσεις

Ἄς θεωρήσουμε τὴ χημικὴ ἀντίδραση ποὺ διεξάγεται μέσω τριῶν στοιχειωδῶν ἀντιδράσεων κατὰ τὸ μηχανισμὸ

$$A + B \underset{k_2}{\overset{k_1}{\rightleftarrows}} AB$$

$$AB \overset{k_3}{\longrightarrow} A + \Pi$$

καὶ ὅτι ἡ ντετερμινιστική-μακροσκοπικὴ κινητική της ἔχει ὡς ἑξῆς:

$$\frac{d[AB]}{dt} = k_1 [A][B] - k_2 [AB] - k_3 [AB]$$

$$\frac{d[\Pi]}{dt} = k_3 [AB]$$

καί $$\frac{d[A]}{dt} = -k_1 [A][B] + k_2 [AB] + k_3 [AB]$$

Δοθέντος ὅτι

$$[A_O] = [A] + [AB]$$

καί $$[B_O] = [B_0] + [AB] + [\Pi]$$

ὅπου A_O καὶ B_O οἱ ἀρχικές (t = O) συγκεντρώσεις τῶν A καὶ B ἀντιστοίχως, ἄν δεχθοῦμε στάσιμη κατάσταση ὡς πρὸς AB, δηλαδὴ

$$\frac{d[AB]}{dt} \simeq 0$$

τότε

$$k_1 \left([A_O] - [AB] \right) [B] = (k_2 + k_3) [AB]$$

καὶ κατὰ συνέπεια

$$\upsilon \frac{d[\Pi]}{dt} = \frac{k_3 [A_O] [B]}{\frac{k_2 + k_3}{k_1} + [B]}$$

Θὰ ἐπιχειρήσουμε μιὰ στοχαστική-μακροσκοπικὴ σπουδὴ τῆς κινητικῆς αὐτῆς τῆς ἀντιδράσεως.

Γι' αὐτὸ τὸ σκοπὸ ἂς ὑποθέσουμε ὅτι, ἄν διαθέτουμε ἀπὸ ἕνα μόριο ἀπὸ τὰ A, B καὶ AB, τότε:

— ἡ πιθανότητα σχηματισμοῦ ἑνὸς μορίου AB στὸ χρονικὸ διάστημα (t, t + Δt) εἶναι $\lambda_1 \Delta t + O(\Delta t)$.

— ἡ πιθανότητα ἀποσυνθέσεως τοῦ AB κατὰ τὴ στοιχειώδη ἀντίδραση $AB \rightarrow A + B$ στό (t + Δt) εἶναι $\lambda_2 \Delta t + O(\Delta t)$.

— ἡ πιθανότητα διασπάσεως τοῦ AB κατὰ τὴ στοιχειώδη ἀντίδραση $AB \rightarrow A + \Pi$ στό (t + Δt) εἶναι $\lambda_3 \Delta t + O(\Delta t)$.

— ἡ πιθανότητα τοῦ νὰ μὴν συμβεῖ καμία ἀπὸ τὶς παραπάνω στοιχειώδεις ἀντιδράσεις στό (t + Δt) εἶναι $1 - \lambda_1 \Delta t - (\lambda_2 + \lambda_3) \Delta t + O(\Delta t)$.

— ἡ πιθανότητα τοῦ νὰ συμβοῦν περισσότερες ἀπὸ μιὰ ἀπὸ τὶς παραπάνω στοιχειώδεις ἀντιδράσεις στό $(t + \Delta t)$ εἶναι $O(\Delta t)$.

— εἶναι $\lambda_1 > \lambda_3 < \lambda_2$

— ἡ δλη ἀντίδραση γίνεται ὑπὸ σταθερὸν ὄγκο καὶ σταθερὴ θερμοκρασία.

Ἂν τώρα n_{10} καὶ n_{20} εἶναι οἱ ἀριθμοὶ τῶν μορίων τοῦ A καὶ τοῦ B ἀντιστοίχως πρὶν τὴν ἔναρξη τῆς ἀντιδράσεως καὶ $n_1'(t) := n_1'$, $n_2'(t) := n_2'$, $n_3'(t) := n_3'$ καὶ $n_4'(t) := n_4'$ εἶναι οἱ ἀριθμοὶ τῶν μορίων τοῦ A, τοῦ B, τοῦ AB καὶ τοῦ Π κατὰ τὴ δεδομένη χρονικὴ στιγμὴ t ἀπὸ τὴν ἔναρξη τῆς ἀντιδράσεως, τότε προφανῶς θὰ ἰσχύουν οἱ σχέσεις

$$n_{10} = n_1'(t) + n_3'(t) \tag{1}$$

$$n_{20} = n_2'(t) + n_3'(t) + n_4'(t) \tag{2}$$

Λόγω τῶν (1) καί (2), ἀρκεῖ νὰ ἐξετάσουμε μόνο τὶς τυχαῖες μεταβλητὲς $n_2(t)$, $n_3(t)$ ἢ ὁποιοδήποτε ἄλλο ζεῦγος πλὴν τῶν (n_1, n_3) καί (n_2, n_4). Ἂν ἐπιλέξουμε τὸ ζεῦγος (n_2, n_3), τότε οἱ μεταβάσεις μὲ μὴ μηδενικὲς πιθανότητες θὰ εἶναι:

Μετάβαση t	t + Δt	Στοιχειώδης ἀντίδραση	Πιθανότητα
$(n_2 + 1, n_3 - 1)$	(n_2, n_3)	$A + B \rightarrow AB$	$\lambda_1 (n_2 + 1)(n_{10} - n_3 + 1)\Delta t + O(\Delta t)$
$(n_2 - 1, n_3 + 1)$	(n_2, n_3)	$AB \rightarrow A + B$	$\lambda_2 (n_3 + 1)\Delta t + O(\Delta t)$
$(n_2, n_3 + 1)$	(n_2, n_3)	$AB \rightarrow A + \Pi$	$\lambda_3 (n_3 + 1)\Delta t + O(\Delta t)$
(n_2, n_3)	(n_2, n_3)	καμιά	$1 - \lambda_1 n_2 (n_{10} - n_3)\Delta t - (\lambda_2 + \lambda_3) n_3 \Delta t + O\Delta(t)$

Ἂν $p(n_2, n_3 \cdot t)$ εἶναι ἡ πιθανότητα ὥστε t χρονικὲς μονάδες μετὰ τὴν ἔναρξη τῆς ἀντιδράσεως νὰ ὑπάρχουν n_2 καὶ n_3 μόρια τῶν B καὶ AB ἀντιστοίχως, τότε

$$\begin{aligned} p(n_2, n_3 \cdot t + \Delta t) = {} & p(n_2, n_3 + 1 \cdot t)\lambda_3 (n_3 + 1)\Delta t + p(n_2 - 1, n_3 + 1 \cdot t)\lambda_2 \\ & (n_3 + 1)\Delta t + p(n_2 + 1, n_3 - 1 \cdot t)\lambda_1 (n_{10} - n_3 + 1)\Delta t + \\ & + p(n_2, n_3 \cdot t)\left[1 - \lambda_1 n_2 (n_{10} - n_3)\Delta t - (\lambda_2 + \lambda_3) n_3 \Delta t\right] \end{aligned}$$

ὁπότε

$$\begin{aligned} \frac{d}{dt} p(n_2, n_3 \cdot t) = {} & \lambda_3 (n_3 + 1) p(n_2, n_3 + 1 \cdot t) + \lambda_2 (n_3 + 1) p(n_2 - 1, n_3 + \\ & + 1 \cdot t) + \lambda_1 (n_2 + 1)(n_{10} - n_3 + 1) p(n_2 + 1, n_3 - 1 \cdot t) - \\ & - \lambda_1 n_2 (n_{10} - n_3) p(n_2, n_3 \cdot t) - \\ & - (\lambda_2 + \lambda_3) n_3 p(n_2, n_3 \cdot t) \end{aligned} \tag{3}$$

Ὁρίζουμε τὴ γεννήτρια συνάρτηση

$$\varphi\,(s_2, s_3 \cdot t) = \sum_{n_3=0}^{n_{10}} \sum_{n_2=0}^{n_{20}} p\,(n_2, n_3 \cdot t)\, s_2^{n_2} s_3^{n_3},$$

$$\mu\grave{\varepsilon}\ |\, s_i \,| \leqslant 1, \quad i = 1, 2 \tag{4}$$

Ἂν πολλαπλασιάσουμε τὴ διαφόρο-διαφορικὴ ἐξίσωση (3) ἐπὶ $s_2^{n_2} s_3^{n_3}$ καὶ ἀθροίσουμε γιὰ τὰ n_2 καὶ n_3 θὰ ἔχουμε

$$\frac{\partial \varphi}{\partial t} = \left\{\lambda_3 + \lambda_2 s_2 - (\lambda_2 + \lambda_3) s_3\right\} \frac{\partial \varphi}{\partial s_3} + \lambda_1 n_{10} (s_3 - s_2) \frac{\partial \varphi}{\partial s_2}$$

$$+ \lambda_1 s_3 (s_2 - s_3) \frac{\partial^2 \varphi}{\partial S_2 \, \partial S_3} \tag{5}$$

Γιὰ νὰ λύσουμε τήν (5), ἅς ὑποθέσουμε ὅτι $n_{10} \gg n_3$ κάτι ποὺ δικαιολογεῖται τοὐλάχιστον στὴν ἀρχὴ τῆς διεξαγωγῆς τῆς ἀντιδράσεως καὶ ποὺ στὴν πραγματικότητα ἰσχύει γιὰ κάθε t ἄν $\lambda_2 > \lambda_1 \gg \lambda_3$ καὶ $\lambda_4 \ll \lambda_3$, ὅπου αὐτὴ ἡ τελευταία σχέση ἀποδίδει τὸ ὅτι ἡ ἀντίδραση Α + Π ⟶ ΑΒ μπορεῖ νὰ ἀγνοεῖται ἀκόμη καὶ σὲ μεγάλους χρόνους.

Ἔτσι, θὰ ἔχουμε

$$n_{10} - n_3 \simeq n_{10} \tag{6}$$

ὁπότε ἡ (3) δίνει

$$\frac{d}{dt} p\,(n_2, n_3 \cdot t) = \lambda_3 (n_3 + 1)\, p\,(n_2, n_3 + 1 \cdot t) + \lambda_2 (n_3 + 1)\, p\,(n_2 - 1, n_3 + 1 \cdot t) + \lambda_1 n_{10} (n_2 + 1)\, p\,(n_2 + 1, n_3 - 1 \cdot t) - \lambda_1 n_{10} n_2\, p\,(n_2 n_3 \cdot t) - (\lambda_2 + \lambda_3)\, n_3\, p\,(n_2, n_3 \cdot t) \tag{7}$$

καὶ κατὰ συνέπεια

$$\frac{\partial \varphi}{\partial t} = \left\{\lambda_3 + \lambda_2 s_2 - (\lambda_2 + \lambda_3) s_3\right\} \frac{\partial \varphi}{\partial s_3} + \lambda_1 n_{10} (s_3 - s_2) \frac{\partial \varphi}{\partial s_2} \tag{8}$$

Τὸ συνοδεῦον σύστημα τῆς (8) εἶναι

$$dt = \frac{ds_2}{\lambda_1 n_{10} (s_2 - s_3)} = \frac{ds_3}{(\lambda_2 + \lambda_3) s_3 - \lambda_2 s_2 - \lambda_3 s_3} = \frac{d\varphi}{0} \tag{9}$$

Ἀπὸ τό (9) ἔχουμε ὅτι

$$\varphi = c_1, \qquad \text{ὅπου } c_1 \text{ μιὰ σταθερά,} \tag{10}$$

καὶ

$$\frac{ds_2}{dt} = \lambda_1 n_{10} (s_2 - s_3)$$

$$\frac{ds_3}{dt} = (\lambda_2 + \lambda_3) s_3 - \lambda_2 s_2 - \lambda_3$$

ποὺ μπορεῖ νὰ γραφεῖ ὡς

$$S' = \Lambda S + \lambda \tag{11}$$

ὅπου

$$S = \begin{bmatrix} s_2 \\ s_3 \end{bmatrix}, \quad S' = \begin{bmatrix} \frac{ds_2}{dt} \\ \frac{ds_3}{dt} \end{bmatrix}, \quad \Lambda = \begin{bmatrix} \lambda_1 n_{10} & -\lambda_1 n_{10} \\ -\lambda_2 & \lambda_2 + \lambda_3 \end{bmatrix} \text{ καὶ } \lambda = \begin{bmatrix} 0 \\ -\lambda_3 \end{bmatrix}$$

Γιὰ νὰ λύσουμε τήν (11), θὰ λύσουμε πρῶτα τὴν ὁμογενῆ διαφορικὴ ἐξίσωση

$$S' = \Lambda S \tag{12}$$

Πρὸς τοῦτο, ἡ χαρακτηριστικὴ ἐξίσωση γιὰ τὸν πίνακα Λ μᾶς δίνει

$$\mu = \frac{1}{2} \left\{ (\lambda_1 n_{10} + \lambda_2 + \lambda_3) \pm \sqrt{[(\lambda_1 n_{10} + \lambda_2 + \lambda_3)^2 - 4\lambda_1 \lambda_3 n_{10}]} \right\} \tag{13}$$

Ἀλλά, $\lambda_1 > \lambda_3 < \lambda_2$ ὁπότε $\lambda_2 - \lambda_3 > 0$
καὶ $\lambda_i \geqslant 0$ μὲ τοὐλάχιστον ἕνα $\lambda_i > 0$, $i = 1, 2, 3$.
Συνεπῶς ἔχουμε

$$(\lambda_1 n_{10} + \lambda_2 + \lambda_3)^2 - 4\lambda_1 \lambda_3 n_{10} = \lambda_1^2 n_{10}^2 + \lambda 2 + \lambda_3^2 + 2\lambda_2 \lambda_3 + 2\lambda_1 n_{10} (\lambda_2 - \lambda_3) \geqslant 0$$

καὶ ἑπομένως τὰ μ_1 καὶ μ_2 εἶναι πραγματικοὶ καὶ διακεκριμένοι μεταξύ τους.

Ἂν τώρα p_1 καὶ p_2 εἶναι τὰ ἰδιοδιανύσματα ποὺ ἀντιστοιχοῦν στὶς ἰδιοτιμὲς μ_1 καὶ μ_2 ἀντιστοίχως, τότε προφανῶς

$$p_1 = \begin{bmatrix} 1 \\ 1 - \frac{\mu_1}{\lambda_1 n_{10}} \end{bmatrix} \text{ καὶ } \quad p_2 = \begin{bmatrix} 1 \\ 1 - \frac{\mu_2}{\lambda_1 n_{10}} \end{bmatrix}$$

Ἄρα, ἡ λύση τῆς (12) δίνεται ἀπὸ τὴν

$$S_h = e^{t\Lambda} C \tag{14}$$

ὅπου $S_h = \begin{bmatrix} s_{2,h} \\ s_{3,h} \end{bmatrix}$ καὶ C εἶναι ἕνα διάνυσμα 2 × 1 μὲ συνιστῶσες τὶς αὐθαίρετες σταθερὲς c_2 καὶ c_3.

Ἂν τώρα P εἶναι ὁ πίνακας

$$\begin{bmatrix} 1 & 1 \\ D_1 & D_2 \end{bmatrix} \tag{15}$$

ὅπου $D_1 = 1 - \dfrac{\mu_1}{\lambda_1 n_{10}}$ καὶ $D_2 = 1 - \dfrac{\mu_2}{\lambda_1 n_{10}}$ καὶ ἂν $\Delta := P^{-1} \Lambda P$, τότε

$$e^{t\Lambda} = e^{tP\Delta P^{-1}} = Pe^{t\Delta}P^{-1} = P \begin{matrix} e^{\mu_1 t} & 0 \\ 0 & e^{\mu_2 t} \end{matrix} P^{-1} \tag{16}$$

Ἀντικαθιστῶντας τὴ (16) στὴ (14) ἔχουμε

$$S_h = \frac{\lambda_1 n_{10}}{\mu_1 - \mu_2} \begin{bmatrix} D_2 e^{\mu_1 t} - D_1 e^{\mu_2 t} & e^{\mu_2 t} - e^{\mu_1 t} \\ D_1 D_2 (e^{\mu_1 t} - e^{\mu_2 t}) & D_2 e^{\mu_2 t} - D_1 e^{\mu_1 t} \end{bmatrix} \begin{bmatrix} c_2 \\ c_3 \end{bmatrix} \tag{17}$$

Ἐπειδὴ τὸ $S_p = \begin{matrix} 1 \\ 1 \end{matrix}$ εἶναι, προφανῶς, μιὰ μερικὴ λύση τῆς (11), ἕπεται ὅτι ἡ γενικὴ λύση της θὰ δίνεται ἀπὸ τὴν

$$S = S_h + S_p = \begin{bmatrix} s_2 \\ s_3 \end{bmatrix} = \frac{\lambda_1 n_{10}}{\mu_1 - \mu_2} \begin{bmatrix} D_2 e^{\mu_1 t} - D_1 e^{\mu_2 t} & e^{\mu_2 t} - e^{\mu_1 t} \\ D_1 D_2 (e^{\mu_1 t} - e^{\mu_2 t}) & D_2 e^{\mu_2 t} - D_1 e^{\mu_1 t} \end{bmatrix} \begin{bmatrix} c_2 \\ c_3 \end{bmatrix} + \begin{bmatrix} 1 \\ 1 \end{bmatrix} \tag{18}$$

ἀπὸ ὅπου προκύπτει ὅτι

$$s_2 = \frac{\lambda_1 n_{10}}{\mu_1 - \mu_2} \left\{ (D_2 e^{\mu_1 t} - D_1 e^{\mu_2 t}) c_2 + (e^{\mu_2 t} - e^{\mu_1 t}) c_3 \right\} + 1 \tag{19}$$

καὶ

$$s_3 = \frac{\lambda_1 n_{10}}{\mu_1 - \mu_2} \left\{ (D_1 D_2 (e^{\mu_1 t} - e^{\mu_2 t}) c_2 + (D_2 e^{\mu_2 t} - D_1 e^{\mu_1 t}) c_3 \right\} + 1 \qquad (20)$$

Ἀπὸ τίς (19) καί (20) εὑρίσκουμε ὅτι

$$c_2 = \frac{\mu_1 - \mu_2}{\lambda_1 n_{10} (D_2 - D_1)^2} \left[(D_2 e^{-\mu_1 t} - D_1 e^{-\mu_2 t}) (s_2 - 1) - (e^{-\mu_1 t} - e^{-\mu_2 t}) (s_3 - 1) \right] \qquad (21)$$

καί

$$c_3 = \frac{\mu_1 - \mu_2}{\lambda_1 n_{10} (D_2 - D_1)^2} \left[(D_2 e^{-\mu_2 t} - D_1 e^{-\mu_1 t}) (s_3 - 1) - D_1 D_2 (e^{-\mu_2 t} - e^{-\mu_1 t}) (s_2 - 1) \right] \qquad (22)$$

Ἀλλά, ἐπειδὴ ἀπὸ τὴν (10) ἔχουμε $\varphi = c_1$, ἡ πλήρης λύση τῆς (8) δίνεται ἀπὸ τὴν

$\varphi (s_2, s_3 \cdot t) = \psi (c_2, c_3) \mid$ ψ αὐθαίρετη συνάρτηση τῶν c_2 καί c_3, ποὺ ἱκανοποιεῖ τὴν $\varphi (s_2, s_3 \cdot 0) = s_2^{n_{20}}$,

$$= \psi \left\{ \frac{\mu_1 - \mu_2}{\lambda_1 n_{10} (D_2 - D_1)^2} \left[(D_2 e^{-\mu_1 t} - D_1 e^{-\mu_2 t}) (s_2 - 1) - (e^{-\mu_1 t} - e^{-\mu_2 t}) (s_3 - 1) \right], \frac{\mu_1 - \mu_2}{\lambda_1 n_{10} (D_2 - D_1)^2} \left[(D_2 e^{-\mu_2 t} - D_1 e^{-\mu_1 t}) (s_3 - 1) - D_1 D_2 (e^{-\mu_2 t} - e^{-\mu_1 t}) (s_2 - 1) \right] \right\} \qquad (23)$$

Ἡ $\varphi (s_2, s_3 \cdot t)$ ἱκανοποιεῖ τὴν $\varphi (s_2, s_3 \cdot 0) = s_2^{n_{20}}$

ὁπότε
$$s_2^{n_{20}} = \psi \left[\frac{(\mu_1 - \mu_2)(s_2 - 1)}{\lambda_1 n_{10} (D_2 - D_1)}, \frac{(\mu_1 - \mu_2)(s_3 - 1)}{\lambda_1 n_{10} (D_2 - D_1)} \right] \qquad (24)$$

Θέτουμε

$$z_i := \frac{(\mu_1 - \mu_2)(s_i - 1)}{\lambda_1 n_{10} (D_2 - D_1)}, \quad i = 2,3 \qquad (25)$$

ὁπότε

$$s_i = 1 + \frac{\lambda_1 n_{10} z_i (D_2 - D_1)}{\mu_1 - \mu_2}$$

καὶ ἀπὸ τὴν (24) ἔχουμε

$$\psi (z_2, z_3) = \left\{ 1 + \frac{\lambda_1 n_{10} z_2 (D_2 - D_1)}{\mu_1 - \mu_2} \right\}^{n_{20}}$$

ὥστε τελικῶς ἡ γεννήτρια πιθανοτήτων εἶναι

$$\varphi(s_2, s_3 \cdot t) = \psi(c_2, c_3)$$

$$= \left\{1 + \frac{\lambda_1 n_{10}(D_2 - D_1)}{\mu_1 - \mu_2} c_2\right\}^{n_{20}}$$

$$= \left[1 + \frac{\lambda_1 n_{10}(D_2 - D_1)^2}{\mu_1 - \mu_2} \frac{\mu_1 - \mu_2}{\lambda_1 n_{10}(D_2 - D_1)^2} \left\{(D_2 e^{-\mu_1 t} - \right.\right.$$

$$\left.\left. - D_1 e^{-\mu_1 t})(s_2 - 1) - (e^{-\mu_1 t} - e^{-\mu_2 t})(s_3 - 1)\right\}\right]^{n_{20}}$$

$$= \left\{1 + \frac{(D_2 e^{-\mu_1 t} - D_1 e^{-\mu_2 t})(s_2 - 1) - (e^{-\mu_1 t} - e^{-\mu_2 t})(s_3 - 1)}{D_2 - D_1}\right\}^{n_{20}}$$

$$= \left\{1 - \alpha(t) - \beta(t) + \alpha(t) s_2 + \beta(t) s_3\right\}^{n_{20}} \qquad (26)$$

ὅπου

$$\alpha(t) = \frac{\lambda_1 n_{10}}{\mu_1 - \mu_2} \left[\left(1 - \frac{\mu_2}{\lambda_1 n_{10}}\right) e^{-\mu_1 t} - \left(1 - \frac{\mu_1}{\lambda_1 n_{10}}\right) e^{-\mu_2 t}\right] \qquad (27)$$

καὶ

$$\beta(t) = \frac{\lambda_1 n_{10}}{\mu_1 - \mu_2} (e^{-\mu_2 t} - e^{-\mu_1 t}) \qquad (28)$$

Ἔτσι, δείξαμε τὸ ἑξῆς:

Θεώρημα

Γιὰ τὴ θεωρία μας, μὲ $[n_2(t), n_3(t)]$ σὰν τυχαία διανυσματικὴ μεταβλητή, ὅπου $n_2(t)$ καὶ $n_3(t)$ ὁ ἀριθμὸς τῶν μορίων, ὑπὸ σταθερὸν ὄγκο, τῶν Β καὶ ΑΒ ἀντιστοίχως κατὰ τὴ χρονικὴ στιγμὴ t ἀπὸ τῆς ἐνάρξεως τῆς ἀντιδράσεως καὶ τὴν παραδοχὴ ὅτι $n_{10} - n_3(t) \simeq n_{10}$ σὲ κάθε χρονικὴ στιγμὴ t, ἂν μὲ $p(n_2, n_3 \cdot t)$ συμβολίσουμε τὴν πιθανότητα τοῦ νὰ ὑπάρχουν κατὰ τὴν t στιγμὴ n_2 μόρια τοῦ Β καὶ n_3 μόρια τοῦ ΑΒ δοθέντος ὅτι γιὰ $t = 0$ ὑπῆρχαν n_{10}, n_{20}, 0 καὶ 0 μόρια τῶν Α, Β, ΑΒ καὶ Π ἀντιστοίχως καὶ ἂν ὁρίσουμε τὴν γεννήτρια συνάρτηση

$$\varphi(s_2, s_3 \cdot t) = \sum_{n_3=0}^{n_{10}} \sum_{n_2=0}^{n_{20}} p(n_2, n_3 \cdot t) s_2^{n_2} s_3^{n_3}$$

τότε εἶναι

$$\varphi(s_2, s_3 \cdot t) = \left[\alpha(t) s_2 + \beta(t) s_3 + 1 - \alpha(t) - \beta(t)\right]^{n_{20}}$$

ὅπου τὰ α(t) καὶ β(t) δίνονται ἀπὸ τὶς (27) καί (28) ἀντιστοίχως καὶ τὰ μ_1 καὶ μ_2 εἶναι οἱ πραγματικὲς καὶ διακεκριμμένες ρίζες τῆς

$$\mu^2 - \mu(\lambda_1 n_{10} + \lambda_2 + \lambda_3) + \lambda_1 \lambda_3 n_{10} = 0$$

Ἀπὸ τὸ θεώρημά μας αὐτὸ ἔχουμε

$$p(n_2, n_3 \cdot t) = \frac{n_{20}!}{n_2!\, n_3!\, (n_{20} - n_2 - n_3)!} \left\{\alpha(t)\right\}^{n_2} \left\{\beta(t)\right\}^{n_3} \left\{1 - \alpha(t) - \beta(t)\right\}^{n_{20}-n_2-n_3} \qquad (29)$$

Μοντέλα τῆς θεωρίας

Ἡ σημαντικότερη κατηγορία μοντέλων τῆς προηγουμένης θεωρίας προέρχεται ἀπὸ τὴν κινητικὴ τῆς κλάσεως ἐκείνων τῶν ἐνζυμικῶν ἀντιδράσεων, ποὺ χωροῦν διὰ τοῦ μηχανισμοῦ

$$E + S \underset{k_2}{\overset{k_1}{\rightleftharpoons}} ES \overset{k_3}{\rightarrow} E + P$$

κατὰ τὸν ὁποῖο ἕνα ἔνζυμο E ἀντιδρᾶ μὲ ἕνα ὑπόστρωμα S καὶ δίνει κάποιο σύμπλοκο ES, ποὺ διασπᾶται πρὸς τὸ προϊὸν P καὶ ὅπου k_1, k_2 καὶ k_3 εἶναι οἱ ἀντίστοιχες ντετερμινιστικὲς εἰδικὲς ταχύτητες ἀντιδράσεως. Ἡ κινητικὴ αὐτῆς τῆς κλάσεως ἐνζυμικῶν ἀντιδράσεων εἶναι γνωστὴ ὡς κινητικὴ τῶν Michaelis-Menten[28], ἐπειδὴ πρῶτοι αὐτοί, τὸ 1913, τὴν ἀντιμετώπισαν κατὰ τρόπο συστηματικό, ἐνῶ σχετικὲς ἀπόψεις εἶχαν διατυπωθεῖ ἤδη ἀπὸ τοὺς A. Brown[29] τὸ 1902 καὶ V. Henri[30] τὸ 1903.

Κατὰ τὴ ντετερμινιστικὴ-μακροσκοπικὴ θεωρία τῶν Michaelis-Menten, ποὺ στηρίζεται στὴν παραδοχὴ ἀποκαταστάσεως ἰσορροπίας μεταξὺ τοῦ ES καὶ τῶν E καὶ S, ἡ ἀρχικὴ ταχύτητα u_0 αὐτῶν τῶν ἀντιδράσεων δίνεται ἀπὸ τὸν τύπο

$$u_0 = \frac{u_{max}\,[S_0]}{\dfrac{k_2}{k_1} + [S_0]}$$

ὅπου u_{max} ἡ μεγίστη τιμὴ τῆς ταχύτητας, δηλαδὴ $u_{max} = k_3\,[E_0]$ καί $[S_0]$, $[E_0]$ οἱ ἀρχικὲς συγκεντρώσεις τῶν S καὶ E ἀντιστοίχως. Ἀργότερα, τὸ 1925, οἱ Briggs καὶ Haldane[31] κριτικάρισαν τὴν παραδοχὴ τῶν Michaelis-Menten περὶ ὑπάρξεως ἰσορροπίας μεταξὺ τοῦ συμπλόκου ἐνζύμου-ὑποστρώματος καὶ τῶν ἀντιδρώντων, εἰσήγαγαν τὴν παραδοχὴ στασίμου καταστάσεως ὡς πρὸς τὸ ES, δηλαδὴ

$$\frac{d\,[ES]}{dt} \simeq 0$$

καὶ ἀπέδειξαν ὅτι ἡ παραδοχὴ ἰσορροπίας κατὰ Michaelis-Menten ἐστερεῖτο οὐσιαστικῆς σημασίας. Οἱ Briggs-Haldane, στηριζόμενοι στὴν παραδοχὴ στασίμου καταστάσεως (ἡ ὁποία εἶναι γενικὰ ἔγκυρη πλὴν τῆς ἀρχικῆς περιόδου τῆς ἀντιδράσεως, πρὶν ἀποκατασταθεῖ ἡ στάσιμη κατάσταση, καθὼς καὶ πρὸς τὸ τέλος τῆς ἀντιδράσεως, ὅταν πλέον δὲν ἰσχύει ὅτι $[S] \gg [E]$), ἀπέδειξαν διὰ μεθοδολογίας ντετερμινιστικῆς-μακροσκοπικῆς τὴ γενικότερη ἐξίσωση

$$u = \frac{u_{max}\ [S]}{\dfrac{k_2 + k_3}{k_1} + [S]}$$

ἡ ὁποία ὑπερκαλύπτει, σὰν μερικὴ περίπτωση της, τὴν ἀντίστοιχη ἐξίσωση τῶν Michaelis-Menten.

Ἀπὸ τὶς στοχαστικές-μακροσκοπικὲς θεωρίες τῆς κινητικῆς τῶν ἐνζυμικῶν ἀντιδράσεων τοῦ τύπου «ἕνα ὑπόστρωμα-ἕνα προϊόν», ἡ θεωρία τῶν C. Heyde καὶ E. Heyde[32] ἀνεπτύχθη κατὰ διαφορετικὸ τρόπο σὲ ἀναφορὰ πρὸς τὶς τυχαῖες μεταβλητὲς $n_1(t)$, $n_4(t)$ καὶ μὲ χρήση τῆς προσεγγίσεως

$$n_{20} - n_{10} - n_1(t) - n_4 \simeq n_{20} \tag{30}$$

ὁδήγησε στὴ διαμόρφωση τῆς διαφορικῆς ἐξισώσεως

$$\frac{\partial \varphi_H}{\partial t} = \left[-(\lambda_2 + \lambda_3 v)\,u^2 - (\lambda_1 n_{20} - \lambda_2 - \lambda_3)\,u + \lambda_1 n_{20} \right] \frac{\partial \varphi_H}{\partial u}$$
$$- n_{10} \left[\lambda_2 + \lambda_3 - u\,(\lambda_2 + \lambda_3)\,v \right] \varphi_H \tag{31}$$

ὅπου φ_H εἶναι ἡ γεννήτρια συνάρτηση πιθανοτήτων γιὰ τὸ ζεῦγος (n_1, n_4), δηλαδὴ

$$\varphi_H(u, v \cdot t) = \sum_{n_1=0}^{n_{10}} \sum_{n_4=0}^{n_{20}} p\,(n_1, n_4 \cdot t)\,u^{n_1} v^{n_4}$$

Δι' ἐπιλύσεως τῆς (31) οἱ C. Heyde-E. Heyde ἔλαβαν

$$\varphi_H = \varphi_H (u, v \cdot t) =$$

$$= \left[\frac{\{1 - e^{-\lambda_1 n_{20} t [\alpha(v) + \beta(v)]}\} + \lambda \{\alpha(v) + \beta(v) e^{-\lambda_1 n_{20} t} (\alpha(v) + \beta(v))\}}{\alpha(v) + \beta(v)} \right]^{n_{10}}$$

$$\cdot e^{n_{10} t [\lambda_1 n_{20} \alpha(v) - \lambda_2 - \lambda_3]}$$

δπου

$$\alpha(v) = \frac{2(\lambda_2 + \lambda_3) v}{\lambda_1 n_{20} - \lambda_2 - \lambda_3 + [(\lambda_1 n_{20} - \lambda_2 - \lambda_3)^2 + 4\lambda_1 n_{20} (\lambda_2 + \lambda_3 v)]^{1/2}}$$

καὶ

$$\beta(v) = \frac{2(\lambda_2 + \lambda_3 v)}{-\lambda_1 n_{20} + \lambda_2 + \lambda_3 + [(\lambda_1 n_{20} - \lambda_2 - \lambda_3)^2 + 4\lambda_1 n_{20} (\lambda_2 + \lambda_3 v)]^{1/2}}$$

Ἐπίσης, γιὰ τὴν περιθώριο κατανομὴ τοῦ n_1 ἔλαβαν

$$n_1(t) \sim Bi\left[n_{10}, \frac{\lambda_2 + \lambda_3 + \lambda_1 n_{20} e^{-(\lambda_1 n_{20} + \lambda_2 + \lambda_3) t}}{\lambda_1 n_{20} + \lambda_2 + \lambda_3} \right]$$

Τὰ ἀποτελέσματα τῆς στοχαστικῆς θεωρίας, ποὺ ἀναπτύχθηκε παραπάνω, συμφωνοῦν μὲ ἐκεῖνα τῆς θεωρίας τῶν C. Heyde-E. Heyde. Πράγματι, γιὰ τὶς τιμὲς τοῦ t ποὺ ἡ παραδοχὴ (30) τῶν C. Heyde-E. Heyde συμφωνεῖ μὲ τὴν παραδοχὴ (6), ἡ ἀπόδειξη τῆς συμφωνίας τῶν δύο θεωριῶν ἔχει ὡς ἑξῆς:

Κατὰ τὴ στοχαστικὴ θεωρία ποὺ ἀναπτύχθηκε ἔχουμε

$$n_3(t) \sim Bi(n_{20}, \beta(t))$$

Ἂν

$$\{\varphi_{n_1}(\sigma)\}_H := E_H(e^{i\sigma n_1})$$

$$\{\varphi_{n_1}(\sigma)\}_\Sigma := E_\Sigma(e^{i\sigma n_1})$$

δπου οἱ δεῖκτες Η καὶ Σ ἀναφέρονται ἀντιστοίχως στοὺς τύπους τῆς θεωρίας C. Heyde-E. Heyde καὶ τῆς θεωρίας ποὺ ἀναπτύχθηκε παραπάνω, τότε

$$\{\varphi_{n_1}(\sigma)\}_H = \left\{ \lambda_1 n_{20} \frac{[1 - e^{-(\lambda_1 n_{20} + \lambda_2 + \lambda_3) t}]}{\lambda_1 n_{20} + \lambda_2 + \lambda_3} + \right.$$

$$\left. + \left[\frac{\lambda_2 + \lambda_3 + \lambda_1 n_{20} e^{-(\lambda_1 n_{20} + \lambda_2 \lambda_3) t}}{\lambda_1 n_{20} + \lambda_2 + \lambda_3} \right] e^{i\sigma} \right\}^{n_{10}} \qquad (32)$$

$$= e^{i\sigma n_{10}} \Big[\frac{\lambda_1 n_{20}}{\lambda_1 n_{20} + \lambda_2 + \lambda_3} \Big\{ (\lambda_1 n_{20} + \lambda_2 + \lambda_3) t + (\lambda_1 n_{20} + \lambda_2 + \lambda_3)^2 \frac{t^2}{2} \ldots \Big\} + e^{-i\sigma}$$

$$+ \Big\{ \lambda_2 + \lambda_3 + \lambda_1 n_{20} - \lambda_1 n_{20} (\lambda_1 n_{20} + \lambda_2 + \lambda_3) t + \lambda_1 n_{20} (\lambda_1 n_{20} + \lambda_2 + \lambda_3)^2 \frac{t^2}{2} +$$

$$+ \ldots \Big\} \frac{1}{\lambda_1 n_{20} + \lambda_2 + \lambda_3} \Big]^{n_{10}}$$

$$= e^{i\sigma n_{10}} \Big[1 + \lambda_1 n_{20} t (e^{-i\sigma} - 1) + \lambda_1 n_{20} (\lambda_1 n_{20} + \lambda_2 + \lambda_3) \frac{t^2}{2} (e^{-i\sigma} - 1) + \ldots \Big]^{n_{10}}$$

$$= e^{i\sigma n_{10}} \Big[1 + \lambda_1 n_{10} n_{20} t (e^{-i\sigma} - 1) \Big] + O(t^2) \qquad (33)$$

καὶ

$$\{ \varphi_{n_3} (\sigma) \}_\Sigma = \{ \varphi_{n_{10} - n_1} (\sigma) \}_\Sigma$$

$$= e^{i n_{10} \sigma} \{ \varphi_{n_1} (-\sigma) \}_\Sigma$$

$$= \Big\{ \frac{\mu_1 - \mu_2 - \lambda_1 n_{10} (e^{-\mu_2 t} - e^{-\mu_1 t})}{\mu_1 - \mu_2} + \frac{\lambda_1 n_{10} (e^{-\mu_2 t} - e^{-\mu_1 t}) e^{i\sigma}}{\mu_1 - \mu_2} \Big\}^{n_{20}}$$

ὁπότε

$$\{ \varphi_{n_1} (\sigma) \}_\Sigma = e^{i n_{10} \sigma} \{ \varphi_{n_3} (-\sigma) \}_\Sigma$$

$$= e^{i\sigma n_{10}} \Big[\frac{\mu_1 - \mu_2 - \lambda_1 n_{10} (e^{-\mu_2 t} - e^{-\mu_1 t})}{\mu_1 - \mu_2} + \frac{\lambda_1 n_{10} (e^{-\mu_2 t} - e^{-\mu_1 t}) e^{-i\sigma}}{\mu_1 - \mu_2} \Big]^{n_{20}}$$

$$= e^{i\sigma n_{10}} \Big[1 + \lambda_1 n_{10} t (e^{-i\sigma} - 1) + \frac{\mu_1 + \mu_2}{2} \lambda_1 n_{10} t^2 (1 - e^{-i\sigma}) + \ldots \Big]^{n_{20}}$$

$$= e^{i\sigma n_{10}} \Big[1 + \lambda_1 n_{10} n_{20} t (e^{-i\sigma} - 1) + O(t^2) \Big] \qquad \text{δ.ε.δ.}$$

Abstract

A stochastic theory for the kinetics of certain non elementary reactions

Stochastic theories of chemical kinetics are those whose Mathematical background is based on stochastic processes.

Compared with the deterministic theories of chemical kinetics, they have the advantage that they express more directly the statistical character of the chemical reactions and that they include as particular cases the corresponding deterministic theories.

Their only «disadvantage» is that, as they have not yet been studied

systematically, they do not cover, at the present stage of their development, a great number of realistic chemically reactive systems.

As examples indicative of the application of the stochastic methodology to chemical kinetics, two stochastic theries are developed, one for elementary reactions and another for non elementary ones. Some of their models are discussed and the conclusions are compared with the corresponding ones of the bibliography.

References and Notes

1. Johnston, H.S.: *J. Amer. Chem. Soc.* **87,** 3791 (1965)
2. Boudart, M.: *Kinetics of chemical processes,* Prentice-Hall, New Jersey (1968).
3. Laidler, K.J.: *Theories of chemical reaction rates,* Mc Graw-Hill, New York (1969).
4. Bunker, D.L.: *Accts, Chem. Res.* **7,** 195 (1974).
5. Lalande, A.: *Vocabulaire technique et critique de la philosophie,* (10me édition), P.U.F., Paris (1972).
6. Feller, W: *An introduction to probability theory and its applications,* Vol. I (3d edition), Wiley, New York (1968).
7. Kramers, H.A.: *Physica* **7,** 284 (1940).
8. Delbrück, M.: *J. Chem. Phys.* **8,** 120 (1940).
9. Bharucha-Reid, A.T.: *Elements of the theory of Markov processes and their applications,* Mc Graw-Hill, New York (1960).
10. Bartholomay, A.F.: *Bull. Math. Biophys.* **20,** 175 (1958).
11. Montroll, E.W. and Shuler, K.E.: *Adv. Chem. Phys.* **1,** 361 (1958).
12. Ishida, K: *Kyoritsu Kagaku Raiburari* (Japan.) **9,** 90 (1974).
13. Doob, J.L.: *Stochastic processes,* Wiley, New York (1953).
14. Papoulis, A.: *Probability, random variables and stochastic processes,* Mc Graw-Hill, New York (1965).
15. Markov, A.A.: *Izv. fiz. math. obch. pri Kazanck-un-te* (2) (Rus) **15,** 135 (1906).
16. Çinlar, E.: *Introduction to stochastic processes,* Prentice-Hall, New Jersey (1975).
17. Kolmogorov, A.N.: Math. Ann. **104,** 415 (1931).
18. (a) Bailey, N.T.: *The elements of stochastic processes,* Wiley, New York (1964).
    (b) Cox, D.R. and Miller, H.D.: *The theory of stochastic processes,* Chapman and Hall, London (1972).
    (c) Parzen, E.: *Stochastic processes,* Holden-Day, San Francisco (1962).
19. Dieudonné, J.: *Calcul infinitésimal,* Hermann, Paris (1968).
20. Van Hove, L.: *Physica* **23,** 441 (1957).
21. Ishida, K.: *Bull. Chem. Soc.* Japan **33,** 1030 (1960).
22. Mc Quarrie, D.A.: *J. Chem. Phys.* **38,** 433 (1963).
23 Kim, S.K.: *J. Chem. Phys.* **28,** 1057 (1958).
24. Osipov, A. and Stupochenko, E.: *Soviet Phys. Uspekhi* **6,** 47 (1963).
25. Wei, J.: *J. Chem. Phys.* **36,** 1578 (1962).
26. Mc Shane, E.Z.: *Stochastic calculus and stochastic models,* Academic Press, New York (1974).
27. Boucher, E.A.: *J. Chem. Educ.* **51,** 580 (1974).
28 Michaelis, L. and Mente, M.L.: *Biochem. Z.* **49,** 333 (1913).
29. Brown, A.Z.: *Trans. Chem. Soc.* **81,** 373 (1902).
30. Lehninger, A.L.: *Biochemistry,* (2d edition), Worth, New York (1975).
31. Roberts, D.V.: *Enzyme Kinetics,* Cambridge, London (1977).
32. (a) Heyde, C.C. and Heyde, E.: *J. Theor. Biol.* **25,** 159 (1969).
    (b) Heyde, C.C. and Heyde, E.: *J. Theor. Biol.* **30,** 395 (1971).

Chimica Chronika, New Series, 9, 179-187 (1980)

PARAMAGNETIC CENTERS IN X-RAY IRRADIATED Ni, $Zn(NH_4)_2$ $(SO_4)_2 \cdot 6H_2O$ SINGLE CRYSTALS

P. ONOUFRIOU and C. BATAS
University of Ioannina, B. Physics Laboratory, Ioannina, Greece

Summary

Analysis of the E.S.R. spectra of X-ray irradiated single crystals of $Zn(NH_4)_2$ $(SO_4)_2 \cdot 6H_2O$ doped with Ni shows that three types of paramagnetic centers are formed. They are related to the Zn-O directions in the unit cell. Their hyperfine splitting tensors A and their electronic splitting tensors g are found to have axial symmetry.

Key words: Electron Spin Resonance spectroscopy, irradiation defects, hyperfine splitting factors, electronic splitting factors.

Introduction

It is known that ionazing radiation produces stable paramagnetic centers in a number of inorganic and organic solids. It has been shown in previous papers[1,2] that Zn $(NH_4)_2$ $(SO_4)_2 \cdot 6H_2O$ upon irradiation at room temperature produces long-lived paramagnetic defects. This paper presents an analysis of the six paramagnetic defects produced in Ni doped $Zn(NH_4)_2$ $(SO_4)_2 \cdot 6H_2O$ single crystals.

Experimental

Ni doped single crystals were grown from aqueous solutions[3] of $ZnSO_4 \cdot 7H_2O$, $(NH_4)_2SO_4$ and $NiSO_4 \cdot 6H_2O$. The saturated aqueous solution which had originally a temperature of 40°C was cooled gradually to the room temperature at the rate of 0.5°C degrees/hour. The crystals were irradiated for 4 hours at room temperature with a copper target X-ray tube operating at 40 KV and 14mA. Crystals were 5cm away from the window of the tube.

The relative concentration of the Zn to Ni atoms in the doped crystals was about 13:1 and it was evaluated by fluorescence analysis.

Tutton salt $Zn(NH_4)_2$ $(SO_4)_2 \cdot 6H_2O$ is monoclinic containig four nitrogen atoms and four sulfur atoms in the unit cell[4,5]. Every Zn atom is surrounded by six aqueous molecules. Cell dimensions are a_0=9.223Å, b_0=12.500 Å, c_0= 6.237 Å and the angle ß= $106^0 52'$. The space group is C^5_{2h} $(P_{2\ 1/a})$.

Crystal axes were identified by means of a precession camera photographs and were aligned for E.S.R. observations with an optical goniometer.

The E.S.R. spectra were taken with an X-band spectrometer in a TE_{011} cylintrical cavity and 100 KHz modulation.

Results

A typical E.S.R. spectrum of the irradiated crystal of Ni, $Zn(NH_4)_2$ $(SO_4)_2 \cdot 6H_2O$ is presented in FIG. 1. It consists of two sets of lines labeled P and Q. The two sets may be distinguished by the fact that at room temperature the P set decreases in intensity after irradiation with a half life of 2 days while the Q set was still there after 9 months.

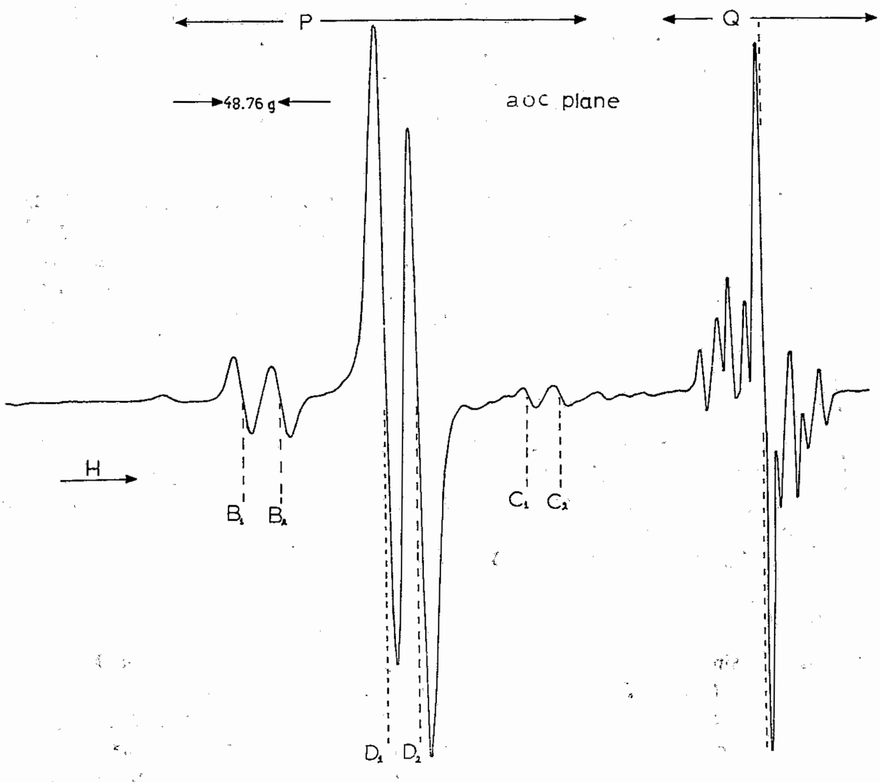

FIG. 1: *E.S.R. spectrum of irradiated Ni, Zn* $(NH_4)_2$ $(SO_4)_2 \cdot 6H_2O$ *single crystal. The first derivative of the spectrum is shown. The magnetic field was on the* aoc *plane at an angle* $\Theta=30°$ *from the* a *axis. The spectrum was taken 5 hours after irradiation.*

Within P set there are three subsets D,B,C of two lines each. Rotation of the magnetic field produces a variation of the center of gravity, a variation of the line spacing and a change in the relative intensities of the D,B,C subsets.

FIG. 2a and FIG. 2b show the angular variation of the g factor and the hyperfine splitting factor A respectively for subset D.

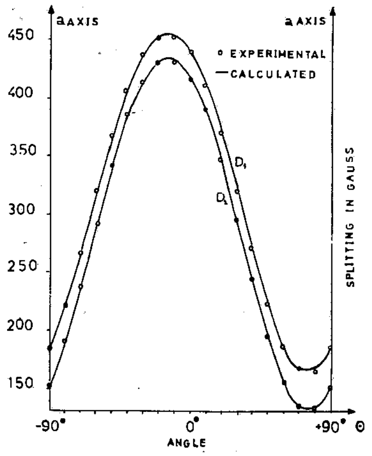

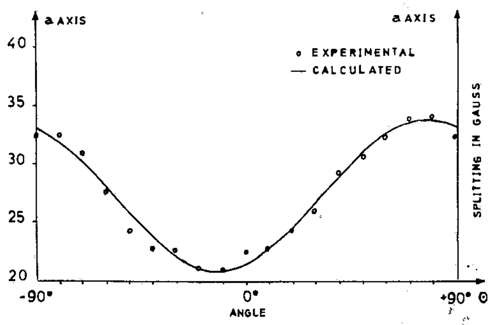

FIG. 2a: *Angular variation of the electronic splitting factor g of the subset lines D when the magnetic field lies on the aoc plane.*

FIG. 2b: *Angular variation of the hyperfine splitting factor A of the subset lines D when the magnetic field lies on the aoc plane.*

E.S.R. spectra were taken from the plane of the axes a,c,FIG. 3, while a axis was pointed to zero magnetic field angle of the rotating base and b axis was vertical.

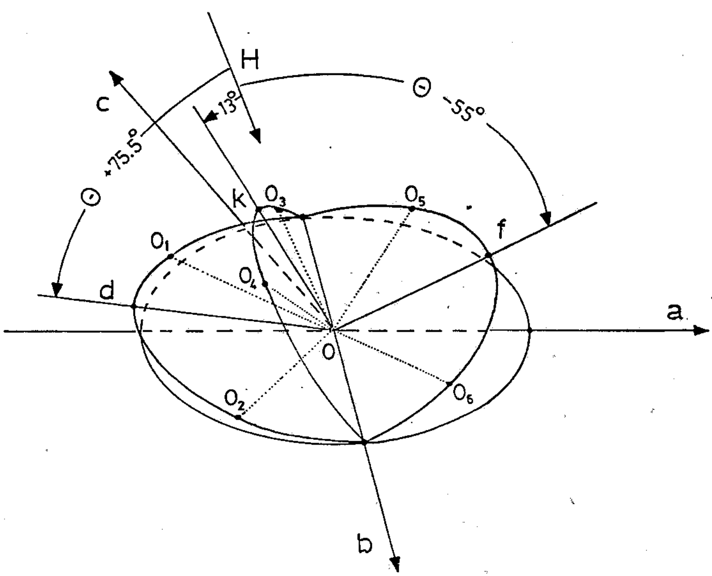

FIG. 3: *Relative directions of the crystal axes a,b,c and the four planes aoc, bod, bof, bok from which E.S.R. spectra were taken.* oo_1, oo_2, oo_3, oo_4, oo_5, oo_6 *are the calculated directions of the Zn-O axes in the crystal cell.*

From FIG. 2a and 2b we can see that g and A factors have their minimum and maximum values respectively at an angle $\Theta = +75.5°$. This angle corresponds to the direction od, FIG. 3, on the plane aoc.

From FIG. 4a, 4b we can see that at an angle $\Theta = -55°$ g and A factors of subset B have extreme values. This angle defines the direction of on the plane aoc, FIG. 3.

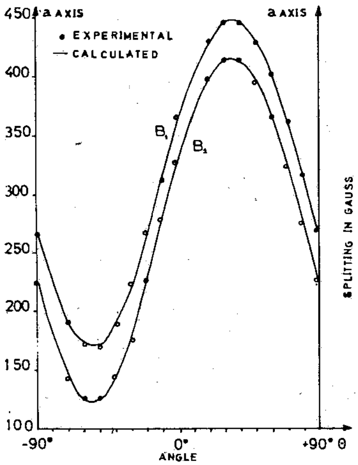

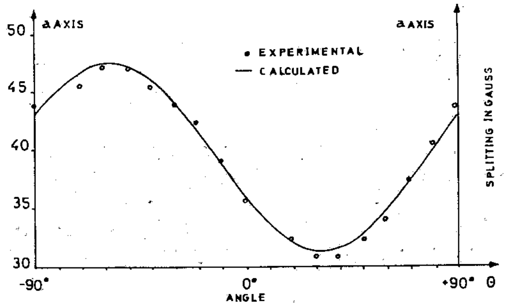

FIG. 4a: *Angular variation of the electronic splitting factor g of the subset lines B when the magnetic field lies on the aoc plane.*

FIG. 4b: *Angular variation of the hyperfine splitting factor A of the subset lines B when the magnetic field lies on the aoc plane.*

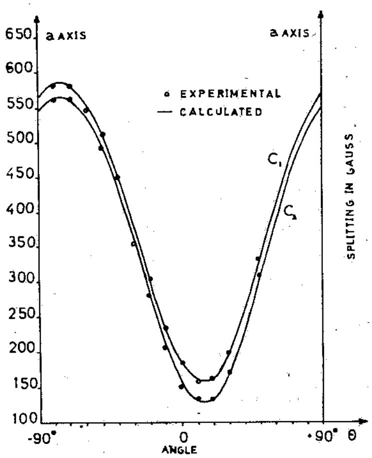

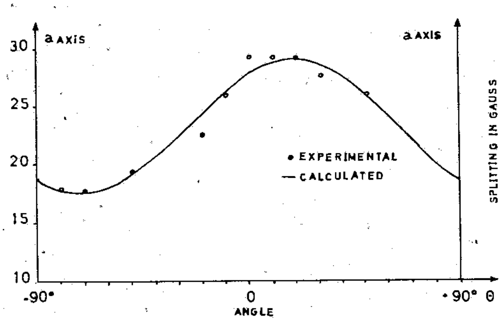

FIG. 5a: *Angular variation of the electronic splitting factor g of the subset lines C when the magnetic field lies on the aoc plane.*

FIG. 5b: *Angular variation of the electronic splitting factor A of the subset lines C when the magnetic field lies on the aoc plane.*

The angular variation of g and A factors for subset C can be seen in FIG. 5a, 5b. Angle $\Theta = +13°$ defines the direction ok on the plane aoc, FIG. 3.

Then E.S.R. spectra were taken from the planes bod, bof and bok FIG. 3, while b axis was horizontal and was pointing to zero magnetic field angle of the rotating base. Each of the subsets D,B and C. was analysed into two new groups $D_1^1D_2^1$, $D_1^2D_2^2$ FIG. 6, $B_1^1B_2^1$, $B_1^2B_2^2$ FIG. 7, $C_1^1C_2^1$, $C_1^2C_2^2$ FIG. 8.

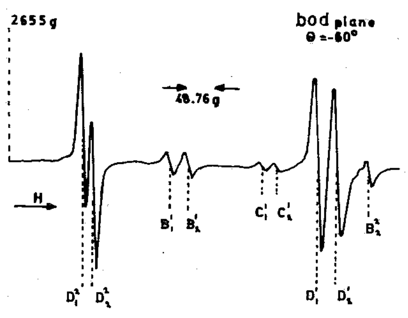

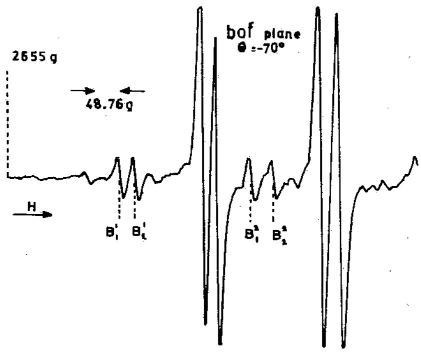

FIG. 6: *E.S.R. spectrum (P set) from irradiated Ni, Zn* $(NH_4)_2$ $(SO_4)_2 \cdot 6H_2O$ *single crystal. The magnetic field was on the bod plane at an angle* $\Theta = -60°$ *from the b axis. The spectrum was taken 5hr after irradiation.*

FIG. 7: *E.S.R. spectrum (P set) from irradiated Ni,* $Zn(NH_4)_2$ $(SO_4)_2 \cdot 6H_2O$ *single crystal. The magnetic field was on the bof plane at an angle* $\Theta = -70°$ *from the b axis. The spectrum was taken 5hr after irradiation. The first derivative of the spectrum is shown.*

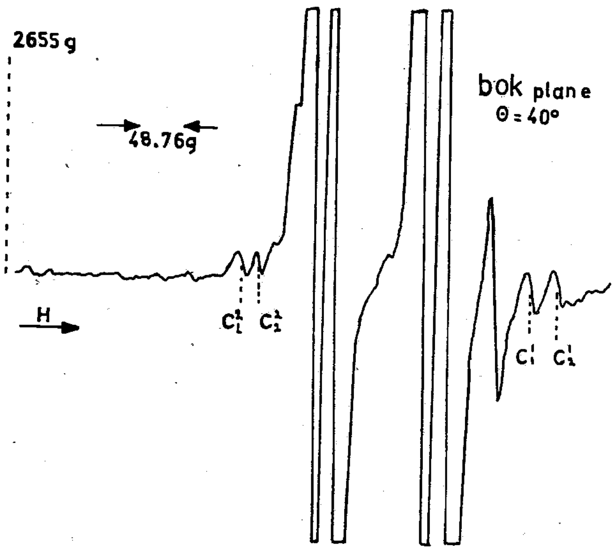

FIG. 8: *E.S.R. spectrum (P set) from irradiated Ni,* $Zn(NH_4)_2$ $(SO_4)_2 \cdot 6H_2O$ *single crystal. The magnetic field lies on the bok plane at an angle* $\Theta = 40°$ *from the b axis. The spectrum was taken 5hr after irradiation. The first derivative of the spectrum is shown.*

The angular variation of the electronic splitting factors g and the hyperfine splitting factors A for the new lines are given in FIG. 6a, 6b, FIG. 7a, 7b and FIG. 8a, 8b.

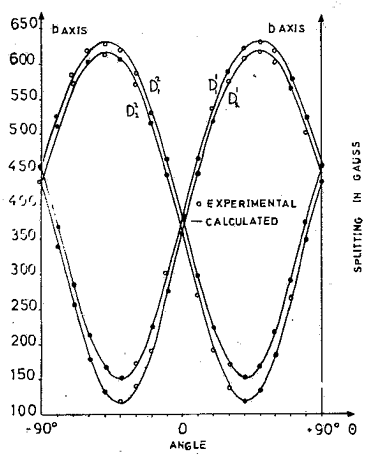

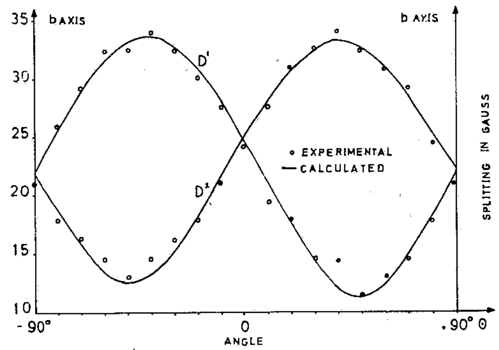

FIG. 6a: *Angular variation of the electronic splitting factors g of the two group lines D^1, D^2 when the magnetic field lies on the bod plane.*

FIG. 6b: *Angular variation of the hyperfine splitting factors A of the group lines D^1, D^2 when the magnetic field lies on the bod plane.*

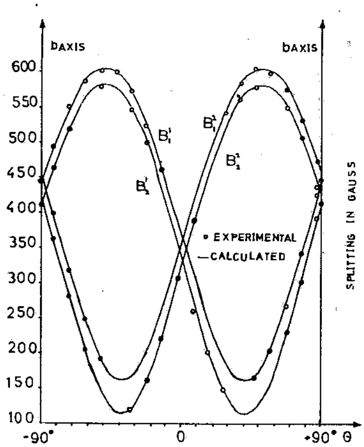

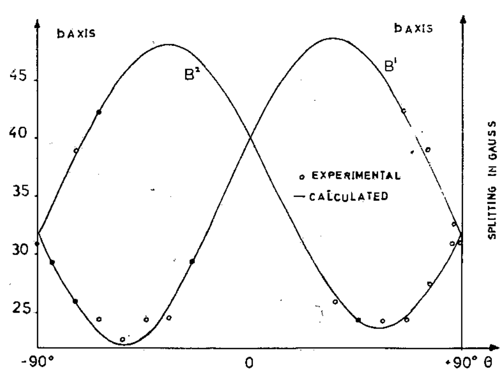

FIG. 7a: *Angular variation of the electronic splitting factors g of the two group lines B^1, B^2 when the magnetic field lies on the bof plane.*

FIG. 7b: *Angular variation of the hyperfine splitting factors A of the group lines B^1, B^2 when the magnetic field lies on the bof plane.*

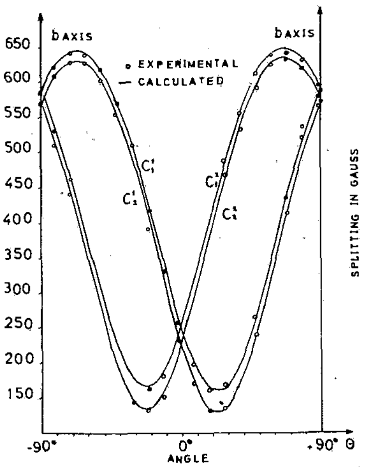

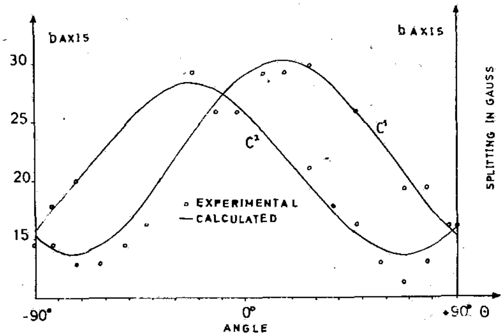

FIG. 8a: *Angular variation of the electronic splitting factors g of the group lines C^1, C^2 when the magnetic field lies on the bok plane.*

FIG. 8b: *Angular variation of the hyperfine splitting factors A of the group lines C^1, C^2 when the magnetic field lies on the bok plane.*

Analysis

Each of the groups of the E.S.R. spectra in the FIG. 6, 7, 8 is composed of two lines with relative intensity 1:1. This spectrum will arise if the unpaired electron in the defect interacts with one nucleus of spin $^1/_2$. We are therefore led to assign the spectrum to the H^+ which can be produced by irradiation in the crystal cell.

From the crystal structure's analysis it is known that every Zn atom is surrounded by 6 aqueous molecules. We have defined the possible directions of the Zn-O axes in the basecentered unit cell which correspond to the 6 directions oo_6, oo_5, oo_3, oo_4, oo_1, oo_2 in FIG. 3.

The diagonal values of the g_{D^1} and g_{D^2} tensors show axial symmetry at angles $\Theta = -49°$ and $\Theta = 49.5°$ on the bod plane. These directions are very close to directions oo_1, oo_2 of FIG. 3, within an error of $\pm 3°$.

g_{B^1} and g_{B^2} tensors show axial symmetry at angles $\Theta = -50°$ and $\Theta = 51°$ on the bof plane, while g_{C^1}, g_{C^2} tensors show axial symmetry at angles $\Theta = -68°$ and $\Theta = 66.5°$ on bok plane. The above given directions are very close to directions oo_5, oo_6 and oo_3, oo_4 respectively within an error of $\pm 3°$.

It is also characteristic that A_{D^1}, A_{D^2} tensors of the hyperfine splitting show axial symmetry on the same directions as g_{D^1} and g_{D^2} tensors within an error of $\pm 5°$, Table I.

From the number of the created paramagnetic centers, the number of lines and their relative intensity in each spectrum, and the relation of the axial symmetry of the g and A tensors to Zn-O axes in the crystal cell, we are led to the conclusion that the paramagnetic centers are related to the hydrogen ions that can be produced by X-ray irradiation in the $6H_2O$ molecules surrounding the Zn atom.

The observed E.S.R. spectra may be derived from the spin Hamiltonian

$$H = \beta S g H + S \sum_k A_k I_k$$

where ß is the Bohr magneton, H the magnetic induction, S and I_k the electronic and nuclear spin operators (subscript K indicates nucleus) g the electronic spectroscopic splitting tensor, A the hyperfine tensor. The nuclear Zeeman term does not affect the resonance spectrum under the conditions of these experiments.

g and A are diagonalized tensors.

In case of axial symmetry the diagonial values of g tensor can be calculed from equation.

$$g^2 = g_{II}^2 \cos^2 \Theta + g_\perp^2 \sin^2 \Theta$$

and the diagonal values of A tensor from equation

$$g^2 A^2 = g_{II}^2 A_{II}^2 \cos^2\Theta + g_\perp^2 A_\perp^2 \sin^2\Theta$$

where Θ is the angle of the magnetic field.

The diagonal values of we found for the g and A tensors are given in Table I.

TABLE I: *Components of the electronic splitting tensors g and the hyperfine splitting tensors A for the six paramagnetic centers in the Ni, $Zn(NH_4)_2$ $(SO_4)_2 \cdot 6H_2O$ single crystal. The standard deviation of all g entries is ±0.0005 and the standard deviation of all A entries is ±0.05 gauss.*

	g tensor				A tensor			
	Angle Θ°	g_{II}	Angle Θ°	$g_\perp$	Angle Θ°	A_{II} gauss	Angle Θ°	A_I γαθσσ
D[1]	−41	2.4532	−49	2.0853	+48.5	33.59	−41.5	11.24
D[2]	+40.5	2.4528	+49.5	2.0868	−49.5	33.17	+40.5	12.54
B[1]	+40	2.4265	−50	2.0877	−53.5	47.87	+36.5	22.27
B[2]	−39	2.4243	+51	2.0884	+56	48.00	−34	23.68
C[1]	+22	2.4661	−68	2.0920	−73.5	30.22	+16.5	13.90
C[2]	−23.5	2.4675	+66.5	2.0962	+67	28.26	−23	13.59

The presence of Ni in the single crystal is necessary for the creation of these paramagnetic defects. Undoped crystals after irradiation give only the Q set of lines, FIG. 1. Doped crystals after irradiation give the Q set of lines with the same characteristics of the undoped crystal and the P set of lines. The intensity of the P line set increases with Ni concetration[6,7] in the single crystal under the same conditions of irradiation and crystal dimensions.

Περίληψη

Παραμαγνητικὰ κέντρα σὲ μονοκρυστάλλους Ni, Zn $(NH_4)_2$ $(SO_4)_2 \cdot 6H_2O$ ποὺ ἀκτινοβολήθηκαν μὲ ἀκτῖνες X.

Ἡ ἀνάλυση τῶν φασμάτων συντονισμοῦ ἠλεκτρονικῆς στραφορμῆς, ποὺ ἐλήφθησαν ἀπὸ μονοκρυστάλλους Ni, Zn $(NH_4)_2$ $(SO_4)_2 \cdot 6H_2O$ μετὰ ἀπὸ τὴν ἀκτινοβόληση τους μὲ ἀκτῖνες X, δείχνει ὅτι δημιουργοῦνται παραμαγνητικὰ κέντρα ποὺ δίνουν δύο ὁμάδες φασματικῶν γραμμῶν, τὴν P καὶ Q, μὲ διαφορετικὴ αἰτία προέλευσης.

Ἡ ὁμάδα γραμμῶν P ἀποτελεῖται ἀπὸ ἕξη συνολικὰ φασματικὲς ὁμάδες μὲ δύο φασματικὲς γραμμὲς σὲ κάθε ὁμάδα. Οἱ φασματικὲς ὁμάδες ἀνὰ δύο εἶναι ἰσοδύναμες καὶ παρουσιάζουν ἀνισοτροπία στὴ στροφὴ τοῦ μαγνητικοῦ πεδίου.

Προσδιορίστηκαν οἱ διαγώνιες τιμὲς τῶν παραγόντων g γιὰ ὅλες τὶς ὑποομάδες φασματικῶν γραμμῶν ποὺ βρίσκονται στὴν ὁμάδα P καθὼς καὶ οἱ διαγώνιες τιμὲς τῶν παραγόντων ὑπέρλεπτης ὑφῆς A. Βρέθηκε ὅτι ἡ διεύθυνση τοῦ ἄξονα τῶν ἀτόμων Zn-O ποὺ βρίσκονται στὴν κρυσταλλικὴ κυψελίδα, εἶναι καὶ ἡ διεύθυνση ἀξονικῆς συμμετρίας τοῦ τανυστὴ g μετὰ τὴ διαγωνιοποίησή του. Αὐτό, σὲ συνδυασμὸ μὲ τὸν ἀριθμὸ τῶν κέντρων ποὺ παρατηροῦνται, τὴ μορφὴ καὶ τὴν ἔνταση τῶν φασματικῶν γραμμῶν, ὁδηγεῖ στὸ συμπέρασμα, ὅτι τὰ παραμαγνητικὰ κέντρα συνδέονται μὲ τὰ H^+, ποὺ δημιουργοῦνται ἀπὸ τὴν ἀκτινοβόληση μὲ ἀκτῖνες X, στὰ μόρια τοῦ H_2O ποὺ περιβάλλουν τὰ ἄτομα τοῦ Zn.

References

1. Batas, C and Karavelas, S.: *Paramagnetic centers in X-ray irradiated Zn $(NH_4)_2$ $(SO_4)_2$ $6H_2O$ single crystals,* Chimika Cronika, New Series, **4,** 75 (1975).
2. Cole, T.: *Paramagnetic defects in irradiated NH_4CLO_3, J. Chem. Phys.* **35,** 1169 (1961)
3. Borcherts, R.H.: *An E.P.R. investigation of VO^{+2} and X-ray produced V^{+2} in Tutton salt,* University of Michigan, Final report, Part I, p. 15, (1963).
4. Wyckoff, R.W.G.: Crystal structures, Vol. 3, (2d edition), pp. 822-824, Wiley & Sons, N.Y. (1965).
5. Al' Tshuler, S.A. and Cozyrev, B.M.: Electron Paramagnetic Resonance, p. 93, Academic Press, N.Y. (1964).
6. Griffiths, J.H.E. and Owen, J.: *Paramagnetic resonance in the Nickel Tutton salt,* Proc. Roy. Soc. A, 213 (1952).
7. Giurgiu, L.V. et al.: *Temperature and irradiation influence on Cu^+E.S.R. spectrum,* Abst. of Conf. on Magn. Resonance and Rel. phenomena, Inst. Atomic Phys., p. 117, Bucharest, Romania (1971).

Chimica Chronika, New Series, 9, 189-199 (1980)

DYNAMIC VISCOELASTICITY AND STRESS-STRAIN PROPERTIES OF VULCANIZATES REINFORCED WITH REACTIVE AND INERT FILLERS

NIKOS K. KALFOGLOU
Laboratory of Chemical Technology, University of Patras, Patras-Greece

Summary

The dynamic mechanical and near-equilibrium stress-strain behavior of polybutadiene vulcanizates prepared using the optimum amount of curative, was compared. These rubbers, prepared from bromine terminated liquid polymer, were reinforced with equivalent amounts of reactive and of inert fine silica filler and of normal carbon black. The products were cured with the equivalent amount of an aliphatic amine to obtain tetrafunctional crosslinks. Dynamic mechanical spectra were obtained between −110°C to 200°C and stress-strain measurements at medium elongations were carried out at 25°C. No significant shift of the glass transition temperature was observed. In the rubbery region the inert filler causes a higher increase in stiffness and damping than the reactive silica filler. At medium elongations tensile properties indicate the improvement achieved by using the active filler in terms of higher strength and lower hysteresis. In general, the results indicate that rubbers loaded with reactive silica fillers behave very similarly to carbon black reinforced vulcanizates.

Key words: Reinforced elastomers, Liquid polymers, Surface modified fillers, Dynamic mechanical spectra.

Abbreviations and terminology

phr: parts per hundred parts (by weight) of rubber.
Br∼PB∼Br: bromine terminated polybutadiene
telechelic polymer: low molecular weight polymer with a functional group at each end of the molecule
gum vulcanizate: unfilled vulcanized rubber
curing, curative: vulcanization, vulcanization agent.

Introduction

The commercial value of elastomer reinforcement has stimulated much research activity towards the elucidation of the physical and chemical aspects of the phenomenon[1-5].

More recently, the development of a class of low molecular weight liquid telechelic polymers giving, under mild curing conditions, gum vulcanizates of comparable strength as traditional elastomers was reported[6-8]. These are bromine terminated polybutadienes and their chemistry allows the design of model reinforced elastomers by controlling the degree of reaction of surface modified fillers with the rubbery matrix[9,10].

The aim of this experimental study was to compare the mechanical behavior of filled elastomers prepared from a bromine terminated polybutadiene, containing the same loading of carbon black, of reactive and of inactive silica filler, all cured with the optimum and equivalent amonts of curative[9] to obtain a network with tetrafunctional crosslinks. The testing included dynamic mechanical tetrafunctional crosslinks. The testing included dynamic mechanical measurements at an extended temperature range and near-equilibrium stress-strain and mechanical hysteresis measurements. In addition to revealing moduli and tensile reinforcement differentiation under static and dynamic conditions caused by the different fillers, it was of interest to examine changes in the relaxation spectra caused by matrix-interacting and inert fillers.

Experimental

Materials Preparation

The samples were prepared from bromine terminated polybutadiene $BrCH_2$ $-CH{=}CH\ (CH_2)_n\ CH{=}CH{-}CH_2Br$ ($\bar{M}_n$ about 10000), at the Technical Research and Development Division, Polymer Corp., Sarnia, Canada. The preparative techniques were described by Fisher and Edwards[9,10]. The silica filler used (Cab-O-Sil HS-5) was made inactive by surface esterification with n-butanol. Reactive silica filler was prepared by reaction with an aminosilane (Union Carbide A-1100) followed by methylation. Curing of the liquid polymer was carried out using methylated triethylene-tetramine (MTETA). Before the cure, the semiliquid filled or unfilled polymer was preformed under pressure within a metal frame bounded by Teflon sheets. The whole assembly was then allowed to cure without pressure, at 60°C for 48 hrs. The following reactions describe the methods used to prepare the inert and reactive fillers and the attachment of the latter to the rubbery matrix.

Preparation of inert silica filler

$$\underset{\text{filler}}{\text{Si}\}\text{-OH}} \xrightarrow[\text{BuOH}]{\text{Esterif}} \text{Si}\}\text{-OBu}$$

Preparation of reactive filler

$$\text{Si}\}\text{-OH} \xrightarrow[(EtO)_3\,Si(CH_2)_3\text{-}NH_2]{\text{Silane}} \text{Si}\}\text{-O-}\overset{\text{OEt}}{\underset{\text{OEt}}{\text{Si}}}\text{-}(CH_2)_3\text{-}NH_2 \rightarrow$$

$$\xrightarrow{\text{Methylation}} \text{Si}\}\text{-O}\overset{\text{OEt}}{\underset{\text{OEt}}{\text{Si}}}\text{-}(CH_2)_3\text{-}N(CH_3)_2$$

Polymer chain extension

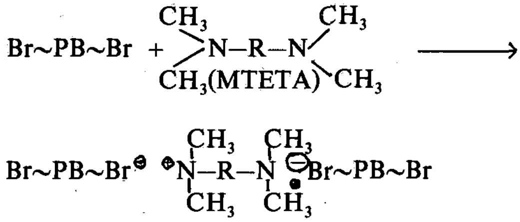

where, $R = -CH_2(CH_2-\overset{CH_3}{N}-CH_2)_2CH_2-$

Crosslinking of the polymer is accomplished through similar quaternization reactions by the non-terminal tertiary amine groups of MTETA.

Filler attachment

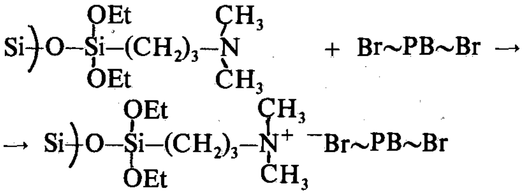

Sample designation and description is given in Table I.

TABLE I: *Sample Description and Designation.*

Sample	Method of Preparation
S1	Liquid polymer cured with the optimum amount (2,6 phr) of MTETA required to give a network with tetrafunctional crosslinks.
S2	The same polymer containing 30 phr of esterified inert filler crosslinked with 2,6 phr MTETA.
S3	The same polymer containing 30 phr of reactive filler crosslinked with 1,6 phr MTETA. Less amount of curative was used to take into account the activity of filler which was equivalent to 1,0 phr of MTETA.
S4	The same polymer reinforced with 26 phr carbon black (Neotex 130) which is equivalent to the same volume fraction as the silica and cured with 2,6 phr of MTETA.

Measurements

Dynamic mechanical testing was carried out between −110°C to 200°C at 110 Hz using the Rheovibron Viscoelastometer Model DDV-IIC of Toyo Baldwin Co., Ltd., Tokyo, Japan. A slow stream of precooled nitrogen prevented moisture from condensing on the sample. In calculating the quantity $|E^*|$ the small deformation of the instrument clamps was taken into account. Typical specimens dimensions were 3,0 cm × 0,3cm × 0,06cm.

Near-equilibrium stress-strain properties were studied at 25°C by the incremental addition of weights at constant rate (50 g/5 min) at the lower film strip, suspended in a thermostated glass chamber. The extension was obtained by measuring the distance between two fiduciary lines on the film with a traveling microscope to an accuracy of 0,2 mm. Typical specimens dimensions were 2,50cm × 0,50cm × 0,06cm.

Results and Discussion

Dynamic Mechanical Properties

In Figures 1 and 2 the thermomechanical spectra of the elastomers studied are reported. A duplicate run on S2 has been included to indicate the degree of reproducibility attained. No significant shift of the low temperature relaxation E'' (at −73°C) was observed among the various specimens. This has been explained[11] as due to the small amount of the rubbery matrix which is influenced by the filler at these loadings, even though our silica filler has a higher specific area (325 m^2/g) from that used in previous work[11,12]. In Figure 1 the loss modulus variation indicates an increase of internal friction in the order S1<S4<S3<S2. This is attributed to the varying degree of attachment of the filler to the elastomer matrix decreasing in the above order. A similar trend is indicated from the temperature dependence of the loss tangent not reported here. At room temperature damping values increase in the order S1<S3<S4<S2. At these small deformations this may indicate[2] some secondary filler aggregation which is highest for the non reactive and lowest for the reactive filler. As Dannenberg notes[4], chemical interaction may improve dispersion of particulates within the matrix. The same mechanism is also operative for the carbon filled elastomer due to a chemisorptive interaction possiple for a normal carbon black.

In Figure 2 the temperature dependence of the storage modulus indicates the differing stiffness caused by the fillers used. Highest stiffness is shown by the elastomer filled with the inert filler. In the same Figure the modulus value calculated using various mechanics models proposed[13], is also included. No satisfactory agreement was obtained. The closest value to the experimentally determined modulus E was obtained using the Guth-Gold expression.

$$E=E_0\ (1+2{,}5c + 14{,}1c^2)$$

where, E_0 is Young's modulus of the rubber matrix and c is the volume fraction of the filler. For this model the value E/E_0 predicted is 1,44 while the experimentally determined values range from 3,38 (for S2) to 1,97 (for S4). The data can be explained by a larger effective filler concentration due to an immobilized rubbery layer covering the filler particle, along the lines suggested by Smit's work[14], or by a layer of bound rubber interacting through entanglements[15]. Using the Guth-Gold equation and the experimentally determined ratio E/E_0, the immobilized layer for S2 is found to be about 19 A^0 thick, for S3 14 A^0 and for S4 approx. one tenth of the average carbon particle diameter. These values are of the same order of magnitude reported by

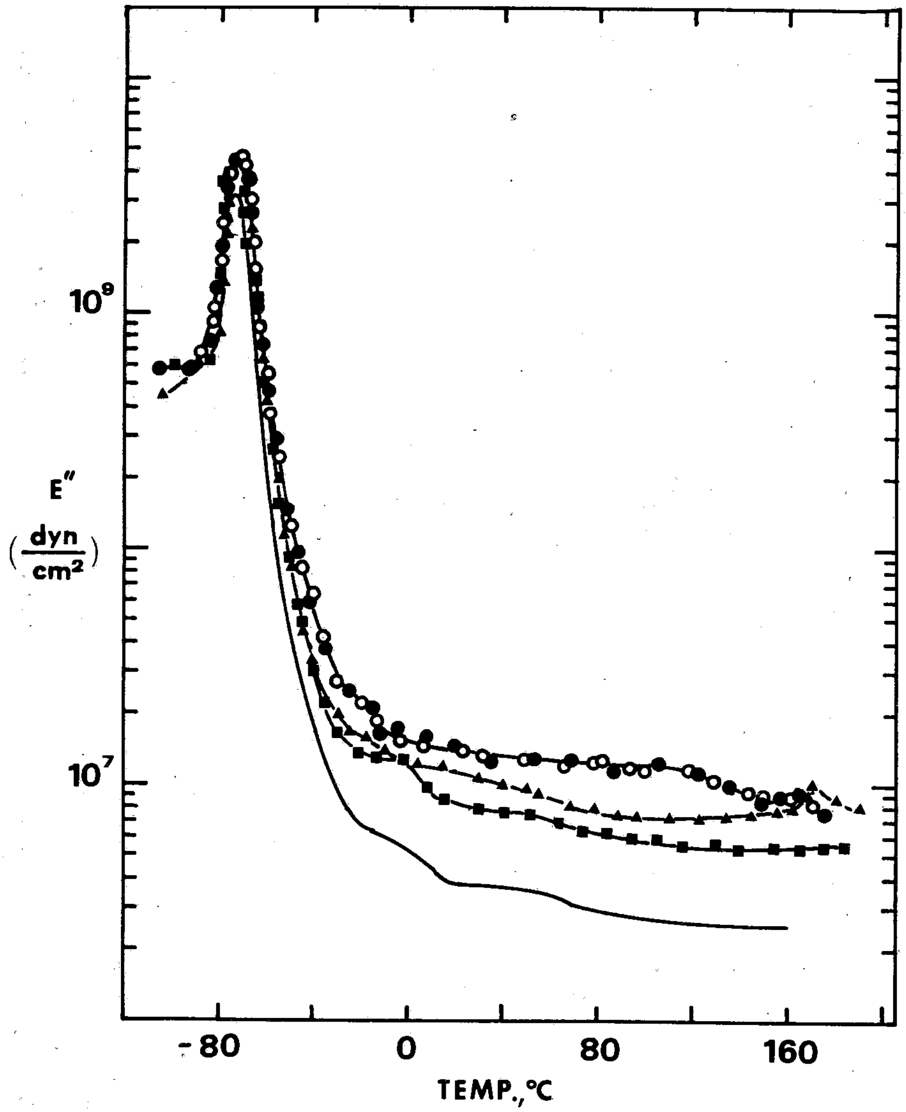

FIG. 1: *Temperature dependence of loss modulus E″ at 110 Hz: (O), sample S2; (●), sample S2 duplicate run; (▲), sample S3; (■), sample S4; (–), sample S1.*

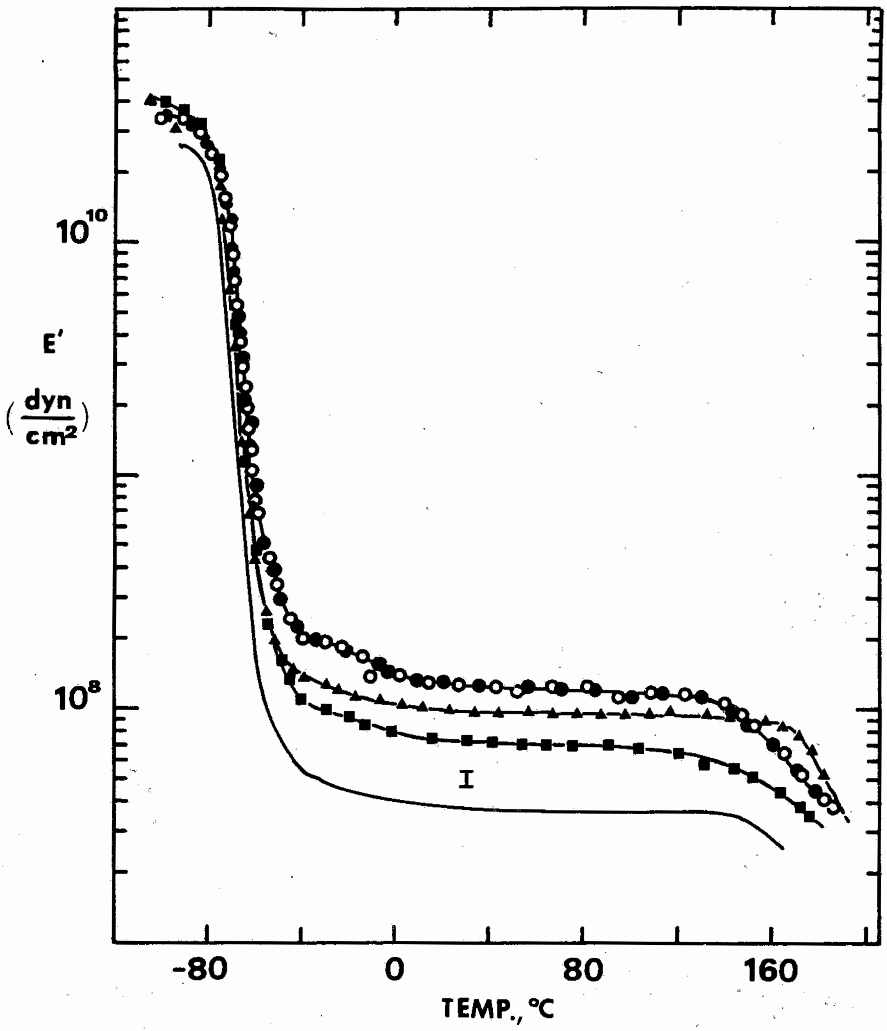

FIG. 2: *Temperature dependence of storage modulus E′ at 110 Hz: (O), sample S2; (●), sample S2 duplicate run; (▲), sample S3; (■), sample S4; (—), sample S1; (I), calculated values from models in Ref. 13.*

Smit[14] and Medalia[16] on the basis of rheological studies. It is perhaps pertinent to mention that the layer of esterified butanol covering the silica particles in S2 has a thickness of approx. 9 A^{o} and the layer of the coupling agent, (up to the point where the flexible PB chain is joined), on the filler in S3, is about 10 A^{o} thinck. This reduces the value of the bound rubber layer thickness closer to that reported by Slichter and his associates[17].

Figure 2 shows also a significant gain in thermal stability of the rubbery network (S3) when it is reinforced by the reactive filler. The incorporation of the filler in the network through its crosslinking effect retards the onset of melt flow.

Stress-strain properties

Figures 3 and 4 and Table II summarize tensile near-equilibrium properties of these vulcanizates at medium elongations, ($\lambda \simeq$ 2-3). In Figure 3 the specimens were loaded up to the same nominal weight. True stress σ was calculated assuming affine deformation. Two loading cycles were carried out for the filled elastomers and before the second loading, the sample was allowed to relax at room temperature for 24 hrs.

To compare more accurately reinforcement and hysteresis, specimens were also tested up to the same elongation, (see Fig. 4).

Figures 3 and 4 demonstrate the reinforcing effect of the chemically bonded filler as compared to inert filler and the carbon black. Table II indicates that stress softening, defined as the percentage decrease of the area under the stress-strain curve between successive loadings, increases in the series S4<S2<S3. This seems to support the Mullins[16] mechanism of reinforcement according to which stress softening is not directly responsible for the increase in strength. From Table 2 it is also seen that the degree of softening increases with the degree of stiffness as measured by the E′ values in Figure 2.

TABLE II: *Comparison of Tensile Testing Data of the Elastomers Studied.*

Property	Samples			
	S1	S2	S3	S4
Modulus E′[a] at 25°C, x 10^{-7}, (dyn/cm²)	3,7	12,2	9,6	7,3
Tensile strength at λ=2,0, (kg/cm²)	27,0	54,0	75,0	41,0
Stress softening %	—	17,9	7,7	6,3
Hysteresis[b] %	9,5	24,7	15,0	15,7

a From dynamic mechanical testing.
b First loading cycle.

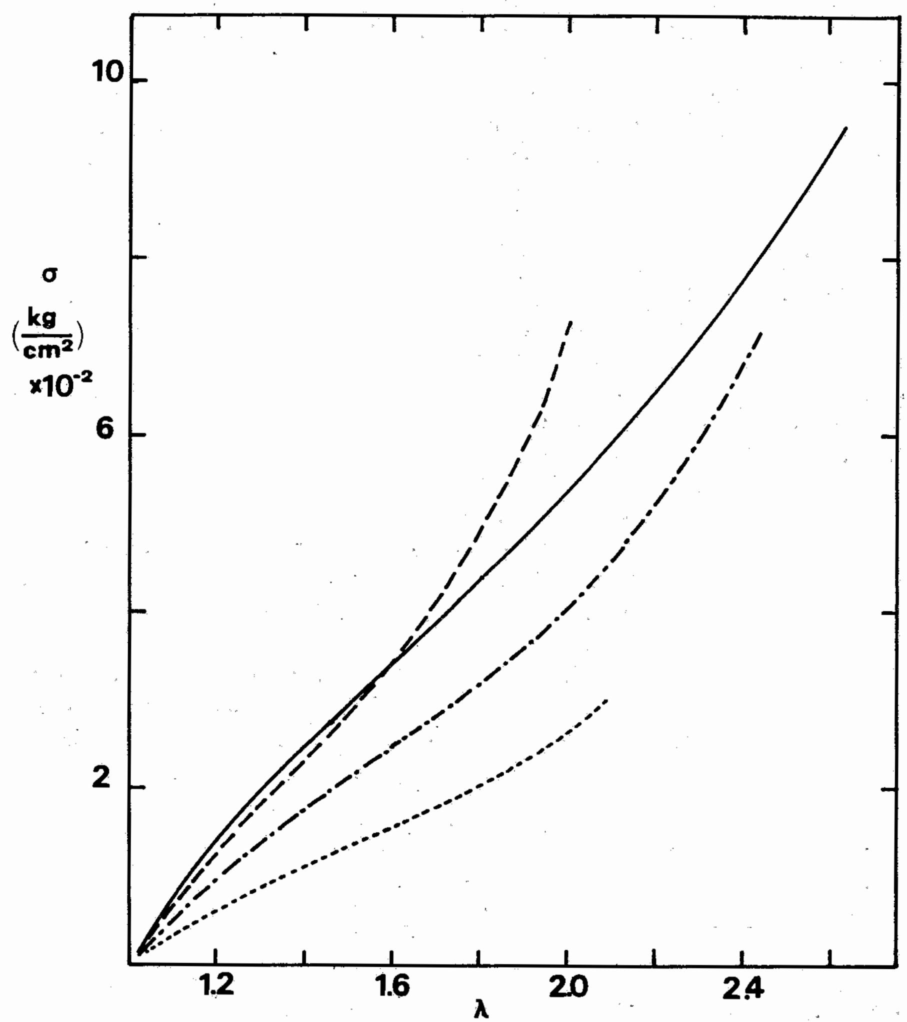

FIG. 3: *True stress-strain properties at 25°C: (——), sample S1; (-.-), sample S4; (–), sample S2; (—), sample S3.*

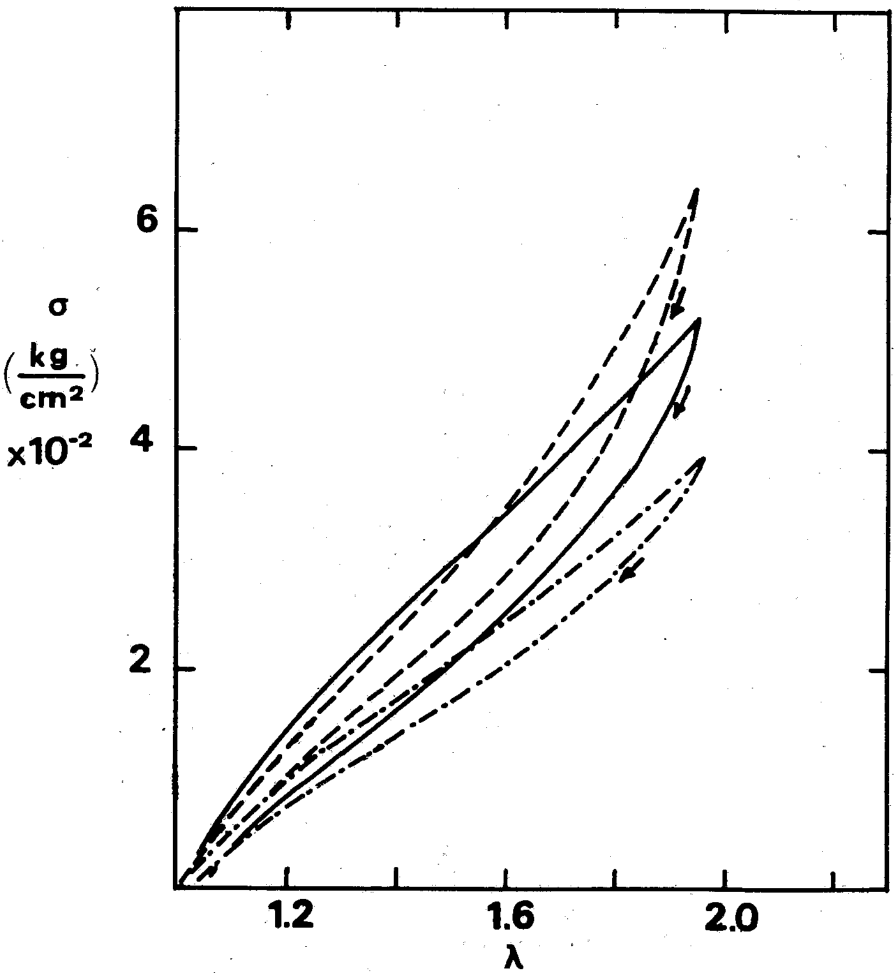

FIG. 4: *First loading cycle at 25°C: (–.–), sample S4; (–), sample S2; (—), sample S3.*

Relative hysteresis losses from stress-strain measurements, see Table II, are in agreement with the areas given by the tanδ spectra. The relative values among the reinforced elastomers show the significant improvement achieved by the use of the active filler providing reinforcement combined with low hysteresis.

Conclusions

1. Bonding of silica active fillers to the rubbery matrix reduces damping and increases the thermal stability of the polybutadiene vulcanizate.
2. The nature of the filler at up to 0.10 volume fraction loading does not influence the glass transition temperature to any significant extent.
3. Reinforcement due to the silica active filler is of a similar nature as that produced by carbon black and can be attributed to strain amplification.
4. Chemical attachment of the filler to the rubbery matrix gives vulcanizates combining high strength with low hysteresis.

Περίληψη

Δυναμικὴ ἰξωδοελαστικότητα καὶ ἰδιότητες τάσεως - ἐφελκυσμοῦ ἐλαστομερῶν ἐνισχυμένων μὲ δραστικὰ καὶ ἀδρανῆ μέσα πληρώσεως.

Γίνεται σύγκριση τῆς δυναμικῆς μηχανικῆς συμπεριφορᾶς καὶ τῶν ἰδιοτήτων τάσεως - ἐφελκυσμοῦ σὲ συνθῆκες ποὺ ἀφίστανται λίγο ἀπὸ τὴν ἰσορροπία, ἐλαστομερῶν ποὺ παρασκευάστηκαν χρησιμοποιῶντας τὴν ἀρίστη ποσότητα τοῦ μέσου βουλκανισμοῦ. Τὰ ἐλαστομερῆ αὐτὰ ποὺ παρασκευάστηκαν ἀπὸ μικροῦ μοριακοῦ βάρους βρωμιωμένο στὰ ἄκρα πολυβουταδιένιο, ἐνισχύθηκαν μὲ ἰσοδύναμες ποσότητες ἐνεργοῦ καὶ ἀδρανοῦς διοξειδίου τοῦ πυριτίου καὶ αἰθάλης βουλκανισμοῦ. Τὰ προϊόντα βουλκανίσθηκαν μὲ ἰσοδύναμες ποσότητες ἀλειφατικῆς ἀμίνης ὥστε νὰ προκύψουν σταυροειδεῖς διασυνδέσεις. Οἱ δυναμικὲς μηχανικὲς ἰδιότητες προσδιορίσθηκαν μεταξὺ −110°C καὶ 200°C καὶ οἱ ἰδιότητες τάσεως - ἐφελκυσμοῦ στοὺς 25°C. Δὲν παρετηρήθη οὐσιώδης μετατόπιση στὴ θερμοκρασία μεταβάσεως ὑάλου T_g. Στὴν περιοχὴ ἐλαστομεροῦς συμπεριφορᾶς τὸ ἀδρανὲς μέσο πληρώσεως αὐξάνει τὸ μέτρο ἐλαστικότητος καὶ τὴν ἀπορρόφηση ἐνεργείας περισσότερο ἀπ' ὅτι τὸ ἀντίστοιχο ἀντιδρὸν διοξείδιο τοῦ πυριτίου. Σὲ μέτριες ἐπιμηκύνσεις οἱ ἰδιότητες ἐφελκυσμοῦ δείχνουν ὅτι ἐπιτυγχάνεται βελτίωση τῶν ἐλαστομερῶν λόγω ηὐξημένης ἀντοχῆς καὶ μειωμένης μηχανικῆς ὑστερήσεως. Γενικὰ τὰ ἀποτελέσματα δείχνουν ὅτι ἐλαστομερῆ ποὺ ἔχουν σὰν μέσο πληρώσεως δραστικό (πρὸς τὴν πολυμερὴ μήτρα) διοξείδιο τοῦ πυριτίου συμπεριφέρονται παρόμοια ὅπως καὶ τὰ ἐνισχυμένα μὲ αἰθάλη ἐλαστομερῆ.

References

1. Reinforcement of Elastomers, Kraus, G., Ed., Intercience Publ., N.Y., 1971.
2. Kraus, G., Adv. Polym. Sci., Vol. 8, Springer - Verlag N.Y., 1971.

3. Medalia, A.I., paper presented at International Symposium on Elastomer Reinforcement, Le Bischenberg, France, September 1973.
4. Dannenberg, E.M., Rubber Chem. Technol., **48,** 410 (1975).
5. Les Bras, J. and Papirer, E., J. Appl. Polym. Sci., **22,** 525 (1978).
6. Beaton, J., Br. Polym. J., **3,** 129 (1971).
7. Dolezal, T., Edwards, D.C. and Wunder, R.H., Rubber World **158,** 46 (1968).
8. Edwards, D.C., Pfisterer, H.A. and Wunder, R.H., Fourth Int. Synthetic Rubber Symposium, London 1969; Rubber and Technical Press, Ltd., London 1969 (1) p. 9.
9. Edwards, D.C. and Fisher, E. : paper presented at D.K.G. Meeting in Wiesbaden, May 1971.
10. Edwards, D.C. Rubber Chem. Technol., **48,** 202 (1975).
11. Kraus, G. and Gruver, J.T., J. Polym. Sci., A-2 **8,** 571 (1970).
12. Droste, D.H., Dibenedetto, A.T., J. Appl. Polym. Sci., **13,** 2149 (1969).
13. Ref. 2, p. 182.
14. Smit, P.P.A., Rheol. Acta **8,** 277 (1969).
15. Schreiber, H.P., Rubin, A.J., J. Appl. Polym. Sci., **11,** 1043 (1967).
16. Medalia, A.I., J. Coll. Interf. Sci., **32,** 115 (1970).
17. Kaufmann, S., Slichter, W.P., Davis, D.D., J. Polym. Sci., A-2, **9,** 829 (1971).
18. Mullins, L., Rubber Chem. Technol., **42,** 339 (1969).

Acknowledgement

The author is indebted to the Staff of the Research and Development Division, Polymer Corp., Sarnia, Ontario, Canada for the generous supply of materials and information.

Chimica Chronika, New Series, 9, 201-205 (1980)

RING OPENING REACTIONS 1. THE TRIAZINONE RING OPENING OF 2H-3,4-DIHYDRO-as-TRIAZINO [3,4-b] BENZOTHIAZOL-3-ONE

MICHALIS D. KAZANIS and PANAYOTIS E. MACHERAS
Laboratory of Pharmaceutical Chemistry,
University of Athens, 104 Solonos Str., Athens 144, Greece.

Summary

The triazinone ring opening of the title compound 3 in the presence of aromatic aldehydes or ketones in hydrochloric acid or methanolic hydrochloric acid is described. The ir and nmr spectra of the resulting asymmetric azines 4 are given.

Key words: 2H-3,4-Dihydro-as-triazino [3,4-b] benzothiazol-3-one, 2-(4'-subst.-phenylidene) hydrazone-3-carb(ometh)oxymethylbenzothiazolines.

Introduction

As a part of a programme directed towards derivatives of 2-amino-benzothiazole with potential pharmacological activities, we studied the triazinone ring opening of 2H-3,4-dihydro-as-triazino [3,4-b] benzothiazol-3-one (3). Allen and Van Allan[1], in an attempt to synthesize 3-carbethoxymethyl-benzothiazoline-2-hydrazone (2a), treated 3-carbethoxymethyl-2-nitrosimino-benzothiazoline (1) with zinc in acetic acid, but the thiazinone 3 was formed instead of the desired hydrazone-ester 2a.

Hydrogenation of the nitrosiminoester 1 using palladium-charcoal catalyst afforded a mixture 2a and 3, which on heating in benzene or ethanol as well as in dillute hydrochloric acid gave exclusively 3[2] (Scheme 1, route a).

In this paper we report that the triazinone ring of 3 can be easily opened, affording the asymmetric azines 4, by treatment with hydrochloric acid or methanolic hydrochloric acid in the presence of aromatic aldehydes or ketones.

Results and Discussion

The required 2H-3,4-dihydro-as-triazino [3,4-b] benzothiazol-3-one (3) was synthesized according to a method described elsewhere[2], by heating under reflux 2-amino-3-carbethoxymethyl-benzothiazolium bromide[3] and hydrazine in ethanol.

Compound 3 was recovered unchanged after prolonged reflux with conc. hydrochloric acid or methanolic hydrochloric acid (see Experimental).

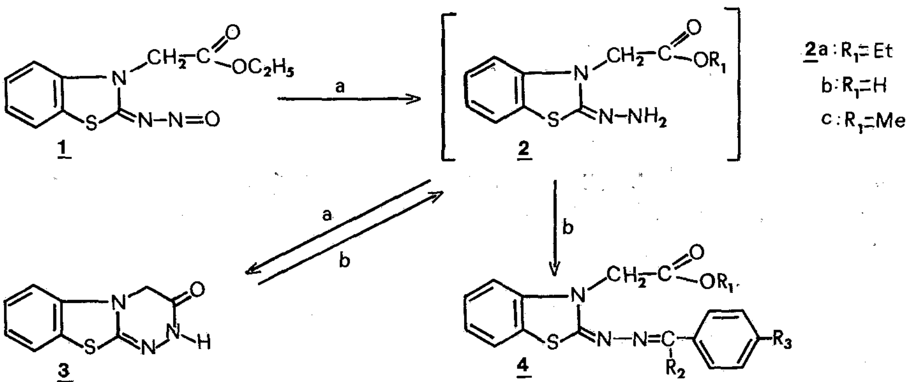

The triazinone ring opening of 3 was achived when refluxed with 4-subst.-benzaldehydes or -acetophenones in conc. hydrocloric acid (Scheme 1, route b), to give 2-(4' subst. -phenylidene) hydrazono-3-carboxymethylbenzothiazolines (Table I, 4a-h, R_1:H). When the reaction was carried out in methanolic hydrochloric acid the corresponding methyl esters, i.e. the 2-(4'-subst.-phenylidene) hydrazono-3-carbomethoxymethylbenzothiazolines where obtained. (Table I, 4i-p, R_1:CH_3)

The formation of the asymmetric azines 4 may be attributed to the postulated intermediates 2b and 2c, which in the absence of the carbonyl compounds recyclize to 3.

The structure of the azines 4 was confirmed by elemental analysis (Table I), ir and ^{1}H-nmr spectroscopy[4] (Table II).

All products 4 showed the characteristic vC=0 ir bands, the acid derivatives (R_1:H) at 1710 cm^{-1} – 1730 cm^{-1}, the esters (R_1:Me) at 1735 cm^{-1} – 1750 cm^{-1}.

In the ^{1}H-nmr spectra compounds 4 a, c, e, g, i, k, m, o, (R_2:H) showed a peak at δ= 8.27 - 8.50 ppm characteristic of the –N = C (H) –Ar formyl proton[5], while compounds 4b, d, f, h, j, l, n, p, (R_2:CH_3) showed a peak at δ= 2,38 - 2,46 ppm for the –N = C (CH_3) -Ar methyl group protons. In the case of compound 4h (R_1, R_2, R_3: CH_3) the protons of R_2, R_3 methyl groups gave one singlet at δ= 2.38 ppm. The peak of the ester methyl group protons of compounds 4 i-p (R_1:CH_3) appeared at δ= 3.72 - 3.78 ppm, while the peak of the ether methyl group of compounds 4g, h, o, p (R_3: OCH_3) appeared at δ= 3.84 - 3.85 ppm (Table II).

Experimental

I *Treatment of 2H-3,4-dihydro-as-triazino [3,4-b] benzothiazol-3-one (3) with a: conc. hydrochloric acid, b: methanolic hydrochloric acid.* An amount of 1.02 gr (5 mmol) of 3 in 50 ml conc. hydrochloric acid was heated under reflux for 24 hours. The resulting reaction mixture was cooled at r.t. and the precipitate filtered to give 0.95 gr of starting material, m.p. 260-262° C (Lit.[2]

TABLE I. *Compounds of general formula 4.*

	R_1	R_2	R_3	Yield %	Recryst. solvents	M.p.(°C)[6]	Molecular formula	Calculated/Found %C	%H	%N
a	H	H	H	65	THF—n-Hex	207-09	$C_{16}H_{13}N_3O_2S$	61.7 61.8	4.2 3.9	13.5 13.4
b	H	CH_3	H	95	THF—n-Hex.	192-98	$C_{17}H_{15}N_3O_2S$	62.8 62.5	4.7 4.8	12.9 12.7
c	H	H	NO_2	90	EtOH	196-98	$C_{16}H_{12}N_4O_4S$	53.9 54.0	3.4 3.4	15.7 15.7
d	H	CH_3	NO_2	95	EtOH	166-68	$C_{17}H_{14}N_4O_4S$	55.1 54.8	3.8 3.8	15.1 14.8
e	H	H	CH_3	95	THF—n-Pent.	220-21	$C_{17}H_{15}N_3O_2S$	62.7 62.5	4.6 4.6	12.9 13.1
f	H	CH_3	CH_3	75	THF—n-Pent.	184-86	$C_{18}H_{17}N_3O_2S$	63.7 63.6	5.0 5.2	12.4 12.2
g	H	H	OCH_3	80	THF—n-Pent.	210-11	$C_{17}H_{15}N_3O_3S$	59.8 59.7	4.4 4.5	12.3 12.2
h	H	CH_3	OCH_3	70	THF—n-Pent.	170-71	$C_{18}H_{17}N_3O_3S$	60.8 60.5	4.8 4.7	11.8 11.6
i	CH_3	H	H	80	C_6H_6	153-54	$C_{17}H_{15}N_3O_2S$	62.7 62.7	4.6 4.6	12.9 13.2
j	CH_3	CH_3	H	70	C_6H_6—n-Pent.	105-07	$C_{18}H_{17}N_3O_2S$	63.7 63.5	5.0 5.0	12.4 12.3
k	CH_3	H	NO_2	90	THF—n-Pent.	216-18	$C_{17}H_{14}N_4O_4S$	55.1 54.8	3.8 3.9	15.1 15.3
l	CH_3	CH_3	NO_2	90	THF—n-Pent.	187-88	$C_{18}H_{16}N_4O_4S$	56.2 55.9	4.2 4.3	14.6 14.7
m	CH_3	H	CH_3	95	C_6H_6—n-Pent.	136-38	$C_{18}H_{17}N_3O_2S$	63.7 63.9	5.0 5.1	12.4 12.3
n	CH_3	CH_3	CH_3	75	C_6H_6—n-Pent.	138-40	$C_{19}H_{19}N_3O_2S$	64.6 64.3	5.4 5.3	11.9 12.0
o	CH_3	H	OCH_3	95	THF—Et_2O	146-48	$C_{18}H_{17}N_3O_3S$	60.8 60.5	4.8 4.8	11.8 11.9
p	CH_3	CH_3	OCH_3	75	THF—Et_2O	143-45	$C_{19}H_{19}N_3O_3S$	61.8 61.8	5.2 5.2	11.4 11.2

260-261°C, 95% recovery). A mixture m.p. with 3 was undepressed. I.r. spectrum was identical with that of 3, ν C=O 1665 cm^{-1}. The same behavior was observed when methanol was added in the reaction mixture.

II. *2-(4′-subst.-phenylidene) hydrazono-3-carbomethylbenzothiazolines.*

(4, R_1:H). A suspension of 3 (1.02 gr 5 mmol) and 5 mmol of the appropriate benzaldeyde or acetophenone in 15 ml conc. hydrochloric acid was refluxed for 3 hrs. After cooling to room temperature the product was filtered off, washed several times with water, dried over P_2O_5 and recrystallized.

III. *2-(4′subst.-phenylidene) hydrazono-3-carbomethoxymethylbenzothiazolines.*

(4, R_1:Me). These derivatives were prepared in a manner similar to the above reaction, except that 20 ml methanol were added into the reaction mixture.

The physical constants, yields and solvents of recrystallisation are listed in Table I.

TABLE II. *Ir and nmr spectral data of Compounds 4.*

Compound	ν C=O cm^{-1}	^{1}H -nmr δ (ppm)
4a	1715	4.94 (s, 2H, CH_2), 7.25-7.92 (m, 9H, ar), 8.42 (s,1H,R_2)
4b	1710	2.44 (s,3H,R_2), 4.96 (s, 2H,CH_2), 7.22-7.99 (m, 9H,ar.).
4c	1730	4.92 (s,2H,CH_2), 7.05-8.13 (m,8H,ar.), 8.50 (s,1H,R_2).
4d	1725	2.46 (s,3H,R_2), 5.04 (s,2H,CH_2), 6.94-8.19 (m,8H,ar.).
4e	1710	2.35 (s,3H,R_3), 4.81 (s,2H,CH_2), 6.99-7.65 (m,8H,ar), 8.27 (s,1H,R_2).
4f	1725	2.36 (s,3H,R_3), 2.39 (s,3H,R_2), 4.90 (s,2H,CH_2), 7.04-7.82 (m,8H,ar.).
4g	1710	3.84 (s,3H,R_3), 4.86 (s,2H,CH_2), 6.98-7.76 (m,8H,ar.), 8.32 (s,1H,R_2).
4h	1710	2.41 (s,3H,R_2), 3.85 (s,3H,R_3), 4.95 (s,2H,CH_2), 6.95-7.94 (m,8H,ar.).
4i	1750	3.72 (s,3H,R_1), 4.99 (s,1H,CH_2), 7.13-7.83 (m,9H,ar.) 8.37 (s,1H,R_2).
4j	1750	2.40 (s,3H,R_2), 3.75 (s,3H,R_1), 5.02 (s,2H,CH_2), 7.03-7.93 (m,9H,ar.).
4k	1750	3.78 (s,3H,R_1), 5.09 (s,2H,CH_2), 7.06-8.17 (m,8H,ar.), 8.48 (s,1H,R_2).
4l	1750	2.45(s,3H,R_2), 3.78 (s,3H,R_1), 5.09 (s,2H,CH_2), 6.95-8.20 (m,8H,ar.).
4m	1745	2.36(s,3H,R_3), 3.74(s,3H,R_1), 4.99(s,2H,CH_2), 7.03-8.71(m,8H,ar) 8.34(s,1H,R_2).
4n	1735	2.38(s,6H,R_2 and R_3), 3.75(s,3H,R_1), 4.91(s,2H,CH_2), 7.01-7.08(m,8H,ar)
4o	1745	3.77(s,3H,R_1), 3.85(s,3H,R_3), 5.00(s,2H,CH_2), 6.95-7.80(m,8H,ar), 8.33(s,1H,R_2)
4p	1745	2.38(s,3H,R_2), 3.77(s,3H,R_1), 3.85(s,3H,R_3), 5.02(s,2H,CH_2), 6.92-7.93(m,8H,ar).

Περίληψη

Ἀντιδράσεις ἀνοίγματος δακτυλίου 1. Ἄνοιγμα τοῦ τριαζινικοῦ δακτυλίου τῆς 2H-3,4-διϋδρο-as-τριαζινο [3,4-b] βενζοθειαζολ-3-όνης.

Ἀναγωγὴ τῆς 3-καρβαιθοξυμεθυλο-2-νιτροζιμινοθειαζολίνης (1) μὲ ψευδάργυρο σὲ ὀξικὸ ὀξὺ δὲν ὁδηγεῖ στὴν ἀντίστοιχη ὑδραζόνη 2α, ἀλλὰ στὴν 2H-3,4-διϋδρο-as-τριαζινο [3,4-b] βενζοθειαζολ-3-όνη (3). Καταλυτικὴ ὑδρογόνωση τοῦ νιτροζιμινο-εστέρος 1 μὲ παλλάδιο-ἄνθρακα παρέχει μῖγμα τῶν 2α καὶ 3, τὸ ὁποῖον ὅταν θερμανθεῖ σὲ βενζόλιο ἢ αἰθανόλη ἢ ἀραιὸ ὑδροχλωρικὸ ὀξὺ δίδει ἀποκλειστικὰ τὴν as-τριαζινόνη 3[2] (Σχῆμα 1, πορεία a).

Βρασμὸς τῆς 3 σὲ πυκνὸ ὑδροχλωρικὸ ὀξὺ ἢ μεθανολικὸ ὑδροχλωρικὸ ὀξὺ ἐπὶ 24 ὧρες δὲν ὁδήγησε στὸ ἄνοιγμα τοῦ δακτυλίου, ἀλλὰ στὴν ἐπαναπόκτηση τῆς 3. Παρουσία ὅμως ἀρωματικῶν ἀλδεϋδῶν ἢ κετονῶν ὁ δακτύλιος τῆς 3 ἀνοίγει (Σχῆμα 1, πορεία b) γιὰ νὰ δώσει τὶς ἀσύμμετρες ἀζίνες 4 (Πίνακας I).

῾Ο σχηματισμὸς τῶν ἀσυμμέτρων ἀζινῶν 4 μπορεῖ νὰ ἀποδοθεῖ στὰ ἐνδιάμεσα 2b καὶ 2c τὰ ὁποῖα, ἀπουσία τῆς καρβονυλικῆς ἑνώσεως, ἐπανακυκλώνουν πρὸς τὴν 3.

῾Η ἐπιβεβαίωση τῆς δομῆς τῶν 4 ἔγινε μὲ τὴν βοήθεια ir καί ^{1}H-nmr φασματοσκοπίας (Πίνακας II).

References and Notes

1. Allen, C.F.H. and VanAllen, J.A.: J. Org. Chem., 13, 603 (1948).
2. Paollini, J.P.: J. Org. Chem., 33, 888, (1968).
3. Parric, J. and Pearson, K.: Chem. and Ind., 1261 (1970).
4. Ir spectra were recorded on a Perkin Elmer Model 177 spectrophotometer using nujoll mulls. ^{1}H-nmr spectra were determined on a 60 MHz instrument in DMSO (D_6), using TMS as internal standard.
5. Jackman, L.H. and Sternhell, S.: Application of Nuclear Magnetic Resonance Spectroscopy in Organic Chemistry, (2nd edition), p. 191, Pergamon, Oxford (1969).
6. Melting points were determined in a Büchi capillary melting point apparatus and are uncorrected.

Acknowledgements

We thank Dr. Ch. Stasinopoulou and Dr. S. Loukas, of N.R.C. «Democritos» for their assistance to nmr spectra determination. We are also indebted to the microanalytical lab. of CNRS (France) and CIBA-GEIGY (Switzerland) for the elemental analysis.

Chimica Chronika, New Series, 9, 207-216 (1980)

CHEMILUMINESCENCE DURING OZONATION OF POLYNUCLEAR HYDROCARBONS

JOHN NIKOKAVOURAS, CHRISTOS PAPADOPOULOS, ANN PERRY and GEORGE VASSILOPOULOS
Nuclear Research Center «Demokritos», Aghia Paraskevi Attikis, Greece.

Abstract

The chemiluminescence accompanying the ozone-oxidation of polynuclear hydrocarbons and derivatives is herein reported; optimum conditions for maximum quantum efficiency are established for the series naphthalene-anthracene-tetracene and anthracene-anthracenaldehyde-anthracenecarboxylic acid, resulting in chemiluminescence quantum yields of the order 10^{-5} einstein mole^{-1}. The fluorescence spectroscopy of reactants and products as well as the spectroscopy of the attendant chemiluminescence are also reported.

Key words: Chemiluminescence, Ozonation, Hydrocarbons.

Introduction

The present work was undertaken as a preliminary investigation of the ozone-oxidation of polynuclear hydrocarbons in order to establish whether such reactions result in light emission and if so, whether light emission is adequate to be employed as a tool in the determination of trace amounts of these hydrocarbons as pollutants. The work was then expanded to cover a study of the chemiluminescence of the series anthracene, 9-anthracenealdehyde, 9-anthracenecarboxylic acid to establish whether ozone-oxidation of a functional group on such hydrocarbons also leads to light emission.

Although the quantum yields of most nonbiological chemiluminescent reactions are quite low-quantum yields 10^{-5} -10^{-3} einstein · mole^{-1} are considered good-modern electronics has made possible very accurate measurements of extremely low light intensities so that chemiluminescence is rapidly becoming a very sensitive analytical tool. Chemiluminescence is already widely employed in the determination of ozone in the outer atmosphere, of various toxic gases in the working environment, of ATP in biological studies, of metals such as iron with a sensitivity higher than that of neutron activation analysis, in clinical chemistry, in forensic science, etc. On the other hand ozonation of polynuclear hydrocarbons higher than naphthalene was expected to proceed mainly via transanular ozonides as in the case with antracene[1], leading to quinones and fullfilling the energetic requirements for emission of light. In this case, the absolute number of photons measured can be correlated with the absolute number of reacting molecules through the quantum yield of luminescence. In addition, under certain conditions, the luminescence intensity can, be correlated with the concentration of the chemical species under study.

Results and Discussion

The chemiluminescence of the series naphthalene-anthracene-tetracene on reaction with ozone was studied in solution as described in the following section. The solvents employed were the lower alcohols, DMF, DMSO, chloroform, carbon tetrachloride and mixtures of chloroform-carbon tetrachloride. The solutions were made neutral or basic with small amounts of pyridine, piperidine, or acidic with a Lewis-acid as aluminum trichloride[2,3]. The highest quantum yields were obtained in a 1:1 chloroform carbon tetrachloride mixture both neutral and in the presence of aluminum trichloride and further study was continued under these conditions.

The light intensity-time diagrams obtained during ozonation of the three hydrocarbons are shown in Fig. 1. As expected, naphthalene ozonation is associated with quite low light intensity and low light sum, apparently due to the low fluorescence in solution of the hydrocarbon itself and that of the expected ozonation product. The order of intensities is tetracene >anthracene >naphthalene while the order of light sums is anthracene>tetracene>naphthalene. The

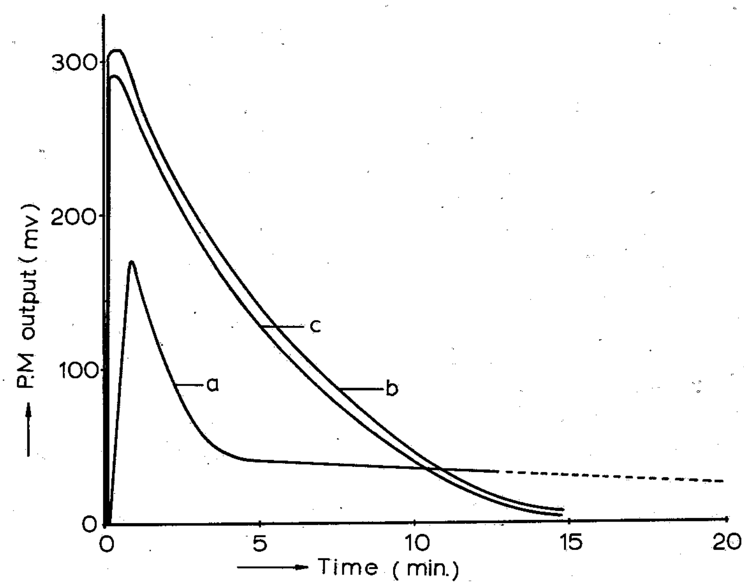

FIG. 1: *Light intensity-Time diagrams of the ozonation reactions of (a) Anthracene, (b) Tetracene and (c) Naphthalene.*

quantum yields measured were 3.3×10^{-5} and 1.0×10^{-5} einstein mole^{-1} for anthracene and tetracene respectively. The spectral distribution of the light emitted during the reaction as well as the fluorescence of reactants and products is shown in Fig. 2 for anthracene and Fig. 3 for tetracene. Comparison, in the case of anthracene, of the reactions' chemiluminescence spectra with the fluorescence spectrum of anthraquinone obtained under identical conditions reveals no resemblance, indicating that in this solvent ozonation of anthracene does not give rise to anthraquinone. Most likely, here, ozone's initial attack occurs at the 1,2-bond, the bond of lowest bond-localization energy, as is the case with osmium tetroxide[1] and then further attack is facilitated by the destruction of aromaticity.

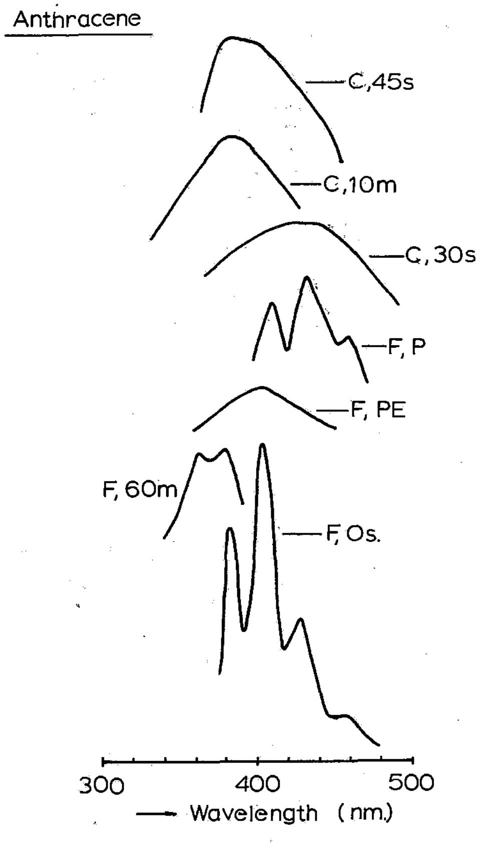

FIG. 2: *F.Os Fluorescence Spectrum of the anthracene reaction mixture before ozonation; F, 60m the same after ozonation for 60 min.; F, PE the same at the end of the chemiluminescence peak (Fig. 1); F, P the same at the chemiluminescence peak (excitation λ_{max} 330 nm); C, 30s chemiluminescence spectrum after ozonation for 30 sec.; C 45s the same after 45 sec.; C, 10m the same after 10 min.*

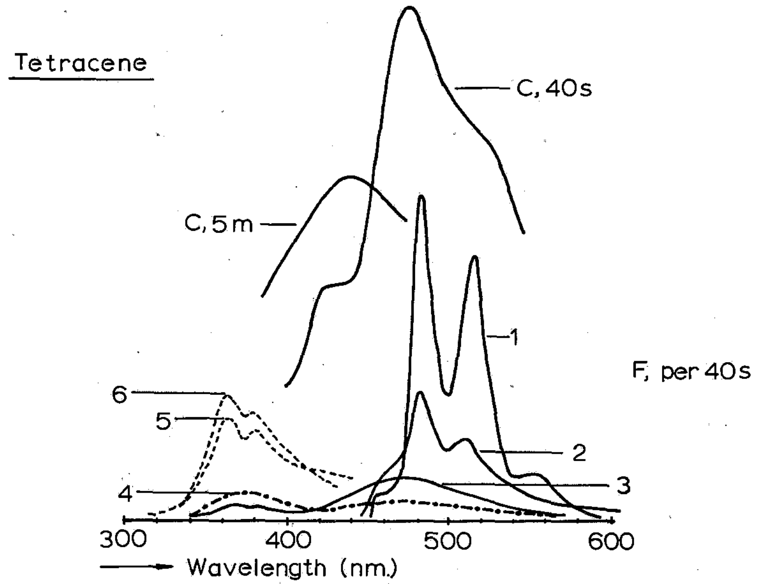

FIG. 3: *1, Fluorescence spectrum of the tetracene reaction mixture before ozonation; 2-6, fluorescence spectra run every 40 sec. as ozonation proceeds (spectra with dotted lines were obtained with increased sensitivity); C, 40s chemiluminescence spectrum after ozonation for 40 sec.; C, 5m the same after ozonation for 5 min.*

Regarding the emitting species, one ought to keep in mind that as a rule the reaction's chemiluminescence spectrum is theoretically identical with the fluorescence spectrum of the primary excited product as both emissions result from de-excitation of the same molecule. Although here we have a complicated situation arising from a multi-stepped reaction, in which we were unable to isolate and identify the product, some conclusions can be drawn, taking into account the intensity-time diagrams (Fig. 1) and the emission spectra (Fig. 2). The first conclusion is that we are dealing not with one, but with two light emissions, one associated with very fast light build-up and decay resulting in a sharp peak and then a second one associated with lower intensity and long duration. This is verified by the set of spectra (Fig. 2) as the reaction proceeds and can be explained in two ways. (a) Ozonation gives rise to the species emitting in the region of 360 nm (Fig. 2, F60m) followed by energy transfer to unreacted anthracene and subsequent emission by the hydrocarbon; then as the concentration of anthracene is diminished and the probability of energy transfer is reduced, the primary emission (C, 10m; F60 m) is de-masked. (b) A short-lived intermediate is produced emitting in the region of the anthracene fluorescence, which is rapidly transformed into a second intermediate through a non-chemiluminescent reaction path, the latter giving rise to the product associated with this emission

(C, 10m; F, 60 m). Explanation (a) is simple, elegant and well founded as energy transfer to and emission by, the reactant is a very common phenomenon in chemiluminescence, yet we are forced to adopt explanation (b) on account of the fluorescence-time diagram shown in Fig. 4. Indeed, here one sees a very fast removal of anthracene, a steady build-up of the product at 360 nm and an intermediate with fluorescence recorded at 500 nm.

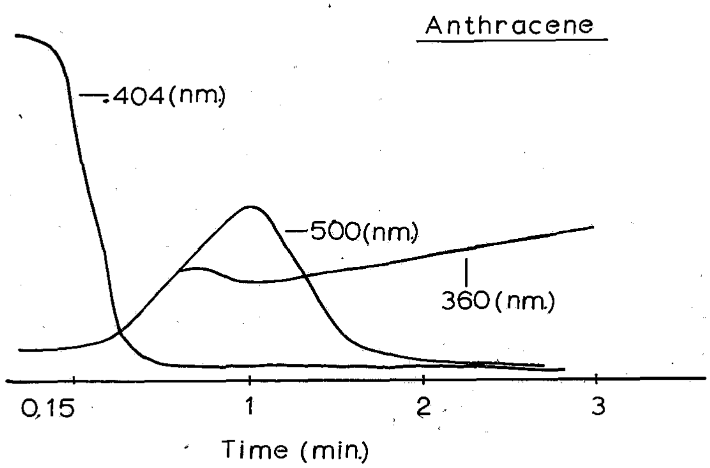

FIG. 4: *Fluorescence intensity-time diagrams at the wave-lengths indicated, as ozonation of an anthracene solution proceeds.*

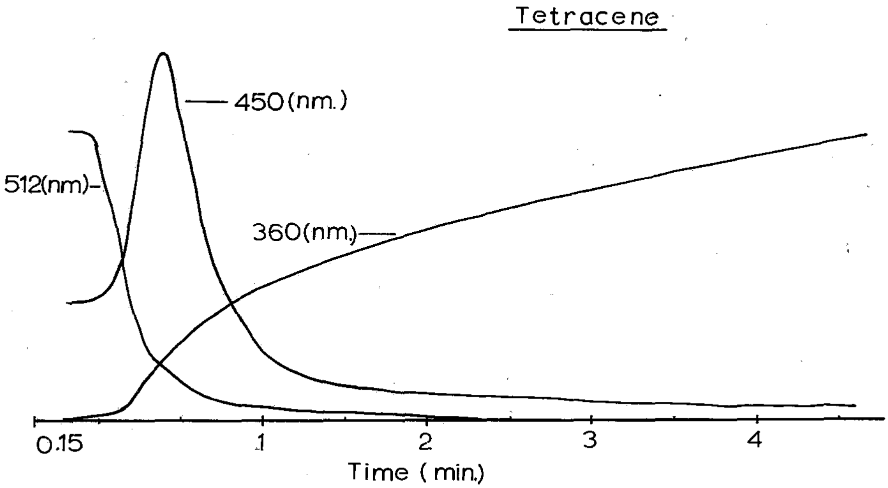

FIG. 5: *Fluorescence intensity-time diagrams at the wavelengths indicated as ozonation of a tetracene solution proceeds.*

Tetracene reacts in the same way as shown in Figure 1, 3 and 5 with one exception; here the chemiluminescence maximum centered at about 430 nm (Fig. 3; C, 5m), corresponding to the chemiluminescence of the valley (Fig. 1), does not shift to lower wavelengths with time indicating that, in the case of tetracene, this emission is due to the second presumed intermediate.

Quantum yields higher by about 20% were obtained on ozonation of the hydrocarbons in carbon tetrachloride in the presence of small amounts of aluminum trichloride, a Lewis acid which has been shown[2,3,4] to improve in certain cases the quantum efficiency of chemiluminescent ozonations. Here, two products were isolated from the anthracene reaction mixture, one of which was identified as anthraquinone, while the other, which we were unable to purify sufficiently for proper identification, was apparently the result of ozone attack at the side rings. Apparently, in the presence of a Lewis acid whose function is to increase the electrophilicity of ozone through formation of a Lewis acid-ozone complex, attack is facilitated at posistions 9 and 10 which are characterized by lowest atom-localization and para-localization energy[1]. The chemiluminescence associated with the reaction under such conditions is mainly due to formation of electronically excited anthraquinone as shown in Fig. 6 where a good match of the anthracene chemiluminescence spectrum and the anthraquinone fluorecence spectrum is easily observed.

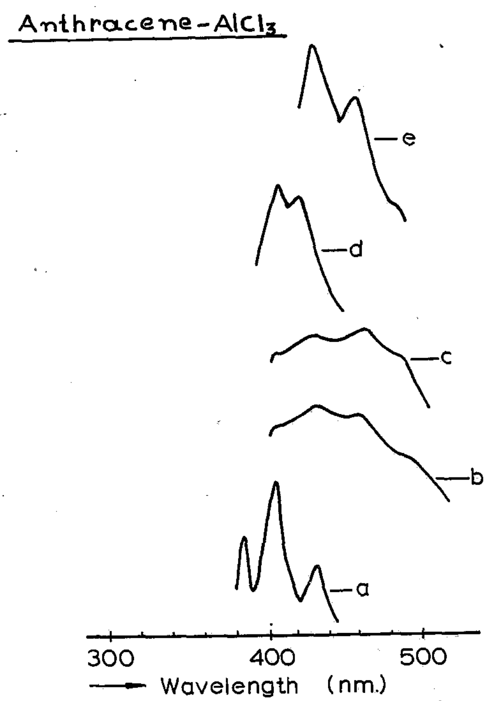

FIG. 6: *Fluorescence and chemiluminescence spectra of anthracene in the presence of* $AlCl_3$ *(a) fluorescence spectrum; (b) chemiluminescence spectrum; (c) anthraquinone fluorescence spectrum; (d) fluorescence spectrum of unidentified product. Excitation* λ_{max} *for fluorescence 300 nm.*

It was interesting to compare at this point the chemiluminescence of this reaction with that of the ozone oxidation of a corresponding aldehyde such as 9-anthracenaldehyde, expected to be chemiluminescent as it has been shown that ozonation of aromatic aldehydes leading to fluorescent-acids is a chemiluminescent process[5,6]. Indeed, ozonation of 9-anthracenaldehyde is a chemiluminescent reaction, but the same is true for 9-anthracenecarboxylic acid, the expected product as can be seen in Fig. 7, where the chemiluminescence intensity-time diagrams are presented together with that of anthracene for comparison.

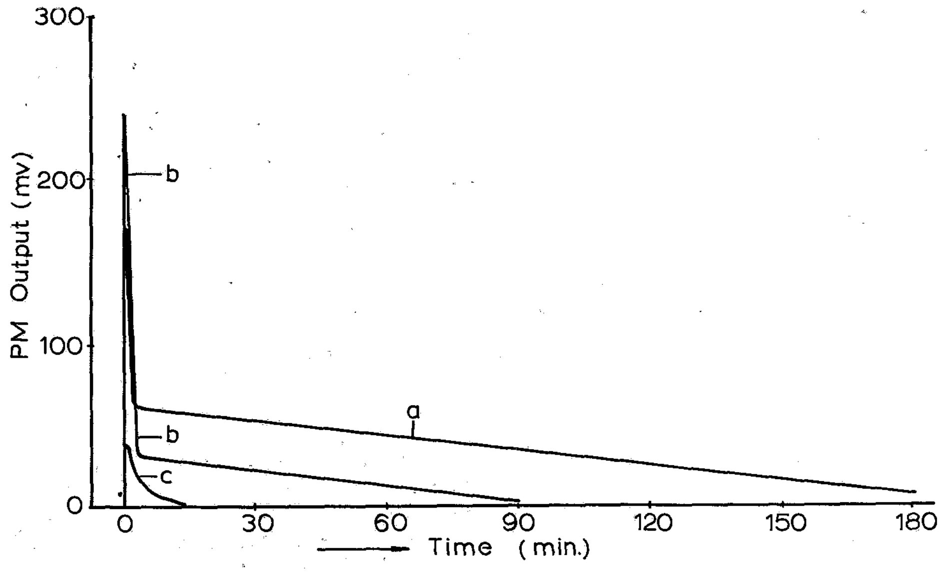

FIG. 7: *Light intensity-time diagrams during the ozonation of (a) anthracene, (b) 9-anthracenaldehyde, (c) 9-anthracenecarboxylic acid.*

Various solvents were again employed in this case and best results were obtained when the reactions were conducted in carbon tetrachloride in the presence of aluminum trichloride. It should be noted here that although the light intensities, due to the aldehyde and the acid, are stronger than that of anthracene, the quantum yield of the anthracene light reaction is much higher due to the longer duration of light emission. Comparison of the emissions' spectra (Fig. 8) reveals that unlike the chemiluminescence accompaying ozonation of mononuclear aromatic aldehydes, in this case, oxidation of the aldehyde to the acid contributes little, if at all, to the total light sum, chemiluminescence mainly arising from attack at the side rings resulting eventually to the same excited product for both aldehyde and acid (Fig. 8; c.f.), followed by energy transfer back to the starting material (Fig. 8; a.b.d.e.).

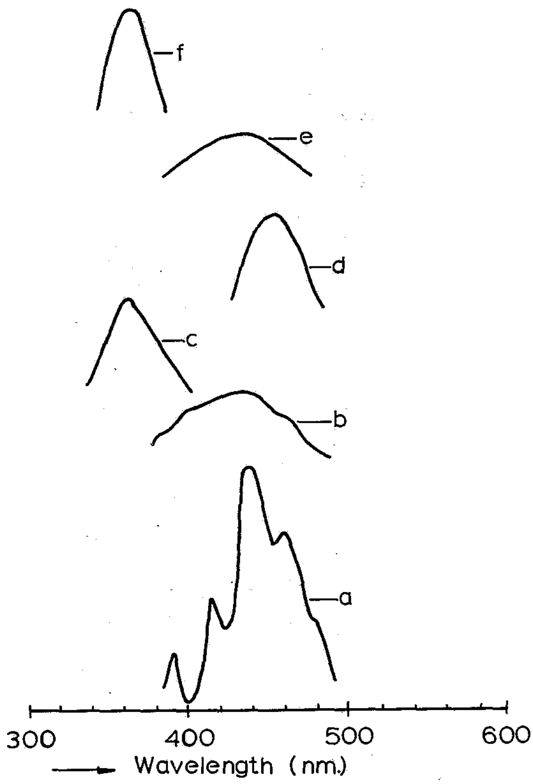

FIG. 8: *(a) Fluorescence spectrum of 9-anthracenaldehyde under conditions of the chemiluminescent reaction; (b) Chemiluminescence spectrum of the 9-anthracenaldehyde light reaction after ozonation for 12 min.; (c) fluorescence spectrum of the 9-anthracenaldehyde reaction mixure after ozonation for 15 m. (d) fluorescence spectrum of 9-anthracenecarboxylic acid under conditions of the chemiluminescent reaction; (e) chemiluminescence spectrum of the 9-anthracenecarboxylic acid light-reaction after ozonation for 10 min.; (f) fluorescense spectrum of the 9-anthracenecarboxylic acid reaction mixture after ozonation for 10 min.*

Conclusions

Ozonation of the polynuclear hydrocarbons examined gives rise to chemiluminescence. With exception of napthalene, the chemiluminescence of the other hydrocarbons is fairly efficient and an analytical method based on chemiluminescence would, in principle, be able to determine quantities of the order of 10^{-6} g. Light reaction in the presence of a Lewis acid leads mainly to electronically excited quinones while in the absence of a Lewis acid the primary excited species is the result of repeated ozone attack at the side rings. Unlike ozonation of mononuclear aldehydes, here ozonation results in chemiluminescence mainly from attack at the ring system. Finally, it is expected that higher hydrocarbons will be more efficiently chemiluminescent due to the stronger fluorescence of both the hydrocarbons themselves and their reaction products.

Experimental Techniques

Production of Ozone: A self-constructed Siemens-type Ozonator was employed giving an ozone-air mixture 0.26% v/v at a flow rate of 340 ml · $min.^{-1}$.
Light Intensity-Time Diagrams: Ozonized air was passed through the reaction mixture in a glass vessel positioned in front of an EMI 9514 B photomultiplier tube operating at 900V and connected with a Varian F-80 recorder. This reaction vessel-photomultiplier system was housed in a self constructed dark chamber with suitable inlets for gaseous and/or liquid reagents. Measurements were conducted with very freshly prepared 20 ml, 10^{-5}M samples of the compounds (spectroscopy grade) under study, in the appropriate solvent; when employed, other reagents such as pyridine, piperidine, aqueous sodium hydroxide e.t.c., were squirted into the solution just prior to the passage of ozone with the aid of a light-proof syringe. When $AlCl_3$ was employed, it was added in the same way as a 1% ethanolic solution (0.2ml).
Chemiluminescence Quantum Yields: The light intensity-time curves recorded in the course of the reaction were integrated with the aid of a very accurate planimeter and the areas obtained were compared with the area recorded during the standard[7,8] luminol light reaction under the same optical geometry. Correction of the light-sums obtained, on account of the S-11 photocathode's spectral response were unnecessary as the chemiluminescence of both reactions roughly falls in the same spectral region. Corrections due to self absorption were also unnecessary as there was very little absorption at the spectral region of the emissions.

Spectra: Excitation and fluorescence spectra were recorded on an Aminco-Bowman spectrophotofluorometer calibrated with a quartz «pen-ray» lamp and are uncorrected. Percent transmittance was determined with the aid of a Cary 14 spectrophotometer while infrared spectra were run on a Perkin-Elmer 521 spectrophotometer. Chemiluminescence spectra were recorded on the spectrophotofluorometer employing fast scanning rates and wide slits, with the excitation source off, at reasonably flat sections of the intensity-time diagrams and were verified by a series of intensity-time diagrams, with the emission monochromator set at intervals of 10nm. The same instrument was employed to follow the fluorescence of reactants and products at selected wavelengths as the reactions proceeded.

Περίληψη

Χημιφωταύγεια κατὰ τὸ ὀζονισμὸν πολυπυρηνικῶν ὑδρογονανθράκων

Περιγράφεται μελέτη τοῦ ὀζονισμοῦ πολυπυρηνικῶν ὑδρογονανθράκων σὲ διάλυμα μὲ σκοπό (α) τὴ διερεύνηση τοῦ κατὰ πόσο μιὰ τέτοια ἀντίδραση συνοδεύεται ἀπὸ ἐκπομπὴ φωτὸς καί (β) κατὰ πόσο οἱ φωτεινὲς ἐντάσεις καὶ ἀ-

ποδόσεις αὐτῶν τῶν ἀντιδράσεων εἶναι ἐπαρκεὶς προκειμένου νὰ χρησιμοποιηθοῦν στὸν προσδιορισμὸ μικροποσοτήτων τέτοιων ὑδρογονανθράκων σὲ συσχετισμὸ μὲ τὴ ρύπανση τοῦ περιβάλλοντος. Ἡ ἐκπομπὴ φωτὸς κατὰ τὸν ὀζονισμὸ τοῦ ναφθαλινίου εἶναι μικρή. Ἀντίθετα ὀζονισμὸς τοῦ ἀνθρακενίου καὶ τετρακενίου συνοδεύεται ἀπὸ χημιφωτάυγεια μὲ φωτονιακὲς ἀποδόσεις τῆς τάξεως τοῦ 10^{-5} Ἀϊνστάϊν ἀνὰ γραμμομόριο. Τόσο οἱ φωτεινὲς ἐντάσεις ὅσο καὶ τὰ φωτεινὰ ἀθροίσματα θεωρητικὰ ἀρκοῦν γιὰ ἀκριβεῖς προσδιορισμοὺς ποσοτήτων τῆς τάξεως τῶν 10^{-6} γραμμαρίων. Ὀζονισμὸς παρουσία τριχλωριούχου ἀργιλίου ἔχει σὰν ἀποτέλεσμα ἐκπομπὴ ἀπὸ ἠλεκτρονικὰ διεγερμένη κινόνη ἐνῶ ἀπουσία του, ἡ φωτεινὴ ἐκπομπὴ προέρχεται ἀπὸ προσβολὴ πλευρικῶν δακτυλίων. Ἀντίθετα μὲ ὅτι συμβαίνει σὲ ὀζονισμοὺς ἁπλῶν ἀρωματικῶν ἀλδεϋδῶν, ἐδῶ ἡ χημιφωταύγεια ὀφείλεται κυρίως σὲ προσβολὴ πλευρικῶν δακτυλίων καὶ ὄχι σὲ ὀξείδωση τῆς ἀλδεΰδης πρὸς ὀξύ.

References

1. Baily, R.S., Chem. Reviews **58B**, 962, (1958).
2. Nicokavouras J. and Vassilopoulos G., Z. Physik. Chem. N.F. **89**, 181, (1974).
3. Nikokavouras J. and Vassilopoulos G., Z. Physik Chem. N.F. **91**, 36, (1974).
4. Nikokavouras J. Vassilopoulos G. and Kanaghinis O., Z. Physik. Chem. N.F. **94**, 31 (1975).
5. Nikokavouras J. and Vassilopoulos G., Z. Physik Chem. N.F. **78**, 325, (1972).
6. Nikokavouras J. and Vassilopoulos G., Z. Physik. Chem. N.F. **84**, 131, (1973).
7. Lee J., Wesley A.S., Ferguson J.F. and Seliger H.H., Bioluminescence in Progress, p. 35. Princeton: Princeton University press. 1966.
8. Lee J. and Seliger H.H., Photochem. and Photobiol. **15**, 227, (1972).

Chimica Chronika, New Series, 9, 217-228 (1980)

STUDIES ON GLYCOSPHINGOLIPIDS OF LECTIN-STIMULATED HUMAN LYMPHOCYTES
II. SURFACE LABELING ON THE PLASMA MEMBRANES*

GREGORY P. EVANGELATOS, CATHERINE VAKIRTZI-LEMONIAS and VASSILIOS M. KAPOULAS
Biology Department, Nuclear Research Center Demokritos, Aghia Paraskevi Attikis, Athens, Greece, and Department of Biochemistry, University of Ioannina, Ioannina, Greece.

Abbreviations: PHA, phytohemaglutinin; GSLs, glycosphingolipids; GL_1, glucosyl-ceramide; GL_2, lactosyl, ceramide; GL_3, galactosyl-lactosyl ceramide; GL_4, globoside; GM_3, hematoside, Sialic-acid-lactosyl-ceramide; GM_1, galactose-N-acetyl galactosamine (sialic acid)-lactosyl ceramide, G_{D1a}, sialic acid-galactose-N-acetylgalactosamine-(sialic acid)-lactosyl ceramide; G_{D1b}, galactose-N-acetylgalactosamine-(sialic acid-sialic acid)- lactosyl-ceramide; PBS, phosphate buffered saline.
Enzymes: Galactose oxidase (E.C. 1.1.3.9)
Neuraminidase (E.C. 3.2.1.18).

Summary

The galactose oxidase-tritiated sodium borohydride method was used for labeling the galactosyl and galactosaminyl moieties of glycosphingolipids present on the surface of normal and phytohemaglutinin-stimulated human lymphocytes. Nonspecific labeling detracts from the applicability of this method in studies with lymphocytes, except if the cells are treated with unlabeled borohydride prior to galactose oxidase attack and the results are based on the percent recovery of the label in galactosyl and galactosaminyl residues by preparative gas liquid chromatography.

Significant specific labeling by the above method was detected only in globoside and disialoganglioside of the G_{D1a} type, as could be judged by their thin layer chromatographic mobility, but no qualitative differences between normal and phytoemaglutinin-stimulated lymphocytes were found. Gas liquid radiochromatographic analysis has further shown that labeling of galactosaminyl residues in all cases was negligible, whereas galacrose contained nearly all the specific label of both, globoside and G_{D1a}, (60% and 40% of the total respectively). It is postulated that galactosaminyl moieties of glycosphingolipids of the lymphocyte membrane surface are in a «cryptic» location, non-available to galactose oxidase attack.

---

* This work was taken in part from the doctoral dissertation of Gregory P. Evangelatos approved by the School of Natural Sciences, National University of Athens, Athens, Greece.

Introduction

Lymphocytes are relatively rich in glycosphingolipids [1-4] localized preferably in the plasma membranes [4], where they contribute considerably in the specificity of receptor sites [5] and of antigenic properties [6], as well as in the regulation of mitotic division through cell contact inhibition [7], and in cell proliferation [4, 8]. The main body of evidence concerning the aforementioned role of glycosphingolipid components of the lymphocyte membrane has been documented by following the alterations of the glycosphingolipid content and composition [4,7], or of the rates of total and individual glycosphingolipid metabolism [8-11] connected with cell physiology. Such a relationship is more generally accepted on the basis that glycosphingolipid patterns in mammalian cells show the greatest organ and species specificity than any other lipid class [4, 12-19].

However, apart from the chemical composition of membrane components, the specificity of cell surface for receptor or antigenic activity, and for intercellular recognition is mainly determined by the organizational status of these molecules on the plasma membrane. Although the majority of cellular glycosphingolipids are in plasma membranes, the first direct evidence with respect to whether and to which extent their carbohydrate moieties are exposed to the external environment, as well as to the possible change in exposure with change in surface function or with surface bound ligands (e.g. lectins, antisera etc.) has been provided by Gahmberg and Hakomori [20]. These investigators developed a method using galactose oxidase [21-23] attack on the carbon 6 of galactosyl and galactosaminyl residues of glycosphingolipids (and glycoproteins), followed by reduction with tritiated sodium borohydride, which allowed the specific labeling of the mentioned sugar residues of the cell surface exposed to the external environment of human erythrocytes [20].

In the course of a research program on the membrane structures and function of human peripheral lymphocytes we have applied the galactose oxidase-NaB^3H_4 method to study any possible changes in availability to this probe of the lipid-bound carbohydrates of lymphocyte membranes connected with their increased mitogenic activity when stimulated by lectines. This possibility was strongly suggested by previously observed extensive enhancement of GSL metabolism in lectin-stimulated cells in comparison to normal or «resting» lymphocytes [9,11], as well as by existing evidence that the membrane GSL patterns show significant differences between normal and leukemic [2,3] or malignant lymphoid [4] cells.

This paper presents the details of reported preliminary data on these lines [24] along with additional evidence concerning the characterization of the labeled products effected through a number of misleading results caused by nonspecific labeling.

Experimental Methods

Materials

Unlabeled sodium borohydride, galactose oxidase (EC 1.1.3.9) of *Polyporus circinatus,* neuraminidase (EC 3.2.1.18) from *Clostridium perfringens* (Type V) bovine brain ganglioside standards (type III) were purchased from Sigma Chemicals Co., USA; NaB^3H_4 (6 Ci/mmole) was supplied by the Radiochemical Centre Amersham, England. All other reagents and media used in this work were described elsewhere [25].

Isolation and cultivation of lymphocytes

Blood from healthy donors was collected in heparinized botlles (8-10 units/ml, final concentration), and lymphocytes were isolated by the Ficoll-Hypaque density gradient centrifugation method [25, 34]. Media were sterilized prior to use by Millipore filtration (4-7-mm HAWP 04700), and all manipulations thereafter were performed under sterile conditions, mostly in siliconized screw caped vials. Isolated lymphocytes were washed three times with PBS or Eagle's minimal medium (pH 7.2), submitted to a short (30 sec) treatment with 0.1N acetic acid to remove any remaining erythrocytes, and washed again with PBS. For cultivation, 0.3-0.4 ml of packed cells were suspended in Eagle's minimal medium, pH 7.2; containing 20% fetal calf serum, penicillin (200 units/ml), streptomycin (100 units/ml) and, when indicated, PHA (170 μg/ml). The suspension was diluted to a cell density of 10^6 cells/ml, monitored by counting in a Neubauer hematocytometer, and cultured at 37° for 48 hr. At the end of this period, PHA stimulated lymphocytes were washed with Eagle's minimal medium and used as the normal cells for labeling.

Surface labeling

The original method of Gahmberg and Hakomori [20], devised for red cells, was essentially applied in the present work, with the following minor modifications in order to minimize nonspecific labeling. These modifications included treatment of lymphocytes with unlabeled $NaBH_4$ prior to galactose oxidase attack, and use of tritiated sodium borohydride of very high specific activity. In detail:

The cell cultures prepared as described above were mixed with 20-40 μl of $NaBH_4$, in 0.1N KOH, to give a final concentiation of 12 μg per ml of cell suspension and incubated for 30 min at 37°. Then, the cells were harvested by centrifugation, washed twice with 2 ml PBS, resuspended in 1 ml PBS and divided in two halves, each corresponding to 0.15-0.20 ml of the original packed cell volume. To the one of the above halves, 40 units of galactose oxidase (EC 1.1.3.9, Sigma, *Polyporus circinatus*) were added, and incubated at 37° for 180 min under continuous shaking. The enzyme was removed by three washings with PBS, the cells were resuspended in 1 ml PBS and to both samples (the galactose oxidase treated, and the untreated control) 2-3 mCi of NaB^3H_4 (6 Ci/nmole) were added. After 30 min at room temperature, the cells were washed at least 5 times with PBS and their lipids extracted.

Isolation of glycosphingolipids

Total lipids were extracted from the cells according to the method of Folch *et al.* [26]. The lower chloroform layer, containing the neutral GSLs and most of the hematoside [25], was submitted to mild alkaline hydrolysis [27] followed by Folch partition. The new chloroform layer was evaporated to dryness, and fractionated on a silicic acid column (7×mm × 10cm) eluted with chloroform (12 ml), ethyl acitate (6 ml), and acetone-methanol, 9:1 (35 ml) plus chloroform-methanol, 1:1 (20 ml). The combined two last eluates, («3rd fraction»), contained the neutral GSLs and about 90% of the hematoside [25].

The aqueous phase of the original Folch extract, containing the residual hematoside and the more complex gangliosides, were dialyzed at 4° overnight against four changes of distilled water. Bovine brain gangliosides (Sigma, type III) were added as carriers to the mixture prior to dialysis, in order to prevent losses of the labeled material [29]. The dialyzed sample was lyophilized, and fractionated on a silicic acid column eluted with chloroform (12 ml). acetone-methanol, 9:1 (25 ml), and acetone-methanol, 1:1 (25 ml) to elute the acidic GSLs [25].

Thin layer radiochromatography

Thin layer chromatographic separations were performed on precoated Silica gel G plates (Merck) activated at 110° for 1 hr prior to use. Neutral GSLs were resolved in the system chloroform-methanol-water, 65:25:4, at 16° (standards were spotted along with the unknowns). Acidic GSLs were resolved in the system chloroform-methanol-2.5N ammonia, 60:40:9 (two developments, with thorough drying in between).

Localization of radioactive GSLs on developed chromatoplates was effected by autoradiography, using Kodak films No PE 4006, with an exposure period of 2-3 weeks. Measurement of the distribution of radioactivity among the various GSLs was accomplished by scraping the desired areas off the chromatoplates into small separatory funnels containing a layer of Celite over a cotton plug, and after addition of 1-2 drops of water to deactivate the adsorbent, the labeled GSLs were eluted with chloroform-methanol (1:1) and methanol. A portion of these eluates was saved for further analysis (see below). Radio-activity was assayed on aliquots of the above eluates evaporated in the scintillation vials by a stream of nitrogen, after addition of 10 ml of a toluene base scintillation fluid [29], on a Packard Tri-Carb (model 3385) liquid scintillation counter. The efficiency of the instrument was 49% for tritium, and monitoring for quenchning was effected by external standardization. Water-soluble radioactive products were counted in 10 ml of Packard emulsifier Insta-Gel.

Preparative gas liquid radiochromography

Localization of the specific labeling of the glycosyl moieties of the various GSL fractions purified by preparative thin layer chromatography was accomplished essentially by the method of Yu and Ledeen [30]. The samples were hydrolyzed by mild acidic methanolysis [31] followed by re-acetylation of the amino groups of hexosamines [32], and the O-trimethylsilyl derivatives of the monosaccharides were prepared according to Sweeley and Walker [33]. Lactose and N-acetyl-galactosamine were added as internal standards prior to the methanolysis step, to serve also as carries preventing loss of label.

Gas liquid chromatography was performed on a glass, 180cm × 3mm (id), column of 3% SE-30 on acid washed Chromosorb G, DCMG. Samples eluted from the column were collected in capillary tubes frozen in liquid nitrogen, and the radioactive products were recovered by washing down from the capillary tubes into scintillation vials. By using tritiated galactose, glucose, and N-acetyl-glucosamine in levels similar to those available in the unknown samples, the recoveries from the column by this technique was about 80%. On this basis, all data were corrected in order to calculate the total recovery of the specific labeling (see below).

Results

The steps of the procedure followed for the successive isolation of normal and PHA-stimulated lymphocytes, labeling of the galactosyl and galactosaminyl moieties exposed to the external cell environment, and for the isolation and purification of the labeled neutral and acidic GSLs are outlined, in a flow-sheet form in Fig. 1. Data on the radioactivities recovered at various steps of this procedure, after extraction of the lipids labeled by NaB^3H_4 from lymphocytes either pre-treated with galactose oxidase, or not, are depicted in Table I.

Nonspecific labeling

As described in the Methods section, some minor albeit necessary modifications of conventional procedures were applied in the present investigation in order to overcome a series of experimental problems. In a first place, lymphocytes isolated by the Ficoll-Hypaque density-gradient centrifugation method [34], were submitted to a short (30 sec) treatment with dilute acetic acid to ensure the removal of any residual erythrocytes. The use of erythrocyte-free lymphocytes was considered of outmost importance because the galactose oxidase NaB^3H_4 method used in this work has been shown to label effectively the GSLs exposed on the external surface of erythrocyte membranes [20].

A second modification concerns the 30 min treatment of cells with unlabeled $NaBH_4$ prior to their attack by galactose oxidase. This treatment was found to eliminate a considerable portion of non-specific labeling, according to data obtained in the course of preliminary experimentation.

However, nonspecific labeling has been one of the most serious experimental problems met during the present investigation, which at last limits significantly the applicability of the galactose oxidase-NaB^3H_4 technique. This

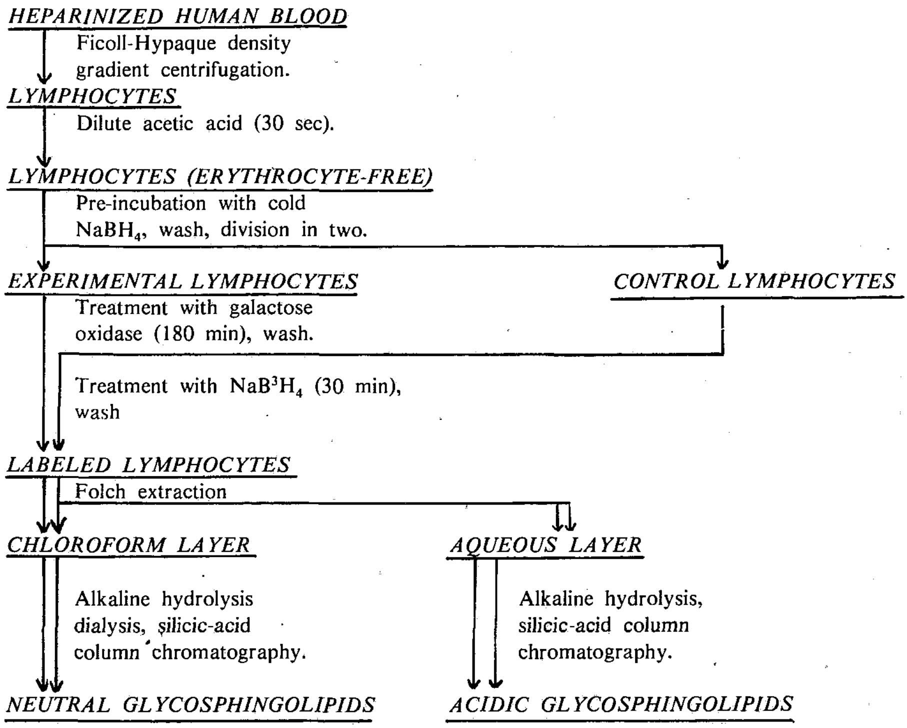

FIG. 1: *Flow sheet of successives teps for surface labeling of human lymphocytes, followed by isolation, fractionation and purification of the labeled neutral and acidic GSLs. PHA stimulation, when indicated (see text), was performed prior to preincubation with dilute acetic acid.*

is evident by the excessive amounts of nonspecific radioactivity present until the final stages of GSL purification, especially striking in the case of lymphocytes unexposed to galactose oxidase attack (see Table I).

Main source of this nonspecific labeling seems to be a great number of exchange reactions. This assumption is strengthened by the finding that the label recovered even originally in the GSL fractions depends on the radioactivity of the sodium borohydride added in a manner which cannot be correlated with the total or/and the specific radioactivity of the added borohydride. More complicated is of course the problem with the gangliosides which are isolated from the aqueous phase after Folch partition, and therefore contain the unreacted borohydride. In other words, the factors influencing the nonspecific labelling differ from experiment to experiment in an unpredictable manner.

Under these circumstances, it is evident that nonspecific labeling may be also unpredictably high even in the pure GSL fractions obtained by eluting the radioactive zones from preparative chromatoplates. Therefore, the only safe way to evaluate the specific labeling of individual GSLs should be based on

TABLE I: *Radioactivity (cpm × 10^{-3}) recovered at various steps during isolation of labeled glycosphongolipids.*
Experiments A, B and PHA (the latter with PHA-stimulated lymphocytes) were performed with 0.20, 0.15, and 0.15 ml of packed cells respectively, pretreated with unlabeled $NaBH_4$ see Methods). After their exposition to galactose oxidase (40 units), the above samples and their respective controls (unexposed to galactose oxidase) were treated with 10^9, 3.6 × 10^9 and 9.2 × 10^9 cpm of $NaBH_4^3$ respectively. Data of controls are given in brackets following the values of the respective galactose-oxidase treated samples.

Preparative step	Exp. A	Exp. B	Exp. PHA
1. Folch-Chloroform extact	9300 (6800)	24600 (30400)	4300 (4200)
2. Alkaline hydrolysate	8000 (4500)	10700 (12600)	4200 (4100)
3. Column fraction 1	1600 (1000)	1400 (2100)	250 (120)
4. Column fraction 2	100 (500)	2400 (5100)	200 (150)
5. Column fraction 3	2300 (1500)	6700 (5200)	3800 (1300)
6. Preparative TLC	151 (67)	2517 (1105)	3700 (1250)
7. Folch-Aqueous phase	1270 (340)	10000 (11000)	5300 (3500)
8. Dialyzed alkaline hydrolyzate	114 (29)	499 (474)	640 (390)
9. Column fraction 3	107 (24)	282 (158)	550 (190)
10. Preparative TLC		274 (150)	540 (182)

TABLE II: *Total radioactivity incorporated into individual glycophingolipids purified by preparative TLC.*
Neutral and acidic glycosphingolipids isolated by silicic-acid column chromatography were purified by preparative TLC as described in the Methods section. Total radioactivity recovered in each individual component is expressed as cpm × 10^{-3}. Numbers in parentheses correspond to respective values of controls (non-exposed to galactose-oxidase action).

Exp.	GL_1	GL_2	GL_3	Globoside	Hematoside	Ganglioside (GD_{1a})
A	7 (7)	16 (7)	27 (15)	88 (25)	12 (13)	ND
B	375 (312)	243 (217)	458 (398)	1375 (145)	66 (33)	274 (150)
PHA	210 (220)	220 (310)	270 (330)	1870 (330)	130 (60)	540 (182)

quantitative estimations of the label localized in the galactosyl and galactosaminyl residues of these lipid components. For this purpose, preparative gas liquid radiochromatographic analysis was carried out under conditions standardized with respect to the overal efficiency of the column, thus permitting an accurate calculation of the radioactivity recovered in the collected eluates as percent of the total counts injected. As indicated in Table III, very low recoveries of radioactivities injected into the column were the result of extensive nonspecific labeling in the smaller neutral GSL molecules, thus justifying our predictions as to the necessity of this further analytical step.

TABLE III: *Percentages of specific labeling of purified individual glycosphingolipids.*
The trimethylsilyl sugar derivatives of each individual GSL recovered by preparative TLC were quantified by GLC and the radioactivity recovered in each GLC-fraction (see Fig. 2) is expressed as percent of the total radioactivity injected. Numbers in parentheses correspond to respective percentages of controls (non-exposed to galactose-oxidase attack).

GLC-fraction	Experiment	Specific labeling (% of injected into column) GL_1	GL_2	GL_3	GL_4+G_{M3}	G_{D1a}
2 (Gal)	A	...	...	...	60.0 (ND)	42.0 (ND)
4 (GalNAC)	A	...	...	...	5.9 (ND)	2.2 (ND)
2+4 (sum)	A	...	...	...	65.9 (ND)	44.2 (ND)
1	B	3.3 (0.1)	1.9 (0.8)	1.9 (2.0)	3.9 (0.6)	5.2 (5.2)
2 (Gal)	B	6.3 (1.7)	4.1 (4.6)	4.2 (2.4)	59.8 (8.4)	40.1 (5.5)
3 (Glc)	B	2.7 (0.5)	2.1 (2.1)	1.4 (1.7)	3.4 (3.6)	1.7 (1.1)
4 (GalNAc)	B	...	...	...	10.9 (7.1)	3.1 (1.2)
5	B	4.5 (0.9)	2.0 (4.3)	5.5 (3.5)	5.9 (10.1)	2.5 (7.1)
2+4 (sum)	B	6.3 (1.7)	4.1 (4.6)	4.2 (2.4)	70.7 (15.5)	42.6 (6.7)
Total	B	16.8 (3.2)	10.1 (9.5)	13.0 (9.6)	83.9 (29.6)	52.6 (30.0)
2 (Gal)	PHA	...	...	...	60.2 (5.2)	41.2 (6.1)
4 (GalNAc)	PHA	...	...	...	10.7 (6.1)	4.1 (2.0)
2+4 (sum)	PHA	...	...	...	70.9 (11.3)	45.3 (8.1)

Labeling pattern of neutral- and acidic GSLs

Typical autoradiograms obtained after thin layer chromatographic separation of the purified neutral- and acidic-GSL fractions (isolated respectively from the chloroform and water phase of the original Folch extraction) are illustrated in Fig. 2. Neutral GSLs yielded one major radioactive zone, the most intense part of which migrated with an R_f slightly lower than the globoside standard (Fig. 2A). The true nature of this labeled component was clarified by neuraminidase treatment on an aliquot of this fraction, followed by Folch partition and re-chromatography of the products [32]. Only negligible amounts of labeled hematoside were identified by this technique (see Table II), while the chloroform soluble product of the neuraminidase treatment co-chromatographed with globoside standards (Fig. 2B).

On the other hand, as shown in Fig. 2C, the purified acidic GSL fraction yielded disialoganglioside of the type C_{D1a} as the single specifically labeled component.

The radioactivity distribution into the zones of chromatoplates corresponding to individual GSLs are depicted in Table II. These data show that differences between counts recovered from galactose oxidase treated lymphocytes and those of the respective untreated controls are significant only in the globoside and G_{D1a} components. To ensure that these two GSL components are the only specifically labeled species, aliquots of all the individual GSLs purified by preparative TLC were further analyzed by preparative gas liquid radiochromato-

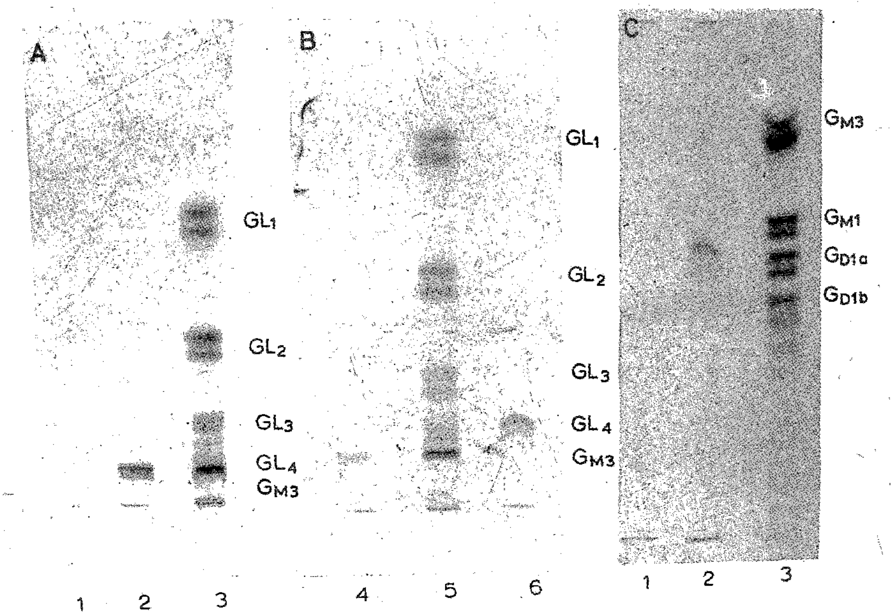

FIG. 2: *Autoradiograms of neutral and acidic GSLs isolated from PHA stimulated lymphocytes. A1, neutral GSLs from PHA stimulated lymphocytes incubated with NaB^3H_4 without prior treatment with galactose oxidase; A2, neutral GSLs from PHA stimulated lymphocytes, treated with galactose oxidase followed by NaB^3H_4; A3 and B5, labeled GSL standards biosynthesized from ^{14}C-galactose as precursor by PHA stimulated lymphocytes; B4, labeled hematoside standard biosynthesized as above; B6, labeled globoside from lane A2 after neuraminidase treatment; C1, acidic GSLs from PHA stimulated lymphocytes incubated with NaB^3H_4 without prior treatment with galactose oxidase; C2, acidic GSLs from PHA stimulated lymphocytes, treated with galactose oxidase followed by NaB^3H_4; and C3, labeled gangliosides standard biosynthesized from ^{14}C-galactose as precursor by PHA stimulated lymphocytes. Developing systems: Plate A, chloroform-methanol-water, 65:25:4 (v/v/v) at 16°; plate B, as for plate A but prolonged development; plate C, chloroform-methanol-2.5N ammonia, 60:40:9 (v/v/v), double development.*

graphy, as described above. As already mentioned, the results depicted in Table III, show that even the total label recovered as percent of that injected, is very low in all other species, except in globoside and G_{D1a}. Namely, from the total label of globoside and G_{D1a} injected into the column, over 40% and 65% respectively were specifically localized in their galactosyl and galactosaminyl moieties.

By combining the described results, it was finally possible to calculate the total specific labeling of individual GSLs in the three typical experiments described in this paper, with a high degree of accuracy (Table IV). On the basis of these data, the specific labeling of globoside is 8 times higher than that of G_{D1a} in both, the normal and the PHA-stimulated lymphocytes.

TABLE IV: *Total specific labeling of individual glycosphingolipids.*
Calculated as the products of total radioactivity bound to each purified GSL (Table II), multiplied by the respective percentages of specific label, i.e. bound to galactose and galactosamine (-sums 2+4 from Table III). Numbers in parentheses correspond to respective controls (non-exposed to galactose-oxidase attack). ND = not determined.

Exp.	Total specific labeling (cpm × 10^{-3})				
	GL_1	GL_2	GL_3	GL_4	GL_{1a}
A	ND	ND	ND	58 (3)	ND
B	23 (5)	10 (10)	11 (10)	970 (15)	119 (10)
PHA	ND	ND	ND	2030 (37)	245 (15)

Discussion

Localization, as well as changes in the organizational status of GSLs in the external surface of normal and PHA-stimulated lymphocytes were seeked by the method of galactose oxidase-tritiated sodium borohydride [20]. Because of its high molecular weight, galactose oxidase cannot enter the cell and therefore, its action is restricted to the attack of galactosyl and galactosaminyl residues of membrane components available to the enzyme on the cell surface. The present results of labeling show that among the GSLs present in the surface of lymphocyte plasma membranes, only globoside and G_{D1a} ganglioside are available to attack by galactose oxidase. Interestingly, the present results did not reveal any significant differences between normal and PHA-stimulated lymphocytes with respect to the organization of these molecules on the plasma membranes.

In analogous experiments with red cells [20], Gahmberg and Hakomori found also no significant differences between embryonic and mature red cells. Using both galactose oxidase attack and binding with antigens specific to G-SLs in mature and embryonic red cells it was shown that the surface GSLs of mature red cells were labeled by the galactose oxidase method, but were only slightly reactive with antigens, such as anti-globoside antisera; while in the embryonic red cells antigens could also react with surface GSLs [20]. This was explained by the assumption that the larger molecular weight of the antigens did not permit their penetration into the region of the GSLs on the surface of adult erythrocytes, while in the immature embryonic cells, the presence of smaller quantities of glycoproteins allowed such an approaching. Such observations have led to the concept of «crypticity» of certain haptens of the cell surfaces [20, 35]. Uncovering of carbohydrates in «cryptic» positions of the cell surface components has been correlated with loss of contact inhibition [35, 36].

Our present findings suggest that almost only galactose (and not galactosamine) was labeled by the galactose oxidase method used. Considering that the ratios of galactose to galactosamine in known tetraglycosyl-ceramides are 2:1, 2:0, and 3:1 [37], our present findings may indicate either that the labeled GSLs are mainly of the 2:0 type, or that galactosaminyl residues were in a «cryptic» position on the plasma-membrane surface. However, since no qualitative differences were identified between normal and PHA-simulated lymphocytes, and at least normal lymphocytes seem to contain mainly the normal GSLs of the 2:1 type, we are inclined to speculate that our findings conform with the possibility of a «cryptic» position of the galactosaminyl residues of GSLs on the lymphocyte surface, which is not altered by lectin stimulation. As in the case of mature and embryonic red cells differing in binding ability with antigens (see above), the use of other probes may be extremely useful to clarify this point.

ΜΕΛΕΤΗ ΤΩΝ ΓΛΥΚΟΣΦΙΓΓΟΛΙΠΟΕΙΔΩΝ ΑΝΘΡΩΠΙΝΩΝ ΛΕΜΦΟΚΥΤΤΑΡΩΝ ΔΙΗΓΕΡΜΕΝΩΝ ΜΕ ΛΕΚΤΙΝΕΣ

ΓΡΗΓΟΡΙΟΣ Π. ΕΥΑΓΓΕΛΑΤΟΣ, ΑΙΚΑΤΕΡΙΝΗ ΒΑΚΙΡΤΖΗ-ΛΕΜΟΝΙΑ καί ΒΑΣΙΛΕΙΟΣ Μ. ΚΑΠΟΥΛΑΣ.

Περίληψη

Ἡ μέθοδος τῆς ὀξειδάσης τῆς γαλακτόζης-τριτιωμένου βοροϋδριδίου τοῦ νατρίου χρησιμοποιήθηκε γιὰ τὴν σήμανση τῶν γαλακτόζυλο - καὶ γαλακτοζαμίνιλο - ὁμάδων τῶν γλυκοσφίγγολιποειδῶν ποὺ βρίσκονται στὴν ἐπιφάνεια τῶν πλασματικῶν μεμβρανῶν κανονικῶν καὶ διηγερμένων μὲ φυτοαιμαγλουτινίνη ἀνθρωπίνων λεμφοκυττάρων. Μὴ εἰδικὴ σήμανση ἐμποδίζει τὴν ἐφαρμογὴ τῆς μεθόδου αὐτῆς στὴν μελέτη τῶν λεμφοκυττάρων ἐκτὸς ἐὰν προηγηθεῖ ἐπεξεργασία τῶν κυττάρων αὐτῶν μὲ μὴ σημασμένο βοροϋδρίδιο πρὶν ἀπὸ τὴν ἐπίδραση τοῦ ἐνζύμου ὀξειδάση τῆς γαλακτόζης. Στὴν περίπτωση αὐτὴ τὰ ἀποτελέσματα ὑπολογίζονται βάση τῆς ἑκατοστιαίας ἀνάκτησης τῆς ραδιενέργειας τῆς γαλακτόζης καὶ τῆς γαλακτοζαμίνης μετὰ ἀπὸ ἀνάλυση μὲ παρασκευαστικὴ ἀεριουγροχρωματογραφία.

Μὲ χρωματογραφία λεπτῆς στιβάδος βρέθηκε σημαντικὴ εἰδικὴ σήμανση μόνο στὸν γλοβοζίτη καὶ στὸν δισίαλογαγγλιοζίτη τύπου G_{D1a}. Δὲν βρέθηκαν ποιοτικὲς διαφορὲς μεταξὺ τῶν κανονικῶν καὶ τῶν διηγερμένων μὲ φυτοαιμαγλουτινίνη λεμφοκυττάρων. Περαιτέρων ἀεριουγροραδιοχρωματομετρικὴ ἀνάλυση ἔδειξε ὅτι ἡ σήμανση τῆς γαλακτοζαμίνης δὲν εἶναι σημαντική. Ἀντίθετα ἡ γαλακτόζη περιέχει ὅλη σχεδὸν τὴν εἰδικὴ σήμανση στὸν γλοβοζίτη 60% καὶ στὸν γαγγλιοζίτη G_{D1a} 40% τῆς ὁλικῆς ραδιενέργειας.

Ἀπὸ τὰ παραπάνω συμπεραίνεται ὅτι οἱ ὁμάδες τῆς γαλακτοζαμίνης τῶν γλυκοσφιγγολιποειδῶν τῆς ἐπιφανείας τῶν μεμβρανῶν τῶν λεμφοκυττάρων εἶναι κατὰ ἕνα τρόπο «καλυμένες» καὶ γιαυτὸ ἡ ὀξειδάση τῆς γαλακτόζης δὲν μπορεῖ νὰ δράσει ἐπάνω τους. Ἀντίθετα οἱ ὁμάδες τῆς γαλακτόζης εἶναι ἐκτεθιμένες καὶ πάνω σὲ αὐτὲς μπορεῖ νὰ δράσει τὸ ἔνζυμο.

References

1. Miras, C.J., Mantzos, J.D. & Levis, G.M. (1966) Biochem. J. **98,** 782-786.
2. Hildebrand, J., Stryckmans, P. & Stoffyn, P. (1971) J. Lipid Res. **12,** 361-366.
3. Goldfried, E.L. (1971) J. Lipid Res. **12,** 531-537.
4. Levis, G.M., Karli, J.N. & Crumpton, M.J. (1976) Biochem. Biophys. Res. Commun. **68,** 336-342.
5. Holmgren, J., Lonnroth, I. & Svennerholm, L. (1973) Infect. Immunity **8,** 208-214.
6. Koscielak, J., Hakomori, S. & Jeanloz, R.W. (1968) Immunochemistry **5,** 441-445.
7. Hakomori, S. (1975) Biochim. Biophys. Acta **417,** 55-89.
8. Levis, G.M. & Kesse-Elias, M. (1974) Lipids **9,** 651-657.
9. Evangelatos, G.P., Vakirtzi-Lemonias, C. & Levis, G.M. (1974) Ninth FEBS Meeting (Budapest) Abstracts p. 229.
10. Evangelatos, G.P., Vakirtzi-Lemonias, C. & Levis, G.M. (1975) Tenth FEBS Meeting (Paris) Abstract 1007.
11. Inouye, Y., Handa, S. & Osawa, T. (1974) J. Biochem. (Tokyo) **76,** 791-799.
12. Yamakawa, T., Irie, R. & Iwanga, M. (1960) J. Biochem. (Tokyo) **48,** 490-507.
13. Dod, B.J. & Gray, G.M. (1968) Biochim. Biophys. Acta **150,** 397-404.
14. Ray, T.K., Skipski, V.P., Barclay, M., Essner, E. & Archibald, F. (1970) J. Biol. Chem. **244,** 5528-5536.
15. Weinstein, D.B., Marsh, J.B., Glick, M.C. & Warren, L. (1970) J. Biol. Chem. **245,** 3928-3937.
16. Klenk, H.D. & Choppin, P.W. (1970) Proc. Nat. Acad. Sci. USA **66,** 57-64.
17. Renkonen, O., Gahmberg, C.G., Simond, K. & Kääriäinen, L. (1972) Biochim. Biophys. Acta, **255,** 66-78.
18. Yogeeswaran, G., Sheinin, R., Wherret, J.R. & Murray, K. (1972) J. Biol. Chem. **247,** 5146-5158.
19. Forstner, G.G. & Wherret, J.R. (1973) Biochem. Biophys. Acta **306,** 446-459.
20. Gahmberg, C.G. & Hakomori, S.I. (1973) J. Biol. Chem. **248,** 4311-4317.
21. Avigad, G., Amaral, D., Asensio, C. & Horecker, B.L. (1962) J. Biol. Chem. **237,** 2736-2742.
22. Morell, A.G., Van den Hamer, C.J.A., Scheinberg, I.H. & Ashwell, G. (1966) **241,** 3745-3749.
23. Hajra, A.K., Bowen, D., Kishimoto, Y. & Radin, N.S. (1966) J. Lipid Res. **7,** 379-386.
24. Vakirtzi-Lemonias, C., Karahalios, C.C., Evangelatos, G.P. & Levis, G.M. (1976) Eighth Intern. Symposium on Carbohydrate Chemistry, Kyoto (Japan) 99.
25. Vakirtzi-Lemonias, C., Evangelatos, G.P., Kapoulas, V.M. & Levis, G.M. (1980) Εθρ. Ξ. Βιοψηεμ. **109,** 541-551.
26. Folch, J., Lees, M. & Sloane-Stanley, G.H. (1957) J. Biol. Chem. **226,** 497-509.
27. Levis, G.M., Evangelatos, G.P. & Crumpton, M.J. (1976) Biochem. J. **156,** 103-110.
28. Kanfer. J.N. & Spielvogel, C. (1973) J. Neurochem. **20,** 1483-1485.
29. Herberg, R.J. (1960) Anal. Chem. **32,** 41-46.
30. Yu, R.K. & Ledeen, R.Q. (1970) J. Lipid Res. **11,** 506-516.
31. Klenk, E. (1942) Z. Physiol. Chem. **237,** 76-86.
32. Holm, M. & Svennerholm, L. (1972) J. Neurochem. **19,** 609-622.
33. Sweeley, C.C. & Walker, B. (1964) Anal. Chem. **36,** 1461-1466.
34. Böym, A. (1968) Scand. J. Clin. Lab. Ievest. **21,** Suppl. 97, 51-76.
35. Hakomori, S. (1973) Adv. Cancer Res. **18,** 265-315.
36. Robbins, P.W. and McPherson, J. (1971) Nature **229,** 569-570.
37. Wiegandt, H. (1971) Adv. Lipid Res. **9,** 249-289.

Chimica Chronika, New Series, 9, 229-238 (1980)

CYCLOPROPANE ANALOGS OF γ-AMINOBUTYRIC ACID

DINESH K. DIKSHIT, SPYRIDON B. LITSAS, ALLEN KRANTZ
Department of Chemistry, State University of New York, Stony Brook, N.Y. 11794.

GAIL BURNETT and CHRISTOPHER WALSH
Departments of Chemistry and Biology, Massachusetts Institute of Technology, Cambridge, Massachusetts 02139.

Summary

To evaluate the potential of using cyclopropane analogs of γ-aminobutyric acid (GABA) as enzyme-suicide inhibitors, *trans*-(2′-aminocyclopropyl) acetic acid (**4**) and *trans*-2-(aminomethyl) cyclopropanecarboxylic acid (**5**) have been synthesized and tested as active-site directed reagents of GABA-transaminase and a homogeneous bacterial ω-amino acid: pyruvate transaminase (ω-AT). The cyclopropylamine, **4**, reversibly inhibits GABA-T and ω-AT with approximate values of K_I= 0.9 and 8 mM, respectively. The cyclopropanecarboxylic acid, **5**, on the other hand, serves as a substrate for both enzymes. The implications of these results for the design of inhibitors of GABA metabolizing enzymes are discussed.

Key Words: Enzyme inhibitors, γ-aminobutyric acid analogs, substituted cyclopnopane synthesis.

Introduction

Enzymatic activation of a double or triple bond by conjugating it to a π-electron system sysceptible to nucleophilic attack has been successfully exploited in the design of enzyme suicide inhibitors[1,2,3]. Cyclopropanes[4] often simulate olefins in their chemical properties and could serve as useful functionality in the construction of such inhibitors.

The ability of cyclopropanone (**1**) and its analogs to trap nucleophiles is well known[5] and is thought to be the basis of action of tranylcypromine[6] (**2**) and other monoamine oxidase inhibitors[7] which are cyclopropylamines. Cyclopropanone (**1**), and perhaps its imine, is the active agent responsible for the inhibition of aldehyde dehydrogenase[8], and for certain toxic effects associated with the mushroom constituent, Coprine (**3**). Also N-benzylcyclopropylamines appear to inactivate cytochrome P-450 monooxygenase coenzymes involved in N-dealkylation of drugs in liver[9].

Although isolated three-member rings possess low chemical reactivity, an adjacent radical, carbonium or carbanionic center renders them unstable to cleavage[10]. Even "Michael-like" addition reactions have been noted for cyclopropanes, where they are activated by electron-withdrawing groups[11]. The conditions under which cyclopropanes, designed to be enzyme suicide in-

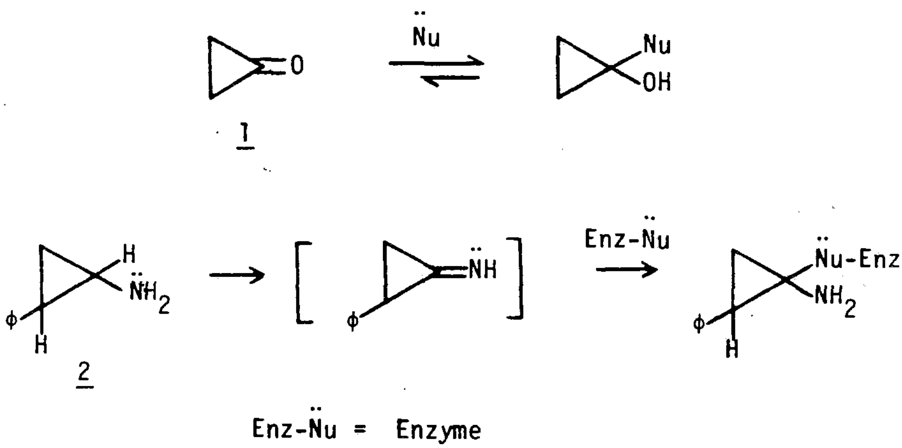

hibitors, express such latent reactivity (i.e. under physiological conditions) are in need of elucidation.

We have investigated the interaction of the cyclopropane analogs of γ-aminobutyric acid (GABA), **4** and **5**, with a bacterial GABA transaminase (EC 2.6.1.19) (GABA-T) and a homogeneous bacterial ω-amino acid: pyruvate transaminase[12]. Some neurological and psychiatric disorders like epilepsy, Huntington's chorea and schizophrenia have been associated with altered brain GABA levels, and there is a need to develop selective reagents which interfere with its metabolism[13,14].

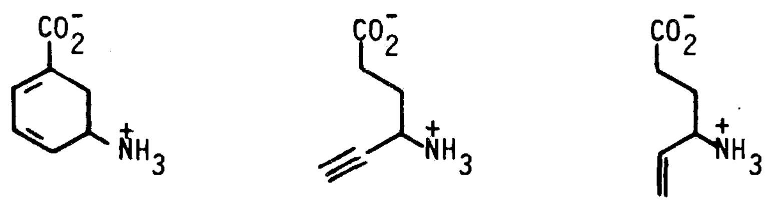

6 7 8

In this connection the natural product, gabaculine (**6**), a rigid, cyclic analog of GABA in extended conformation, has been examined[15,16] and found to inactivate each of these enzymes, whereas the acyclic GABA analogues γ-acetylenic- (**7**) and γ-vinyl-GABA (**8**), were found to inactivate only GABA-T[16,17].

Given the effects of gabaculine (**6**), we have now prepared two additional analogs of GABA, locked in extented conformations by a cyclopropane ring and tested them with the two transaminases. Compound **4** is a cyclopropylamine, compound **5**, a cyclopropane carboxylate.

Results and Discussion

Both GABA-T and ω-amino acid: pyruvate transaminase are pyridoxal phospate (PLP)-linked enzymes. Enzyme-mediated activation of the cyclopropylamine **4** could come about during catalysis either by formation of the initial substrate-coenzyme aldimine **9,** rendering it susceptible to nucleophilic attack at the β-cyclopropylcarbon[11], or as a consequence of enzymic transamination (1,3-proton shift) to generate a potentially reactive product cyclopropylimine **10,** (scheme 1) still attached to the pyridoxamine-P cofactor.

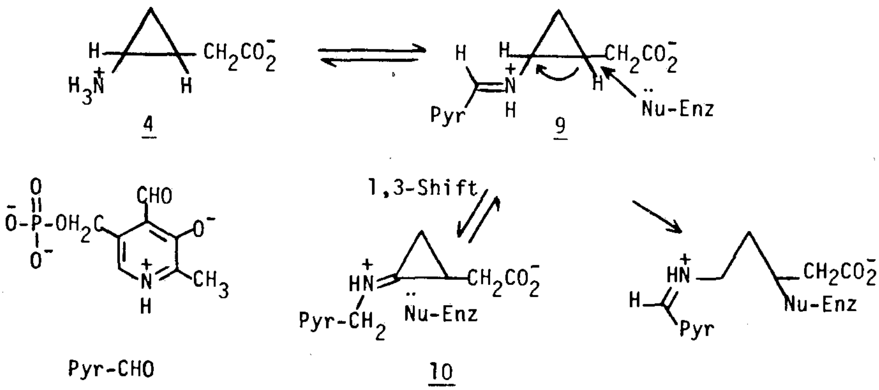

Scheme 1

On the other hand, initial adduct formation between the pyridoxal cofactor and **5,** followed by enzyme-mediated proton removal would generate the stabilized α-carbanion. Precedent exists for facile ring cleavages of cyclopropylcarbinyl carbanions where an ester stabilizes the incipient anion[18,19]. The extent to which the negatively charged carboxylate is neutralized by binding to active site residues should influence the reactivity of the ring toward cleavage, (scheme 2).

The synthesis of **4** commenced with the cupric sulfate decomposition of methyl diazoacetate **12** in the presence of t-butyl but-3-enoate **13** in cyclohexane. Subsequent transformations (sheme 3) centered about the Curtius rearrangement, led to the urethano-ester **18** which was converted to the target amino acid **4** by consecutive hydrolyses.

The amino acid **5,** was prepared by a modification of the route of Ivanskii[20] utilizing hydroboration as the means for selective reduction of the cyano-ester **22.**

Neither cyclopropane analogue of GABA was found to irreversibly inactivate either the bacterial GABAT-T or ω-AT upon incubation at 37° with con centrations up to 50 mM for 20 minutes. The cyclopropylamine, **4,** appears to

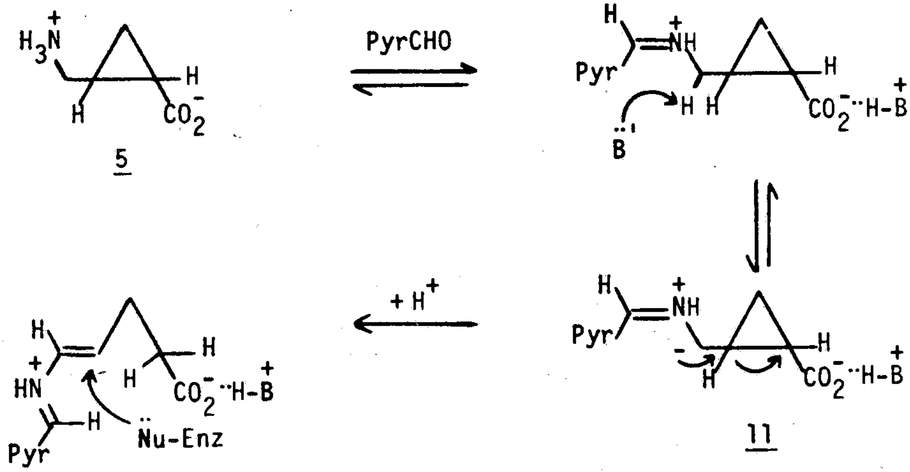

B & B' are part of the enzyme

Scheme 2

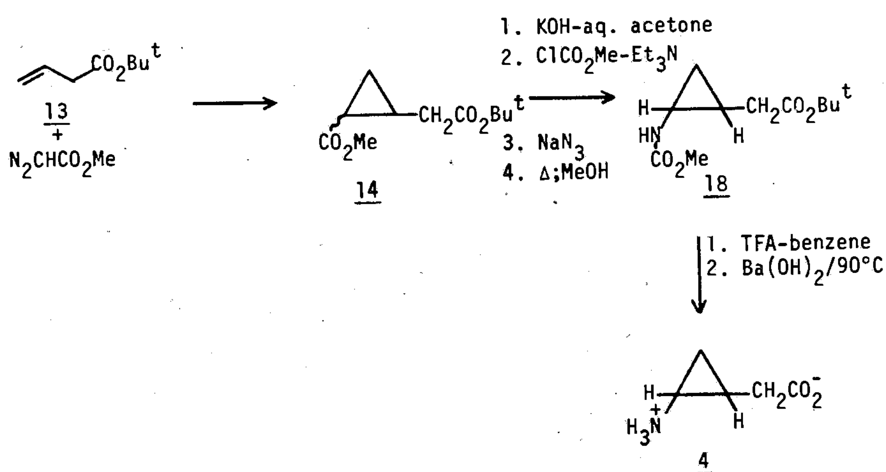

Scheme 3

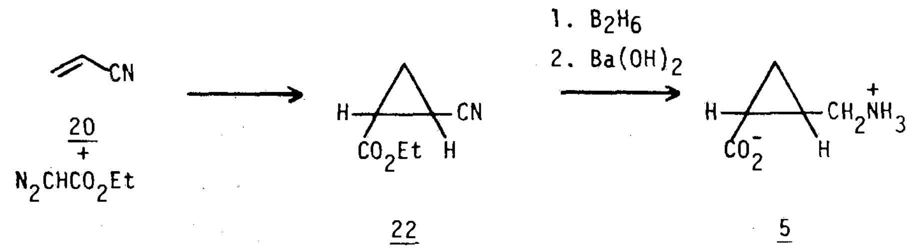

Scheme 4

TABLE I: *Relation of GABA and Its Analogs to GABA-T and ω-AT.*

	Substrate		Inactivator		Reversible Inhibitor	
Compound	GABA-T	ω-AT	GABA-T	ω-AT	GABA-T	ω-AT
GABA	+ K_m=1–18mM	+ K_m=8.0mM	—	—	—	—
Gabaculine	+	+	+	+[a]		
4	—	—	K —	—	K_I=9×10^{-4}M	K_I=8×10^{-3}M
5	+ K_m=6mM	+	—	—		

[a]Kills in every turnover.

be a reversible inhibitor of GABA-T and ω-AT with approximate values of K_1 = 0.9 and 8 mM, respectively. *trans*-2- (Aminomethyl)cyclopropanecarboxylic ancid, **5**, on the other hand, serves as a substrate for each enzyme. With GABA-T, it has an apparent K_m of 5.8 mM at 5.0 mM α-ketoglutarate. The K_m value was not determined for ω-AT, but its turnover rate at 5.0 mM (0.9 U/mg) is comparable to the rates for β-aminobutyrate (1.1 U/mg) of GABA (1.4 U/mg) at 5.0 mM. These data are collected in Table I. A recent paper has also noted that **5** is a substrate for GABA-T from brain mitochondria with a V_{max} which is 48% that of GABA (ref. 20a).

Finally, the cyclopropyl compounds were tested for inactivation of glutamate decarboxylase (GAD), the PLP-enzyme involved in GABA biosynthesis. Activity of GAD was monitored by a continuous assay using a pH indicator, 1,1′-diethyl-2-2′-cyanine iodide (DCI) (21). Once again, neither compound caused irreversible inactivation during 20 minute incubations at concentrations up to 50 mM.

Thus of the three rigid analogs of GABA in extended conformation, only gabaculine exhibits irreversible inactivation. In fact the three cyclic analogs offer three distinct possible inactivation routes by rearrangement or capture of an initial transamination adduct. Gabaculine inactivates because the initial adduct between **6** and GABA-T is processed to a product imine-Pyridoxamine phosphate complex, then isomerized to a stable anthranilyl-PNP linkage[15-17]. Compound **4** on transamination would yield a cyclopropylimine, capturable as a stable 1,2-adduct by a nearby enzyme nucleophile. This strategy is thwarted because neither transaminase will carry out the requisite oxidation of the cyclopropylamine group. The K_I values for reversible inhibition are comparable to the values for GABA with each enzyme.

The inability of the cyclopropylamine **4** to serve as a substrate for GABA-T and ω-AT, despite its interaction with active-site residues, may be reconciled to the difficulty of isomerizing the conjugated imine **9**, to the thermodynamically unfavorable imino cyclopropane **10.** A double bond exocyclic to a cyclopropane contributes 12 kcal/mole of strain energy[22] and this increment should make the 1,3-shift in sheme 3 considerably more difficult than it is for ordinary GABA-like substrates[23].

Cyclopropyl isomer **5** *is* processed catalytically (see also ref. 20a), presumably via stabilized α-carbanion species but no inactivation is detected. Although accumulating product species have not yet been characterized, the lack of inactivation supports the view that fragmentation of the cyclopropyl ring by an adjacent carbanion (to set up a conjugate addition possibly) has not occurred. Thus, anionic cyclopropane fragmentations may not be realizable during catalytic turnover of cyclopropyl α-anion equivalents in these PLP enzyme systems unless additional or more powerful electron-withdrawing groups are appropriately placed on the cyclopropane framework. In this connection we have also examined cyclopropylglycine (**23**), as a mechanism-based inactivator of two other PLP-dependent enzymes, L-alanine transaminase from pigheart and alanine recemase from *E. Coli.* Both enzymes process cyclopropylglycine (for transamination or racemization) but show *no* inactivation.

To date very few strategies for the design of enzyme inhibitors have been developed for cyclopropanes. That **5** is a reasonable substrate ($K_m \sim$ 6mM) for both GABA- and ω-AT should be a guilding principle for the design of cyclopropane suicide substrates of these enzymes. Studies are now in progress to exploit this discovery by determining which substitutions on the cyclopropane framework of **5** lead to ring fragmentation, and thus to viable suicide inhibitors.

Experimental Section

Melting points were determined in open glass capillaries using a Thomas-Hoover Uni-Melt apparatus and are uncorrected. IR spectra were recorded with a Perkin-Elmer model 727 spectrophotometer. NMR spectra were recorded with Varian Associates EM-360 and HFT-80 instruments using tetramethylsilane as the internal standard. A Bruker-360 MHz spectrometer was used to decouple the cyclopropyl protons.

trans-2-(aminomethyl) cyclopropanecarboxylic acid (**5**) was synthesized by an adaptation of the method of Ivanskii[20]. ω-Amino acid: pyruvate transaminase was purified to homogeneity as described[12], while GABA- transaminase was obtained as a partially purified enzyme from *Pseudomonas fluorescens* (Sigma Chemical Company). Enzyme activity of ω-amino acid, pyruvate transaminase was assayed as described[16] by either a continous method using β-aminobutyrate as substrate (for inhibition and inactivation studies), or by a discontinous method in which $|^{14}C|$ pyruvate is converted to $|^{14}C|$ alanine and separated on Dowex 50 H^+ columns. The discontinuous assay is suitable for any ω-amino substrate. Activity of GABA-T was monitored in a continuous assay, coupled to the action of succinic semialdehyde dehydrogenase which is also present in the preparation of GABA-T.

Both substrates, **4** and **5**, were tested as inactivators of ω-AT by incubation at 37°C with 10.0 and 20.0 mM substrate concentrations in the presence of 1.0 mM pyruvate. Aliquots were withdrawn at times up to 30 minutes and assayed for activity. Incubations with GABA-T were carried out at 25°C with 10.0 and 50.0 mM substrate concentrations. Competitive inhibition studies were performed by including either **4** or **5** in assay mixtures containing a known amino acid substrate for each enzyme. Cyclopropylamino acid concentrations of 0.1 to 1.0 mM were used with ω-T, while concentrations of 0.1 to 6.0 mM were used with GABA-T. Finally, enzymatic turnover by GABA-T was determined at cyclopropylamino acid concentrations of 0.2 to 20.0 mM with 5.0 mM α-ketoglutarate, while turnover by ω-AT was determined at 5.0 mM substrate only, due to the large amount of substrate consumed in this assay. Turnover of **5** was also detected in the competition assays.

Elemental analyses were performed by Galbraith Laboratories, Knoxville, Tenessee. Where analyses are indicated by the symbols of the elements, analytical results are within ±0.4% of the theoretical values.

***cis** and **trans**-t-Butyl (2′-carbomethoxy) cyclopropyl acetate* (**14**)

A solution of 110 g. (1.1 mol) of methyl diazoacetate (**12**) in 100 mL of cyclohexane was added dropwise to a well-stirred and refluxing solution of (t-butyl but-3-enoate **13,** 155 g 1.09 mol) in 800 mL of cyclohexane in which 35 g of anhydrous $CuSO_4$ were suspended. After the addition, the mixture was refluxed for 1 hr, and then cooled, filtered, and concentrated. Unreacted **13** (55 g) was recovered by vacuum distillation at 5mm. The residue was treated with a solution of potassium permanganate until the purple color of permanganate persisted. Manganous salts were then filtered off, washed with ether and ethereal extacts, washed with water, dried (sodium sulfate) and concentrated. The crude product was purified by distillation to give 45 g of a 40:60 mixture of *cis* and *trans*-diesters **14** (31%), bp 45-8°/2 mm; IR (Neat) 2850–2900, 1720-40 cm^{-1}; NMR ($CDCl_3$) 0.6—1.93 (m, 4H) 1.47 (s, 9H), 2.20 δ 2.67 (two doublets, 2H, J= 7Hz), 3.66 (s, 3H).

cis and ***trans**-t-Butyl-(2′carboxyclopropy) acetate* **(15)**

A mixture of 10 g (50 mmol) of **14**, 300 mL of 1N KOH and 300 mL of acetone was stirred under N_2 for 30 min., poured over ice-water and extracted with ether (2×150 mL). The aq. lalyer was acidified with conc. HCl to pH 2 and extracted with ether. Concentration of the ether extracts followed by distillation *in vacum,* gave 8 g (85%) of **15** as a colorless liquid, bp 75-80°/2-3 mm; IR (Neat) 1680-1720, 2500-3200 cm^{-1}; NMR ($CDCl_3$) 0.60—1.90 (m, 4H), 1.47 (s, 9H), 2.20 δ 2.53 (two doublets, 2H, J = 7Hz), 6.52 (b, 1H).

***cis** and **trans**-t-Buty [2′N-methoxycarbonylamino) cyclopropyl] acetate* **(18)**

To a solution of 11 g (0.055 mol) of **15** in 84 mL of acetone and 150 mL of water at 0°C was added with stirring 6.1 g (0.06 mol) of Et_3N dissolved in 50 mL of acetone. After ten minutes the reaction mixture was cooled to −10°C and a solution of 5.7 g (0.06 mol) of methyl chloroformate in 50 mL of acetone was added to it dropwise, the mixture was stirred at −10° for 30 min. followed by the addition of 9.0 g (0.138 mol) of NaN_3 dissolved in 40 mL of water over a period of 10 min. The contents which were slowly allowed to rise to room temp (30 min.) were poured into 150 mL of water. Extraction with ether and concentration of the ethereal layer below 30°C gave the carboxazide **16:** IR (Neat) 1700 δ 1720 (CO), 2050 (N_3) cm^{-1}; which was taken up in 300 mL of dry toluene and brought carefully to reflux. Refluxing (1 hr) converted **16** to the isocyanate **17:** IR 2200 (N=C=0), 1720 (CO) cm^{-1}; which was not isolated. Addition of 60 mL of absolute methanol to the refluxing toluene solution of **17,** and continuation of refluxing for 3 hrs, followed by concentration and chromatographic separation of crude **18** over a column of silica gel in chloroform using chloroform-ethylacetate as eluant gave **18** as a thick oil: 4.4 g, 35%; IR (Neat) 3250, 1710 cm^{-1}, NMR ($CDCl_3$) 0.33-1.6 (m, 3H), 1.53 (s, 9H), 2.07-2.64 (m, 3H), 3.65 (s, 3H), 5.42 (bs, 1H).

***trans**-(2′-N-carbomethoxyamino) cyclopropylacetic acid* **(19)**

A solution of 2 g (8.7 mmol) of **18** and 15 mL of trifluoroacetic acid in 50 mL benzene was refluxed under N_2 for 1 hr. After solvent was removed *in vacuo,* the residue was crystallized from ethylacetate-hexane to give 0.73 g of **19** as a white powder: 50%; mp 107°C; IR: (Nujol) 3300, 1715, 1675 cm^{-1}; NMR ($CDCl_3$ = DMSO-D_6) 0.45-1.3 (m, 3H), 1.85-2.4 (m, 3H), 5.6 (s, 3H), 6.65 (bs, 1H).

Anal: calcd. for $C_7H_{11}NO_4$; C, 48.60; H, 6.40; N, 8.10. Found: C, 48.61; H, 6.20; N, 7.91.

***trans**-(2′-Aminocyclopropyl)acetic acid* **(5)**

A mixture of 0.2 g (1.15 mmol) of **19,** 7 g of barium hydroxide, 25 mL of methanol and 100 mL of water was refluxed under N_2 for 10 hrs. Methanol was removed and the residue was acidified with 20% H_2SO_4 to pH 3 and then brought to pH 7 with barium carbonate. The barium salts were separated upon centrifugation from a clear solution which was concentrated under vacuum at 30°C. The crude yield (100 mg, 75%) of residue after repeated recrystallizations (from ethanol using a minimum of water) gave **4** as a white powder: mp 197°C; IR (KBr) 3400, 3200-2300, 2150, 1570, 1390 cm^{-1}m NMR CD_2O relative to HDO peak at δ 4.61 0.45-0.94 (m, 2H), 1.04-1.37 (m, 1H), 2.03 (d, J = 7Hz, 2H), 2.23-2.40 (m, 1H). Double resonance experiments with the decoupling frequency centered at 0.78 δ collapsed the multiplet at 2.23-2.40 δ to a doublet with a typical *trans*-cyclopropyl proton-proton coupling constant (J = 3.8Hz)[24-28].

Περίληψη

Κυκλοπροπανικὰ Ἀνάλογα τοῦ γ-Αμινοβουτυρικοῦ ὀξέος

Γιὰ νὰ ἐξεταστεῖ ἡ δυνατότητα χρησιμοποιήσεως κυκλοπροπανικῶν ἀναλόγων τοῦ γ-αμινοβουτυρικοῦ ὀξέος (GABA) ὡς ἀναστολέων αὐτοκτονίας ἐνζύμων ἔγινε ἡ σύνθεση τοῦ *trans* -(2-αμινοκυκλοπροπυλ) ὀξικοῦ ὀξέος **(4)** καὶ τοῦ trans -2-αμινομεθυλ) κυκλοπροπανοκαρβοξυλικοῦ ὀξέος **(5)** καὶ κατόπιν ἡ δοκιμὴ γιὰ πιθανὴ δράση των ὡς ἀντιδραστηρίων ποὺ ἀδρανοποιοῦν τὸ ἐνεργὸ κέντρο τῆς τρανσαμινάσης τοῦ GABA (GABA-T) καὶ τῆς πυροσταφυλικῆς τρανσαμινάσης (ω-AT) βακτηριακῆς προελεύσεως. Ἡ κυκλοπροπυλαμίνη **(4)** ἀναστέλλει ἀντιστρεπτὰ τὴν GABA-T καὶ τὴν ω-AT μὲ τιμὲς K_I περίπου 0,9 καὶ 8mM ἀντιστίχως. Ἐξάλλου τὸ κυκλοπροπανοκαρβοξυλικὸ ὀξὺ **5**, δρᾶ σὰν ὑπόστρωμα καὶ τῶν δύο ἐνζύμων. Μελετῶνται οἱ ἐπιπτώσεις τῶν ἀποτελεσμάτων αὐτῶν στὸ σχεδιασμὸ ἀναστολέων τῶν ἐνζύμων ποὺ μεταβολίζουν τὸ GABA.

References and Notes

1. Rando, R. R., *Science, 1974,* **185,** 320.
2. Abeles, R.H. and Maycock, A.L., *Accts. Chem. Res., 1976,* **9,** 313.
3. Walsh, C.T. in *Horiz. Biochem. Biophys.,* Quagliarello, R., Palmieri, F., and Singer, T.P., Eds., Addison-Wesley, Reading, Massachusetts, 1980.
4. Turro, N., Gagosian, K.B., Edelson, S.E., Darling, T.R., Williams, ZJ.R., Hammond, W.B., *Trans. N.Y. Acad. Sci., 1971,* **33,** 396.
5. (a) Wasserman, H.H., Clagett, D.C., *J. Am. Chem. Soc.,* 1966, **88,** 5368.
   (b) van Tilborg, W. J. M., Schaafsma, S.E., Steinberg, H., Deboer, Th., *Rec. Trav. Chim. Pays-Bas, 1967,* **86,** 417.
6. Paech, C., Salach, J. I., Singer, T.P., *Biochem. Biophys. Res. Commun.,* in press.
7. Silverman, R.B. and Hoffman, S.J., *J. Am. Chem. Soc., 1980,* **102,** 884.
8. Wiseman. J.S. and Abeles, R.H., *Biochemistry, 1979,* **18,** 427.
9. Hanzlik, R.P., Kishore, V., and Tullman, R., *J. Med. Chem., 1979,* **22,** 759.
10. Charton, M. in *The Chemistry of the Alkenes,* Vol. 2, Patai, S., ed., John Wiley, 1970, Chapter 10, p. 511.
11. Danishefsky, S., *Accts. Chem. Res., 1979,* **12,** 66.
12. Yonaha, K., Toyama, S., Yasuda, M., and Soda, K., FEBS Letts., *1976,* **71,** 21.
13. Emson, P.C., *Int. J. Biochem., 1975,* **6,** 689.
14. Perry, T.L., Hansen, S. and Kloster, M., *N. Engl. J. Med., 1973,* **288,** 337.

15. Rando, R.R., *Biochemistry, 1977,* **16,** 4604.
16. Burnett, G., Yonaha, K., Toyama, S., Soda, K., Walsh, C., *J. Biol. Chem., 1980,* **255,** 428.
17. Metcalf, B.W., Lippert, B., Casara, P. in *Enzyme-Activated Irreversible Inhibitors,* 1978, (Seiler, N., Jung, M.J., and Koch-Weser, J., eds.) pp. 123-134, Elsevier/North-Holland, Amsterdam.
18. Stirling, C.J.M., *Chem. Res., 1978,* **78,** 517.
19. Augustine, R.L. and Pinto, F.J., *J. Org. Chem., 1975,* **40,** 115.
20. Ivanskii, V.I. and Maksimov, V.N., *J. Org. Chem.,* USSR, *1972,* **8,** 54.
20a. Allan, R.D., Curtis, D.R., Headley, P.M., Johnston, G.A.R., Lodge, D. and Twitchin, B., *J. Neurochem., 1980,* **34,** 652.
21. Johnson, R.B., 1979, Master's Thesis, U. Wisconsin, Madison.
22. Wiberg, K.B. and Fenoglio, R.A., *J. Am. Chem. Soc., 1968,* **90,** 3395.
23. Olivo, F., Rossi, C.S., and Siliprandi, N. in *Chemical and Biological Aspects of Pyridoxal Catalysis,* Snell, E.E., Fasella, P.M., Braunstein, A., and Rossi Fanelli, A., eds., The Macmillan Co., New York, 1963, p. 91.
24. Patel, D.J., Howden, M.E.H. and Roberts, J.D., *J. Am. Chem. Soc., 1963,* **85,** 3218.
25. Wiberg, K.B. and Nist, B. J., *J. Am. Chem. Soc., 1963,* **85,** 3218.
26. Prinzbach, H., Hagemann, H., Hartenstein, J.H., and Kitzing, R., *Chem. Ber., 1965,* **98,** 2201.
27. Shono, T., Morikawa, T., Oku, A., Ode, R., *Tetrahedron Lett., 1964,* 791.
28. Wiberg, K.B., Barth, D.E. and Schertler, P.H., *J. Org. Chem., 1973,* **38,** 378.

Acknowledgment

This investigation was supported by a grant from the National Institutes of Health (1 RO 1 NS 13220) to Allen Krantz, by a Biomedical Research Support Grant no. 5507 RR 0573607, and in part by grants to Christopher Walsh from the National Institutes of Health and the American Heart Association.

Chimica Chronika, New Series, 9, 239-246 (1980)

SYNTHÈSE DE QUELQUES DÉRIVÉS HYDROXYLÉS ET DIALKYLAMINO-2 ÉTHYLÉS DU THIAZOLE À NOYAU CONDENSÉ

G.B. FOSCOLOS, G. TSATSAS et E. COSTAKIS
Laboratoire de Pharmacie Chimique, Université d'Athènes, 104, rue Solonos, Athènes (114) Grèce.

La synthèse des derivés dialkylamino-2 éthylés des bromures de l'imidazo [2,1-b]thiazolium-4, thiazolo[3,2-a]pyrimidinium-4 et thiazolo[3,2-a] diazépin-1,3-ium-4 est effectuée par action des bromo-1dialkylamino-4 butanones-2 sur les thiurées cycliques correspondantes. Pour certains de ces dérivés et dans des conditions définies, l'isolement des carbinolamines intermédiaires est possible. De même, la synthèse des bromures des hydroxy-6-tétrahydro-5, 6, 7, 8 thiazolo [3,2-a] pyrimidinium-4 est effectuée par action du dibromo-1,3 propanol-2 sur les aminothiazoles correspondants.

Summary

Synthesis of 2-dialkylaminoethylated and hydroxylated bicyclic fused compounds of thiazole

The synthesis of 2-dialkylaminoethylated compounds of imidazo[2,1-b] thiazol-4-ium, thiazolo[3,2-a]pyrimidin-4-ium and thiazolo[3,2-a][1,3] diazepin-4-ium bromides has been achived by action of 1-bromo-4-dialkylamino-butan-2-ones on the corresponding cyclic thioureas. In some cases and under certain conditions the isolation of intermediates carbinolamines was possible.

On the other hand some 6-hydroxy-5,6,7,8-tetrahydro-thiazolo[3,2-a] pyrimidin-4-ium bromides were obtained by reaction of 1,3-dibromo-2-propanol with the corresponding 2-aminothiazoles.

Key Words

3-(2-Dialkylaminoethyl)-3-hydroxy-2,3,5,6,7,8-hexahydro-thiazolo[3,2-a] pyrimidin-4-ium bromides.
3-(2-Dialkylaminoethyl)-3-hydroxy-2,3,5,6,7,8-hexahydro-9H-thiazolo[3,2-a] [1,3]diazepin-4-ium bromides.
5-(2-Dialkylaminoethyl)-2,3-dihydro-1H-imidazo[2,1-b]thiazol-4-ium bromides.
3-(2-Dialkylaminoethyl)-5,6,7,8-tetrahydrothiazolo[3,2-a]pyrimidin-4-ium bromides.
3-(2-Dialkylaminoethyl)-5,6,7,8-tetrahydro-9H-thiazolo[3,2-a][1,3]diazepin-4ium bromides.
6-Hydroxy-5,6,7,8-tetrahydrothiazolo[3,2-a]pyrimidin-4-ium bromides.

L'étude de la littérature chimique révèle que parmi les nombreux dérivés decrits du thiazole à deux noyaux condensés, il y a des produits possedant des propriétés pharmacologiques et antimicrobiènnes remarquables[1-6]. Cependant la préparation de tels dérivés qui contiennent dans leur molécule une fonction amine aliphatique ou une fonction alcool n'est pas encore décrite, selon nos connaissances.

Dans le présent travail nous étudions d'une part l'introduction de la fonction dialkylaminoéthyle dans le noyau du thiazole des dérivés thiazoliques à noyau condensé (V) et d'autre part la préparation des dérivés (IX) du thiazolo [3,2-a]pyrimidinium-4 hydroxylés en position 6.

Les composés synthétisés avec leurs constantes physiques sont cités dans le tableau I.

En ce qui concerne la synthèse des dérivès dialkylaminoéthylés (V), elle est effectuée par formation du noyau du thiazole en faisant réagir les bromhydrates de bromo-1 dialkylamino-4 butanones-2 (I) sur les thiurées cycliques correspondantes (II) come il est indiqué dans le schéma 1. Cette réaction évolue avec formation intermédiaire des thiocétones (III) qui subissent une addition nucléophile sur leur carbonyle et se transforment en carbinolamines bicycliques (IV); ces dernières fournissent finalement les dérivés thiazoliques (V) avec une élimination spondanée d'eau[2,6,7].

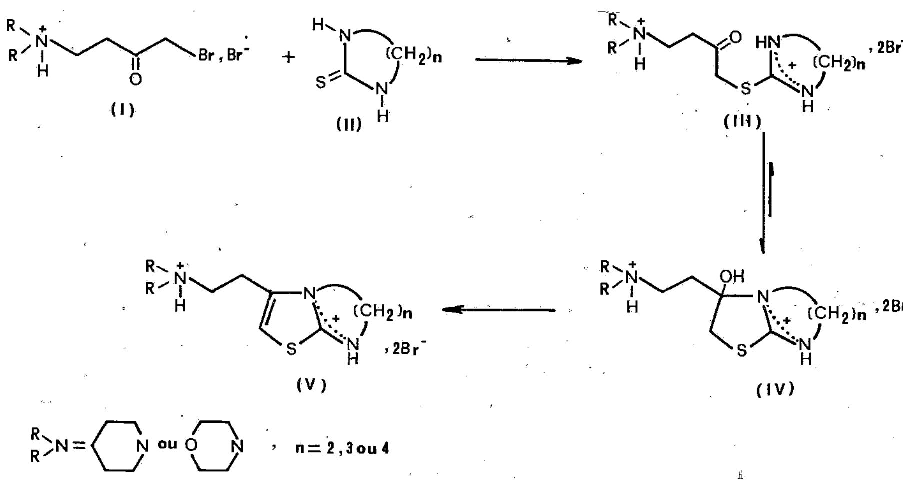

SCHEMA 1

C'est ainsi qu'en faisant réagir l'imidazolinothione-2(3H) avec la bromocétone correspondante (I) dans l'éthanol à chaud ils se forment directement les bromhydrates de bromures des (dialkylamino-2 éthyl)-5, dihydro-2,3-1H-imidazo[2,1-b]thiazolium-4 (Va) et (Vb) sans isolement intermediaire des thiocétones (III) et des carbinolamines (IV). Par contre la réaction des bromocétones (I) aussi bien avec la tetrahydro-3,4,5,6 pyrimidinothione-2(1H) qu'avec la héxahydro-1,3,4,5,6,7-2H-diazepino-1,3-thione-2 dans l'éthanol bouillant fournit respectivement les carbinolamines intermédiaires (voir tableau I) (IVc), (IVd), (IVe) et (IVf). La transformation de ces composés en derivés thiazolo[3,2-a] pyrimidiniques et thiazolo[3,2-a][1,3]diazepiniques (Vc), (Vd) et (Ve), (Vf) respectivement, est effectuée par chauffage dans l'acide acétique glacial.

Les spectres IR des carbionolamines (IV) présentent les absorptions du noyau thiazolinique $\bar{\nu}$ (C=N) vers 1650-1620 cm^{-1} et $\bar{\nu}$ (S—C=N) vers 1550-1525 cm^{-1}. D'une manière semblable les spectra IR des dérivés thiazoliques (V) présentent les trois absorptions du noyau thiazolique $\bar{\nu}$ (C=N) vers 1640-1595 cm^{-1} (thiazole I), $\bar{\nu}$ (C=C) vers 1610-1565 cm^{-1} et $\bar{\nu}$ (S—C=N) vers 1575-1535 cm^{-1} (thiazole II)[8]. Ainsi l'absorption de la vibration de valence $\bar{\nu}$ (C=N) des dérivés thiazoliques (V) est déplacé vers les valeurs de fréquence plus faibles à cause de l'aromatisation du noyau thiazolique.

Les spectres RMN des carbinolamines (IV) dans la DMSO-d_6 donnent trois protons non equivalents au point de vue mangétique, qui sont échangeables en présence de D_2O (δ 10,13-10,26,9,49-9,67 et 7,5-7,7 ppm) tandis que le spectre RMN des dérivés (V) donnent seulement les deux premières des trois absorptions ci-dessus. Cela nous amène à la conclusion que ces absorptions correspondent aux protons des fonctions NH^+, l'absorption avec δ 7,5-7,7 ppm est par consequent dûe à l'hydroxyle des carbinolamines (IV). De plus, les dérivés (V) donnent l'absorption du proton non protegé du noyau thiazolique vers δ6,38-6,78 ppm.

De même durant la fusion des dérivés (IV) on observe une effervescence et par la suite resolidification; le nouveau point de fusion correspond à celui du dérivé (V) correspondant.

Nous n'avons pas reussi à effectuer des analyses élémentaires des composés (IV) à cause de leur transformation en (V) dans les conditions du séchage préalable necessaire.

Plus précisement, dans le cas de la préparation du dérivé benzimidazolique (Vh) le produit intermédiaire formé paraît avoir la structure de la thiocétone ouverte (IIIh); cela résulte du pic caractéristique aigu dû à la vibration de valence du carbonyle qui se situe vers 1705 cm^{-1}. Cela est confirmé par le spectre RMN du (IIIh) qui présente les quatre protons benzimidazoliques sous forme de multiplet symétrique (δ 7,22-7,64 ppm) caractéristique du système AA'BB'. D'autre part dans le spectre RMN du dérivé thiazolique (Vh) le proton thiazolique se présente sous forme de singulet (δ 7,35 ppm) tandis que les protons benzèniques sous forme de multiplet assymétrique (δ 7,44-8,35 ppm) caractéristique du système ABCD.

Enfin il paraît probable que des facteurs stériques peuvent influencer la transformation des carbinolamines (IV) en dérivé (V). C'est ainsi que malgré les expériences répetées et l'augmentation du temps de chauffage dans l'acide acétique nous n'avons par reussi de transformer le bromhydrate de bromure du (diméthylaminométhyl)-5 hydroxy-4a octahydro-2,3,4,5,6,7,8,8a-1H-imidazo [2,1-b]benzothiazolium-4 (IVg) en dérivé (V) correspondant. Il faut noter que contairement aux autres dérivés (IV) malgré le séchage prolongé, le (IVg) donne une analyse élémentaire constante.

Quant à la préparation des bromures de l'hydroxy-6 tetrahydro-5,6,7,8 thiazolo[3,2-a]pyrimidiniums-4 (IX) nous l'effectuons en chauffant 1 mole de dibromo-1,3 propanol-2 (VII) avec deux moles d'amino-2 thiazole (VI) correspondant (Schéma 2).

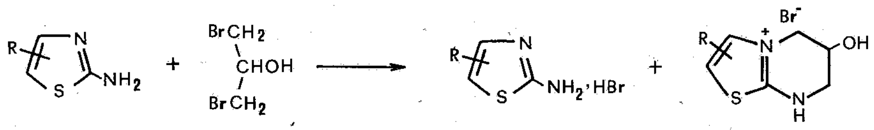

SCHEMA 2

La séparation du produit (IX) du bromhydrate (VIII) qui se forme durant la réaction est réalisée par cristallisation franctionné basée à la plus grande solubilité du (VIII) dans un mélange éthanol-éther.

Partie Expérimentale

Les points de fusion ont été pris dans l'appareil de Büchi et ne sont pas corrigés. Les microanalyses ont été effectuées par le Service Central de Microanalyse du CNRS. Les spectres IR ont été obtenus en dispersion dans le KBr à l'aide d'un spectrophotomètre Perkin-Elmer 177. Les spectres RMN ont été enregistrés sur un appareil Bruker-Hx90 et sur un Varian-A60 en utilisant le DMSO-d_6 et le D_2O comme solvant. Les déplacements chimiques sont donnés en δ (ppm) par rapport au TMS et au DSS en référence interne.

Matières premières. Les thiurées cucliques (II), soit l'imidiazolinothione-2 (3H)[9], la tétrahydro-3,4,5,6 pyrimidinothione-2(1H)[10], l'héxahydro-1,2,3,4,5,6,7-2H-diazepino-1,3 thione-2[11] et la 1H-benzimidazolothione-2(3H)[12] ont été préparées respectivement à partir de l'éthylènediamine, de la propylènediamine-1,3, de la butylenediamine-1,4 et de la o-phènylènediamine par action de CS_2 et cyclisation par la suite des sels internes des acides N-(ω-aminoalkyl)-dithiocarbamidiques formés.

Les piperiodino-4 et morpholino-4 butanones-2 et la (diméthylaminométhyl)-2 cyclohéxanone[13-15] ont été préparées en appliquant la réaction de Mannich sur l'acétone et la cyclohéxanone.

Les bromhydrates des aminobromocétones (I) ont été préparés par bromuration des bases de Mannich ci-dessus à l'aide d'un mélange de brome-acide bromhydrique dans l'acide acétique glacial[16,17].

TABLEAU I

N°	Formule	Rdt %	P.f. (°C)	I.R. Absorption (cm^{-1}) $\bar{\nu}$(C=N)	$\bar{\nu}$(S-C=N)	$\bar{\nu}$(C=C)
III_h	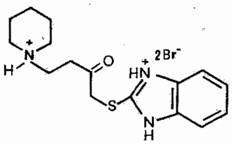	82	206-207	1620	---	1515
IV_c	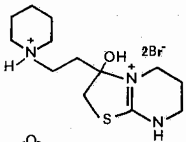	85	199-200	1650	1550	---
IV_d	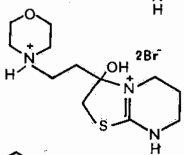	88	202	1640	1550	---
IV_e	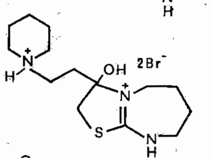	90	234-236	1650	1530	---
IV_f	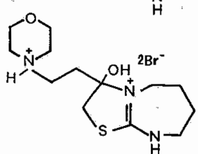	91	257	1640	1525	---
IV_g**	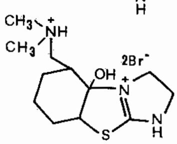	55	255-256	1620	1545	---
V_a**	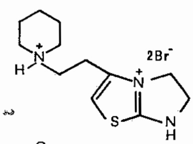	78	239-241	1598	1555	1565
V_b**	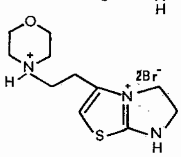	97	202	1597	---	1565

V_c**	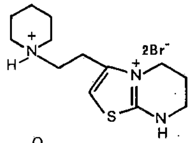	98	279-281	1640	---	1610
V_d**	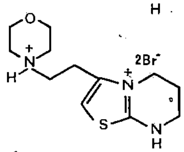	98	270-271	1630	1535	1610
V_e**	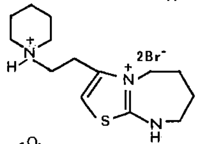	96	249-150	1630	1550	1595
V_f**	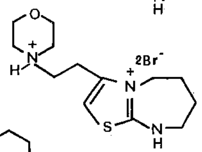	96	274-275	1625	1550	1600
V_h**	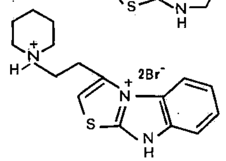	98	280-281	1615	1575	1600
IX_a**	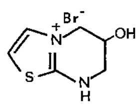	46	191-192	1610*	1520	1590
IX_b**	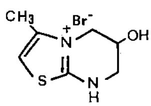	42	217-218	1630*	1520	1600
IX_c**	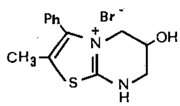	10	230-232	1640*	1530	1600
IX_d**	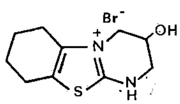	21	205-206	1643*	1515	1605

* Absorption du OH alcoolique en IR $\bar{\nu}$ (OH) 3350-3300 cm^{-1}.

** Analyses élémentaires satisfaisantes ont été obtenues pour C,H, Br, N, S ($\pm$ 0,4 %).

Les dibromo-1,3 propanol-2 (VII) a été synthétisé par bromuration de glycerol à l'aide de brome et de phosphore rouge[18].

Parmi les amino-2 thiazoles utilisés (VI), l'amino-2 thiazole non substitué est commercial, tandis que le méthyl-4 amino-2 thiazole[19], le phényl-4 méthyl-5 amino-2 thiazole[20] et l'amino-2 tetrahydro-4,5,6,7 benzothiazole[21] ont été préparés selon les méthodes decrites dans la bibliographie.

Dérivés (IV) et (III): 0,01 mole de bromhydrate de bromocétone (I) et 0,01 mole de thiurée cyclique (II) sont chauffés à reflux dans 250 ml d'alcool absolu pendant 3 hrs. Après quoi le solvant est éliminé sous pression réduite et le résidu est recristallisé dans un mélange de méthanol-éther.

Dérivés (V): 0,01 mole de dérivé (III) ou (IV) est mis en suspension dans 60 ml d'acide acétique glacial et la mélange est agité pendant 12 hrs à 120°C. Puis, l'acide acetique est èliminé par distillation sous pression réduite et le résidu est recristallisé dans un mélange méthanol-éther.

Dérivés (IX): On chauffe pendant 80 hrs à reflux un mélange de 0,025 mole de dibromo-1,3 propanol-2 (VII) et de 0,05 mole d'amino-2 thiazole substitué ou non dans 25 ml d'éthanol absolu. Puis on laisse pendant 2 hrs à 0°C, ajoute une petite quantité d'éther anhydre jusqu'à commencement de la cristallisation et après refroidissement pendant 2 hrs on filtre les cristaux formés et lave avec de l'éther. On rectistallise dans un mélange méthanol-éther. La concentration des eaux-méres suivie par une addition d'éther permet d'obtenir le bromhydrate de l'amino-2 thiazole utilisé.

Περίληψις

Σύνθεσις 2-διαλκυλαμινοαιθυλιωμένων καὶ ὑδροξυλιωμένων διπυρηνικῶν παραγώγων τοῦ θειαζολίου.

Ἡ παρασκευὴ 2-διαλκυλαμινοαιθυλιωμένων παραγώγων τῶν βρωμιούχων ἰμιδαζο[2,1-b]θειαζολ-4-ίων, θειαζολο[3,2-a]πυριμιδιν-4-ίων καὶ θειαζολο[3,-2-a][1,3]διαζεπιν-4-ίων ἐπιτυγχάνεται δι' ἐπιδράσεως 1-βρωμο-4-διαλκυλαμινοβουταν-2-ονῶν ἐπὶ τῶν ἀντιστοίχων κυκλικῶν θειουριῶν. Ὑπὸ ὡρισμένας συνθήκας καὶ διὰ τινα τῶν προϊόντων εἶναι ἐφικτὴ ἡ ἀπομόνωσις τῶν ἐνδιαμέσων καρβινολαμινῶν. Ὡσαύτως ἡ σύνθεσις τῶν βρωμιούχων 6-ὑδροξυ-5,6,7,8-τετραϋδρο-θειαζολο[3,2-a]πυριμιδιν-4-ίων λαμβάνει χώραν δι' ἐπιδράσεως 1,3-διβρωμο-2-προπανόλης ἐπὶ τῶν ἀντιστοίχων 2-ἀμονοθειαζολίων.

Bibliographie

1. Werbel, L.M. and Battaglia, J.R.: J.Med. Chem. **14** 10 (1971).
2. Sharpe, C.J., Shadbolt, Ashford, A., and Ross, J.W.: J. Med. Chem. **14** 977 (1971).
3. Allewijn, F.T.N., and Demoen, P.J.A.: J. Pharm. Sci., **55** 1028 (1966).
4. Raeymaekers, A.H.M., Allewijin, F.T.N., Vandenberk, J., Demoen, D.J. a., Van Offenwertand, T.T.T. and Janssen, P.A.J.: J. Med. Chem. **9** 545 (1966).
5. Paolini, J.P. and Lendvay, L.J.: J. Med. Chem. **12** 1031 (1969).
6. Snyder,-Jr., H.R. and Benzamin, L.E.: J. Med. Chem. **9** 402 (1966).
7. Fefer, M. and King, L.C.: J. Org. Chem. **26,** 828 (1961).

8. Bassignana-Cogrossi, C. and Candino, M.: Spectrochim. Acta **19** 1885 (1963).
9. Allen. C.F.H., Edens, C.O. and Vanallen, J. Org. Syntheses **26** 34 (1946).
10. McKay, A.F. and Hatton, W.C.: J. Am. Chem. Soc. **78** 1618 (1956).
11. Hall, H.K. and Schneider, A.K.: J. Am. Chem. Soc. **80** 6409 (1958).
12. Van Allen, J.A. and Deacon, B.D.: Org. Syntheses Coll. vol. IV 569 (1963).
13. Roth, H.J. and Dnovak, J.: Arch. Pharm. **196** 243 (1963).
14. Mannich, C, and Braun R.: Ber. **53** 1874 (1920).
15. Frank, R.L. and Pierle, R.C.: J. Am. Chem. Soc. **73** 724 (1951).
16. Land, A.H., Ziegler, C. and Sprague, J.M.: J. Am. Chem. Soc. **69** 125 (1947).
17. Djerassi, C., Missoni, R.H. and Scholz, C.R.: J. Org. Chem. **15** 700 (1950).
18. Braun, G.: Org. Syntheses Coll. Vol. II 308 (1943).
19. Byers, J.R., and Dickey, J.B.: Org. Syntheses Coll. Vol. II 31 (1943).
20. Dodson, R.M. and King, L.C.: J. Am. Chem. Soc. **67** 2242 (1945).
21. Sprague, J.M. and Kissinger, L.W.: J. Am. Chem. Soc. **63** 578 (1941).

Remerciements: Nous remercions le Centre National des Recherches de Grèce, qui, evec son aide financière, a contribué à l' aboutissement de ce travail.